Diploma thesis

Morphologic Alterations of Small Intestinal Mucosa in Patients with Cirrhosis

A Pilot Study

submitted by

Florian Rainer

d.o.b.: 14-02-1987

attaining the academic degree

Doktor der gesamten Heilkunde
(Dr. med. univ.)

at the

Medical University of Graz

under supervision of

Univ. Prof. Dr. Rudolf Stauber

Division of Gastroenterology and Hepatology

Department of Internal Medicine

Medical University of Graz

and

Univ. Prof. Dr. Carolin Lackner

Institute of Pathology

Medical University of Graz

Graz, March 2013 (Rainer Florian)

Eidesstattliche Erklärung

Ich erkläre ehrenwörtlich, dass ich die vorliegende Arbeit selbstständig und ohne fremde Hilfe verfasst habe, andere als die angegebenen Quellen nicht verwendet habe und die den benutzten Quellen wörtlich oder inhaltlich entnommenen Stellen als solche kenntlich gemacht habe.

Affidavit

I hereby declare that the following diploma thesis has been written only by the undersigned and without any assistance from third parties. Furthermore, I confirm that no sources have been used in the preparation of this thesis other than those indicated in the thesis itself.

Graz, 25th of March, 2013 *Florian Rainer*

Acknowledgements

First of all, I would like to express my sincere gratitude to Univ. Prof. Dr. **Rudolf Stauber** and Univ. Prof. Dr. **Carolin Lackner**, my supervisors, not only for encouraging and supporting me in conducting this clinical trial, but also for giving me the perfect example of how to combine clinical and scientific practice.

Moreover, I would like to thank **Andrea Koschell**, who became more a friend than a colleague within our prolonged electron-microscopy meetings; Priv.-Doz. Dr. **Vanessa Stadlbauer-Köllner**, Univ. Prof. Dr. **Peter Fickert**, Dr. **Philipp Douschan**, Dr. **Walter Spindelböck**, **Hannelore Pock**, **Kathrin Schiefer** and the rest of the team of the liver unit for supporting me in conducting this study.

Furthermore, a variety of others were indispensable in the completion of this study:

- Univ. Prof. Dr. **Christoph Högenauer** & Univ. Prof. Dr. **Heinz Hammer** from the endoscopy unit of the Department of Internal Medicine
- Univ. Prof. Dr. **Karl Öttl** & **Doris Payerl** from the Institute of Biochemistry
- Univ. Prof. Dr. **Harald Kessler** & Dr. **Eva Leitner** from the Institute of Hygiene
- Priv.-Doz. Mag. Dr. **Gerd Leitinger** from the Institute of Histology and Embryology

Finally, I would also like to thank my parents, **Erika** and **Peter Rainer**, my brother **Peter**, my sister **Eva**, my cohabitants and my friends for their support and encouragement throughout my studies. My special thanks go to my friends at the Red Cross of Gastein, without whom I probably would never have started my studies.

Abstract

Background: Increased gastrointestinal permeability in cirrhosis is considered an important factor in the etiology of bacterial translocation & its related complications and has repeatedly been confirmed by measuring the urinary excretion of orally administered test substances. Since tight junctions represent the main barrier for macromolecules used in permeability tests, impaired function related to structural alterations is suspected to be involved in the disruption of the gut barrier. However, studies regarding the ultrastructural changes in intestinal mucosa are scarce and have given contradictory results.

Methods: Twelve patients with cirrhosis at an early (n = 7) or advanced (n = 5) stage and ten healthy controls underwent distal duodenal biopsy. Alterations observed on light- and transmission-electron microscopy, with special emphasis on tight-junction ultrastructure, were correlated to intestinal permeability, assessed by the sucrose/lactulose/mannitol test.

Results: Morphological abnormalities on light microscopy included a distended intercellular space (in the basal parts of enterocytes) & vacuolization of the enterocytes' cytoplasm at the villous tips, increased number of denuded villi, edema & fibrosis of the lamina propria and larger capillary diameters in cirrhotic patients. The lactulose/mannitol excretion ratio was increased in cirrhotics. Permeability for mannitol was only decreased in patients with advanced cirrhosis. Electron-microscopy analysis revealed preserved cell/cell-connections at the enterocytes' luminal borders with morphologically intact tight junctions. A slightly increased TJ-gap width was observed only in-between perishing enterocytes and in epithelial areas with distended intercellular spaces (in the basal parts of the epithelium). In contrast, density of the perijunctional actomyosin complex was increased even in areas without distended intercellular spaces or perishing cells. Furthermore, microvilli were shorter and less densely packed; distorted microvilli were only observed in perishing enterocytes.

Conclusion: Among the morphological changes detected by light microscopy (distended intercellular spaces, vacuolization of the cytoplasm, denuded villi, edema & fibrosis of the lamina propria and capillary congestion), only denuded villous tips correlated with an increased lactulose/mannitol ratio. Permeability for mannitol was decreased in advanced cirrhotics, probably associated with a decreased villus/crypt ratio observed in those patients. Ultrastructural analysis revealed a widening of tight-junction gaps in epithelial areas with a distended intercellular space in the basal parts of enterocytes, but, only a tendency to correlate with the lactulose/mannitol ratio was observed. Further studies in larger cohorts are being conducted to confirm our findings and to reach statistical significance in some indicated alterations.

Zusammenfassung

Hintergrund: PatientInnen mit Leberzirrhose neigen zu Infektionen durch Bakterien aus dem Gastrointestinaltrakt, dies steht vermutlich mit einer gestörten Barrierefunktion der Darmschleimhaut in Zusammenhang. In früheren Studien mit ZirrhotikerInnen zeigte sich eine verstärkte Durchlässigkeit des Darmes für Substanzen, die über den parazellulären Transportweg aufgenommen werden. Da die Substanzaufnahme über diesen Weg vor allem durch Tight Junctions reguliert wird, liegt die Vermutung nahe, dass diese an der veränderten Darmdurchlässigkeit beteiligt sind. Studien, welche die ultrastrukturellen Veränderungen der Darmschleimhaut beleuchten sind rar und haben unterschiedliche, zum Teil widersprüchliche Resultate gezeigt.

Methoden: In die Studie wurden zwölf PatientInnen mit Zirrhose im Früh- (n = 7) bzw. Spätstadium (n = 5) und zehn Kontrollen eingeschlossen. Es wurden Biopsien aus dem unteren Dünndarm entnommen und anschließend licht- und elektronenmikroskopisch untersucht. Strukturelle Veränderungen der Darmschleimhaut, vor allem im Bereich der Tight Junctions, wurden mit dem Vorliegen funktioneller Veränderungen verglichen, die mit Hilfe des Sucrose/Lactulose/Mannitol Tests untersucht wurden.

Ergebnisse: In der Lichtmikroskopie zeigten sich ausgeweitete Interzellularspalten (in den basalen Abschnitten der Enterozyten) & ein vakuolisiertes Zytoplasma der Epithelzellen an den Villi-Spitzen, abgeschilferte Villi, Ödem & Fibrose in der Lamina propria und ein größerer Durchmesser der Kapillaren bei den ZirrhotikerInnen. Die Lactulose/Mannitol Ausscheidungsrate war bei ZirrhotikerInnen erhöht. Die Elektronenmikroskopie zeigte gewahrte Zellverbindungen in den luminalen Bereichen der Enterozyten mit morphologisch erhaltenen Tight Junctions. Ein verbreiterter Tight Junctions-Spalt wurde nur in Epithelabschnitten mit untergehenden Zellen oder basal auseinandergedrängten Zellen beobachtet. Die Dichte des umliegenden Aktomyosin-Komplexes war auch in ansonsten unauffälligen Bereichen bei ZirrhotikerInnen erhöht. Die Mikrovilli erschienen kürzer und weniger dicht gestaffelt; deformierte Mikrovilli wurden nur an untergehenden Enterozyten beobachtet.

Fazit: Von den in der Lichtmikroskopie gefundenen Veränderungen (ödematös aufgelockertes Epithel, vakuolisiertes Zytoplasma, abgeschilferte Villi, Ödem & Fibrose in der Lamina propria, kapilläre Stauung) korrelierte lediglich die Anzahl denudierter Villi mit einer erhöhten Lactulose/Mannitol Ausscheidungsrate. Erst bei fortgeschrittener Zirrhose wurde ein erniedrigter Mannitolwert im Harn festgestellt, der wahrscheinlich mit einer bei diesen PatientInnen erniedrigten Villi/Krypten-Ratio in Zusammenhang steht. Die Elektronenmikroskopie zeigte einen verbreiterten Tight Junctions-Spalt in Epithelbereichen mit basal auseinandergedrängten Zellen; hierbei zeigte sich eine Tendenz zur Korrelation mit der Lactulose/Mannitol Ausscheidungsrate. Weitere Untersuchungen in einer größeren Kohorte werden derzeit durchgeführt, um die Bedeutung der nachgewiesenen und angedeuteten Veränderungen weiter zu klären.

Table of contents

Figures

Tables

Abbreviations

A

Å .....Ångström [10^{-10}m]

ACLF .....acute-on-chronic liver failure

AIH .....autoimmune hepatitis

ALT .....alanine transaminase

AP .....alkaline phosphatase

aPTT .....activated partial thromboplastin time

ASH .....alcoholic steatohepatitis

AST.....aspartate transaminase

asymp.....asymptotic

B

BT .....bacterial translocation

C

CCC .....cholangiocellular carcinoma

CCl_4 .....Carbon tetrachloride

CHE .....serum cholinesterase

^{51}Cr-EDTA ...chromium-labeled ethylenediaminetetra acetic acid

CRP.....C-reactive protein

D

Da .....Dalton

DIS.....distended intercellular space

DNA .....deoxyribonucleic acid

E

ET-1 .....endothelin-1

eNOS .....endothelial NO- synthetase

G

GGT .....gamma-glutamyltransferase

GI.....gastrointestinal

H

Hb .....hemoglobin

HCC.....hepatocellular carcinoma

HE.....hepatic encephalopathy

H&E.....haematoxylin and eosin stain

HSC .....hepatic stellate cells

HVPG .....hepatic venous pressure gradient

I

IBD .....inflammatory bowel disease

IDDM .....insulin-dependent diabetes mellitus

i.e. .....id est, that is

IEL.....intraepithelial lymphocytes

IgA.....immunoglobulin A

IFN-γ .....interferon-gamma

INR .....international normalized ratio

J

JAM .....junctional adhesion molecule

K

K .....potassium

L

LDH.....lactate dehydrogenase

LPS .....lipopolysaccharide

M

MAGUK.....membrane associated guanylate kinase

MCV .....mean corpuscular volume [of erythrocytes]

MLN .....mesenteric lymph nodes
mRNA.....messenger ribonucleic acid

N

Na .....sodium
NIEC.....new Italian endoscopic club for the study and treatment of esophageal varices
nm .....nanometer
NO .....nitric oxide

O

OLT .....orthotopic liver transplantation

P

PAC .....perijunctional actomyosin complex
PCR.....polymerase chain reaction
PEG 400.....polyethylene glycol 400
PH .....portal hypertension
PHD .....portal hypertensive duodenopathy
PHE.....portal hypertensive enteropathy
PHG .....portal hypertensive gastropathy
pO_2.....partial pressure of oxygen
PT .....prothrombin time
pts .....points

R

RAS .....renin-angiotensin system
RNA.....ribonucleic acid
RNS .....reactive nitrogen species
ROS .....reactive oxygen species

S

SBP.....spontaneous bacterial peritonitis
SD.....standard deviation
Sig.....significance
Std.....standard

T

TEM.....transmission electron microscopy
TER .....transepithelial electrical resistance
TIPS.....transjugular intrahepatic portosystemic shunt
TNF-α.....tumor necrosis factor alpha
TJ .....tight junction [Zonula occludens]

V

VEGF.....vascular endothelial growth factor

W

WHVP .....wedged hepatic vein pressure

1 Introduction

The human intestine contains 400 to 500 different species of bacteria whose number of cells exceeds the body's own cell count by far (1). Despite the fact that interaction of most of the bacterial residents and the host offers advantages for both sides, some of these microorganisms are potential pathogens and - under particular circumstances - entail the risk of infection and other complications (2,3).

The intestinal epithelial layer forms an enormous surface area where the outside of the body – i.e. the gut lumen - interacts with inside body structures. Nutrients, vitamins, ions and water need to be taken up to the 'inside', whereas bacteria, toxins and other pathogens should stay outside the epithelial layer in the intestinal lumen. Therefore, to prevent infection of the organism, epithelial cells are attached closely via complex cell/cell-connections which simultaneously allow the passage of essential substances. Tight junctions (TJ) are some of these connections that play an important role in the maintenance of the gut barrier and the selection of substances to cross this barrier. Their performance seems to be regulated by a large number of influencing factors; even organs situated far away appear to effect TJ structure and function.

1.1 The Liver and its Pathologies

Performing over 500 different functions for the body (4), the liver plays a major role in metabolism including detoxification, production of enzymes important for digestion and protein synthesis (5). Its complexity makes the liver susceptible to a variety of diseases (4): EU statistics estimates that ***chronic liver disease*** is the fifth most common cause of death in the states of the European Union, which means that more than 70,000 Europeans are dying because of chronic liver diseases every year (6). With regard to Austria, the mortality rate for chronic liver diseases is estimated at 19.4 per 100,000 (7), which is higher than the average value in Europe. In the Western world, chronic alcohol abuse is among the most common reasons for chronic liver disease, whereas in developing countries, viral infections are more prevalent causes (8). To the variety of possible causes for damage, the response pattern of the liver is mostly the same: Progressed damage leads - due to the replacement of the destroyed parenchyma by connective tissue – to a disruption of the normal liver architecture and the development of cirrhosis. (9)

1.1.1 Distortion of Normal Liver Architecture – Cirrhosis

The term cirrhosis originates from the Greek *κιρρός* [kirrhós] which is best translated as orange-colored or tawny, and refers to the color-change of a chronically damaged liver. Cirrhosis was defined by the WHO as *a diffuse process characterised by fibrosis and the conversion of normal liver architecture into structurally abnormal nodules* (10). It is considered the end-stage of a variety of inflammatory and necrotizing liver diseases [Table 1] resulting in the disorganization of the lobular and vascular architecture throughout the whole liver. The pathological hallmark of cirrhosis is the development of fibrous septa and regenerative nodules which represent a stage of liver disease that is hardly reversible if at all. (10)

chronic alcohol abuse (approx. 50% in developed countries)
viral hepatitis (B,C,D; approx. 45% in developed countries)
other causes:
- autoimmune hepatitis
- primary biliary cirrhosis
- drug-induced liver damage
- metabolic diseases (haemochromatosis, Wilson's disease, Alpha-1 antitrypsin deficiency, cystic fibrosis,…)
- cirrhose cardiaque
- Budd-Chiari syndrome
- tropical diseases (schistosomiasis, liver fluke)

Table 1. 'Common Liver Diseases causing Cirrhosis' [adapted from (11)]

1.1.2 Clinical Presentation

The clinical presentation and complications of chronic liver disease arise from a dysfunction of the liver cells (hepatocytes) and/or an alteration of blood flow through the liver (9). For a long period of progression, cirrhosis is a silent disease – most patients remain asymptomatic (compensated cirrhosis) until the appearance of complications (decompensated cirrhosis) occurs. Initial signs for well-compensated cirrhosis are non-specific and can manifest as weight-loss, weakness or fatigue (12). With progressive liver damage, a systemic disease affecting several organs presenting a variety of hepatic and extra-hepatic complications develops. Major complications of cirrhosis include *portal*

hypertension, ascites, spontaneous bacterial peritonitis, hepatic encephalopathy, hepatorenal syndrome, variceal bleeding and hepatocellular carcinoma. (13)

abdominal wall vascular collaterals (caput medusae)
ascites
asterixis
clubbing and hypertrophic osteoarthropathy
constitutional symptoms, including anorexia fatigue, weakness and weight loss
dupuytren's contracture
fetor hepaticus - a sweet-pungent breath odor
gynecomastia
hepatomegaly
jaundice
Kayser-Fleischer ring – a brown-green ring of copper deposit around the cornea, pathognomonic for Wilson's disease
nail changes
palmar erythema
scleral icterus
splenomegaly
testicular atrophy
vascular spiders (spider teleangiectasias, spider angiomata)

Table 2. 'Common Physical Examination Findings in Cirrhotics' [from (12)]

1.1.2.1 Portal Hypertension and Variceal Bleeding

In the setting of chronic liver disease, the intrahepatic vascular resistance is increased and, together with increased splanchnic blood flow, results in the congestion of blood within the splanchnic bed. When portal pressure exceeds a certain threshold, the development and dilatation of ***porto-systemic collaterals*** facilitate the diversion of portal venous blood bypassing the liver (9). Approximately 50 percent of patients with cirrhosis develop varices, most commonly seen in the distal part of the esophagus (14). Moreover, varices constitute a risk of rupture and bleeding; the prognosis of variceal hemorrhage is poor (9).

1.1.2.2 Ascites and Spontaneous Bacterial Peritonitis

Cirrhosis is the leading cause of ***ascites***, a pathologic accumulation of fluid in the peritoneal cavity. It results from an increase in capillary hydrostatic pressure within the splanchnic bed and a decrease in colloid-osmotic pressure that is often seen in patients with advanced liver disease, due to a decreased production of albumin. In cirrhosis, sequestration of fluid in the peritoneal cavity is induced by transudation and therefore, characterized by low protein and LDH, high pH and normal glucose levels (5,11). The kidney is another important factor in the development of cirrhotic ascites, since impaired ability to excrete sodium is an early renal dysfunction in cirrhotic patients and regularly seen before the onset of ascites (15).

Spontaneous bacterial peritonitis (SBP) - the development of infection of fluid in the peritoneal cavity - occurs in up to 10% of ascitic patients (15) - in the absence of any intra-abdominal source -, and is considered one of the most feared complications in patients with cirrhosis (16). It is diagnosed with the detection of more than 250 granulocytes per µl ascitic fluid and often caused by microorganisms that originate in the gut (17). Gram-negative intestinal bacteria, especially Escherichia coli and Klebsiella species, are detected in approximately 70% of culture-positive cases of SBP (18). Currently, there are several mechanisms suspected of playing an important role in its pathogenesis: Portal hypertension, increased intestinal permeability [see 1.5.4.1], impaired defense mechanisms against microorganisms [see 1.5.4.2] and intestinal bacterial overgrowth [see 1.5.4.3].

1.1.2.3 Other Complications of Cirrhosis

Other complications of cirrhosis include ***hepatic encephalopathy*** (HE) – a decrease in neuropsychiatric functions caused by the accumulation of toxic substances that are normally degraded by the liver – and ***hepatorenal syndrome*** – the deterioration of kidney function due to the sequestration of fluid within the splanchnic bed and a subsequent decrease in renal perfusion. (8,9,14)

Furthermore, a chronically damaged liver fails to synthesize coagulants and anticoagulants - that is why patients with cirrhosis suffer more likely from hemorrhage. Additionally, hypersplenism leads to an increased depletion of cells - especially thrombocytes - aggravating the bleeding tendency. Furthermore, liver dysfunction also exerts effects on the pulmonary vascular system, leading to either hepatopulmonary syndrome or portopulmonary hypertension [see (19)]. Cirrhosis is regarded as a facultative

precancerosis and constitutes the main common cause for ***hepatocellular carcinoma*** in Western countries. (9)

1.1.3 Grading of Cirrhosis – the Child-Pugh Score

The prognostic assessment of patients with cirrhosis is based on the Child-Pugh classification which features not only clinical findings (severity of encephalopathy, ascites), but also the performance of synthesis (albumin concentration, coagulation status) and the excretion function (bilirubin levels) of the liver. (9)

Measure	1 point	2 points	3 points
Ascites	None	Mild	Severe
Hepatic Encephalopathy	None	Grade I-II	Grade III-IV
Total bilirubin [mg/dl]	≤ 2	2 - 3	≥ 3
PT INR	< 1.7	1.71 – 2.30	> 2.3
Serum albumin [g/l]	> 35	28 - 35	< 28

Table 3. 'Child-Pugh Score' [from (11)]; PT = prothrombin time; INR = international normalized ratio

The total score ranges between 5 and 15 points; 5-6 points is considered class A, a total score of 7-9 is class B and 10-15 points class C.

1.2 Intestinal Epithelium

Spread from the lower esophageal to the anal sphincter, the *columnar epithelium* of the gastrointestinal tract has to fulfill a variety of well-known tasks involved in the digestion of food and the uptake of water, electrolytes & nutrients to the body (20). Since the gastrointestinal lumen is connected to the 'outside world' (with all of its antigens, toxins, microorganisms etc.), the mucous membrane lining the intestines has to face another important task, namely the construction of a *barrier* against all the substances that should not enter the human body. To keep the balance between those two contrary events, complex tissue organization and different transportation routes with the possibility of tight regulation are necessary (21).

1.2.1 Intestinal Cellular Composition

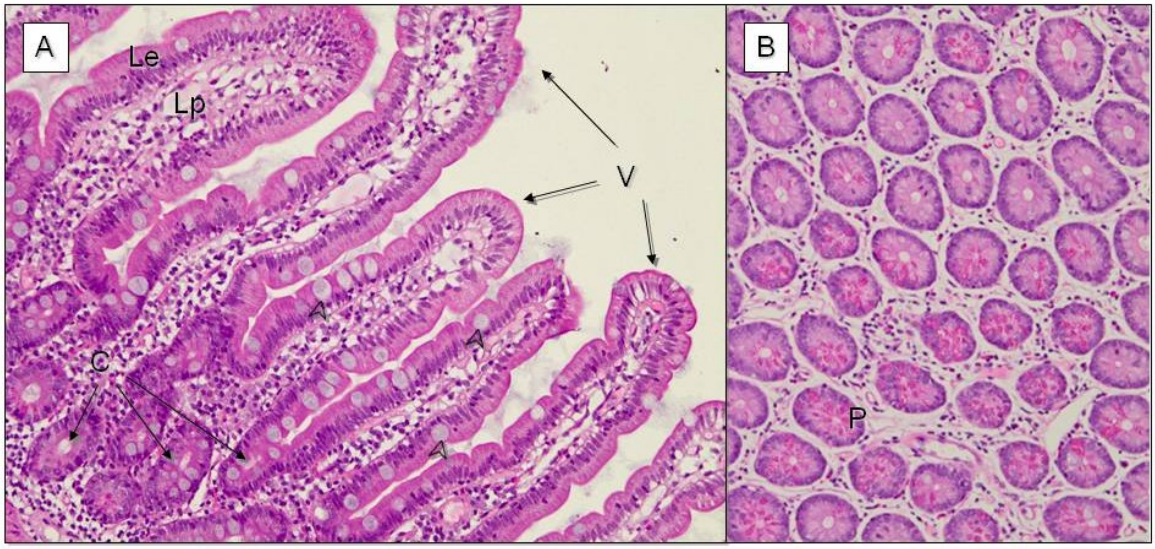

Figure 1. 'Regular Intestinal Mucosa' (A): Villi (V) are formed by protuberances of the lamina propria (Lp) coated with epithelial cells (Le = lamina epithelialis). In-between the villi, crypts (C) are present as indentations of the epithelium into the lamina propria. The epithelial lining consists mostly of enterocytes, interspersed with mucin-secreting goblet cells (arrow tips). (B): Transverse sections of crypts, containing Paneth cells (P) with large eosinophilic granules. (H&E stain. 100x)

The small intestine, where 95% of nutrient absorption takes place, is coated with a single cell-layer that forms *a three-dimensional structure consisting of invaginations or crypts alternating with tips or villi* (22). The villi are finger-shaped protuberances formed by the epithelium and the lamina propria; in between their bases, crypts - or intestinal glands – dip like caves into the lamina propria [Figure 1]. The epithelium consists of ***four different cell types*** that can be found at preferred locations: **Absorptive enterocytes,** wearing microvilli on their apical side to increase surface area available for digestion and absorption, are the predominant cell type at the villi. Few **goblet cells** are present [Figure 2] that produce protective mucins forming a polysaccharide- and glycoprotein-containing glycocalyx layer. In the depth of the crypts, antimicrobial peptide-secreting

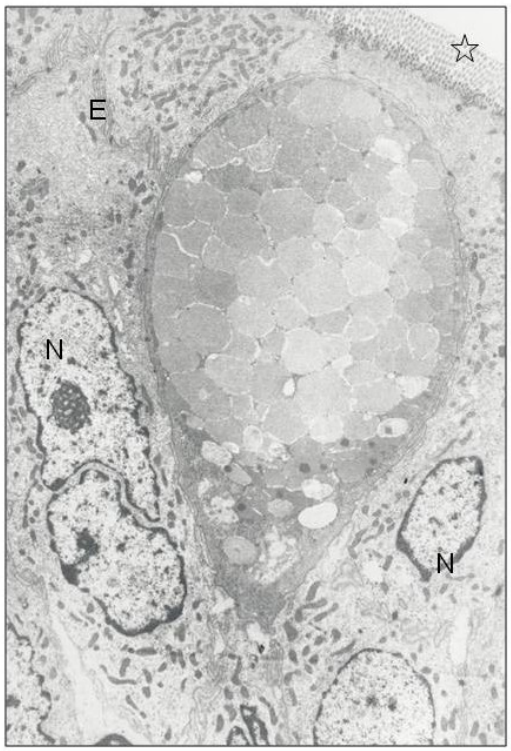

Figure 2. 'Electron Micrograph of Goblet Cell (healthy control patient)**'** The cytoplasm is crowded with numerous fusing secretory granules, forming the typical honeycomb shape. The goblet cell is surrounded by enterocytes (E). (N = nuclei of enterocytes; open star = intestinal lumen)

Paneth cells are found that take part in the nonspecific immune defense. Furthermore, hormone-secreting **enteroendocrine cells,** interspersed in the epithelium of the small intestine, are involved in the secretion of gastrin, secretin, cholecytokinin or serotonin (22-24). The lifespan of enterocytes is in the range of 4-5 days; during this time, they migrate from the depths of the crypts - where their stem cells are also located - to the tips of the villi. Here, they undergo apoptosis and are shed into the gut lumen. (22)

1.2.2 The two Pathways of Intestinal Substance Uptake

The majority of the epithelial barrier is formed by enterocytes that are connected via different types of cell/cell-connections. Regarding the structural set-up of the intestinal mucosa, two ways of substance uptake can be distinguished (25,26):

1) **Transcellular Pathway:**

On the one hand, substances can be taken up via the transcellular pathway, straight through the enterocytes by crossing the lipid bilayer membrane [Figure 3A]. Eukaryotic cell membranes are permeable to lipid substances, whereas water soluble compounds are prevented. Therefore, epithelial cells are equipped with transporters for water soluble compounds the body requires (including amino acids, sugars, electrolytes and fatty acids). This pathway through enterocytes is directional and energy-dependent. (27,28)

2) **Transcellular Pathway:**

On the other hand, substances can cross the epithelial layer via the paracellular space between neighboring enterocytes [Figure 3B]. This pathway is passive & non-directional and results from diffusion or osmosis driven by different concentrations of substances on the two sides of the epithelium (28). Furthermore, it is not regulated by membrane transporters or channels, but rather limited by the junctional complexes that link the epithelial cells. (27)

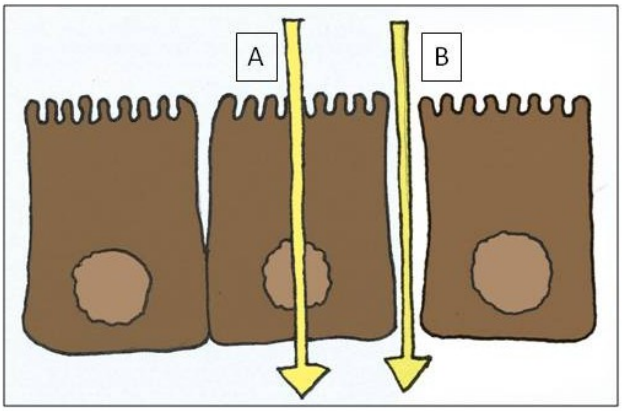

Figure 3. 'Tanscellular (A) **and Paracellular** (B) **Pathway'**
[adapted from (25)]

1.2.3 Structural Components of Junctional Complexes

At the ultrastructural level, different types of cell/cell-connections, localized across the membrane contact areas of epithelial cells, can be identified. They are formed by complex networks of characteristic transmembrane proteins and lipids that establish connections to their counterparts of neighboring cells (27). In 1963, *Farquhar et al.* first discovered and described ***three different junctional complexes*** [Figure 4] located at the lateral surface of adjacent enterocytes (29). Close to the gut lumen, they set up the so-called terminal bar: The most apical part of this tripartite complex is formed by ***tight junctions (TJ, or zonulae occludentes)***, followed by ***zonulae adherentes (ZA, or intermediate junctions)*** and ***maculae adherentes (MA, or desmosomes)***. These structures are not only observed in the epithelium of the intestinal mucosa, but rather occur in every epithelium of the body that separates two different compartments (30,31). A different type of cell connection is represented by ***gap junctions*** that – dispersed all over the contact area of epithelial cells - serve primarily as intercellular pore builders to ensure exchange of substances between two adjacent cells. (32)

ZAs and ***MAs*** are thought to play an important role in the ***mechanical linkage*** of two contiguous cells; in electron microscopy they are represented by dense areas on the inner surface of cell membranes, where filaments of the cytoskeleton and transmembrane proteins insert [Figure 4]. (27)

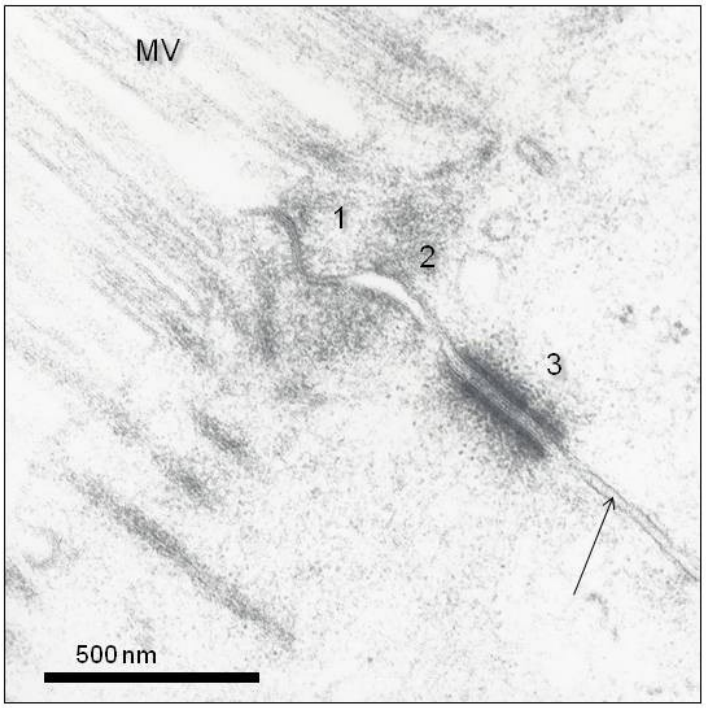

Figure 4. 'Junctional Complex of Adjacent Enterocytes' 1: tight junction; 2: zonula adherens; 3: desmosome; MV: microvilli; the arrow points to the extracellular space between two enterocytes.

1.3 Tight Junctions – Structure and Function

TJs seem to perform a different role compared to that of ZAs and desmosomes: Electron-microscopy images reveal a narrowing of the space between the enterocytes to an almost complete obliteration of the intercellular gap [Figure 4]. Therefore, TJs are considered less a mechanical support, but more a ***structural barrier*** that circumferentially wraps the apical pole of epithelial cells. In fact, TJs regulate the permeation of molecules in-between enterocytes and therefore, constitute the major physical structure ***defining the particular properties of the paracellular transport system*** (33). They create an adjustable barrier that is capable of reacting to influences of the environment and to requirements of epithelial cells. Therefore, the term *tight* junction is an unfortunate one describing TJs as rigid, non-dynamic structures. However, besides their role in the regulation of paracellular diffusion, these multifunctional complexes prohibit diffusion of membrane proteins and lipids located at the apical side of the enterocytes to the basolateral area & vice versa and thus, preserve the different composition of these two areas ('*fence function*' of TJs). Moreover, they are suspected to be involved in cell signaling, transcriptional regulation, cell cycle and vesicle trafficking. (23,26,27,30,34)

Figure 5. 'Electron Micrograph of a TJ between two Epithelial Cells.' Lanthanum Hydroxide (black color) was added to the basolateral side. It diffuses freely through the intercellular space, until it reaches the tight junction (arrow). The marker is precluded from the apical side of the cell and gut lumen. [adapted from (26)]

1.3.1 Molecular Architecture of Tight Junctions

During the last decades, a number of molecular components of TJs have been identified and characterized. Currently, more than 40 proteins are known (34), the role of many is only partly described. The protein constituents of TJs are divided into two groups: ***Adhesive transmembrane proteins*** form the core of TJs; they protrude from the cell membrane into the intercellular space and create the paracellular barrier (35). ***Peripheral proteins*** are located at the cytoplasmatic surface of the junctional complexes and interact with transmembrane components on the one side, and bunches of the perijunctional cytoskeleton (i.e. actin and myosin) on the other side (23). The actomyosin cytoskeleton located near the cytoplasmic surface of TJ forms a circular structure, the contractible actomyosin ring (36). Together with the cytoplasmatic adaptor proteins, the actomyosin ring makes up the dense *'cytoplasmatic plaques'* [or *perijunctional actomyosin complex (PAC)*] near the cell borders observed on electron microscopy [Figure 7]. Together with other scaffolding proteins & signaling complexes, peripheral proteins contribute to the 'non-classical' functions of TJs. (37)

There are at least three important types of transmembrane proteins within the tight junctions: ***occludin, claudin*** and ***junctional adhesion molecule (JAM)***. Each of these protein classes represent groups consisting of a number of subunits or alternatively spliced isoforms. It is suspected that the combination of different protein isoforms affects the 'tightness' of TJs and therefore, the permeability properties of the barrier (27,38-40) [see 1.4].

1.3.1.1 Occludin

Occludin is an approximately 65 kD protein with four transmembrane areas and two extracellular loops; it exists in several isoforms which are thought to be a result of alternative mRNA splicing (41,42). Although occludin was the first TJ transmembrane protein discovered [*Furuse et al*, 1993 (43)], its definite function still remains cryptic. Since occludin-deficient epithelial cells do not present any significant disturbances in the structure and function of TJs, interest in the exploration of occludin has gradually decreased (37). Moreover, occludin-deficient mice are viable and show normal epithelial transport and barrier function (44,45). Nevertheless, in intestinal diseases associated with permeability disruption, including inflammatory bowel (IBD) and celiac disease, expression of occludin seems markedly decreased suggesting a possible role in the pathogenesis of these entities. (37)

1.3.1.2 The Claudin Family of Proteins

Although claudins do not share sequence similarities with occludin, they also consist of four transmembrane-spanning helices with two extracellular loops, but, in contrast, are much smaller with a mass unit of about 20 to 27 kD. Proteins of the claudin family were first discovered in 1998 by Furuse and Tsukita (46) and soon suspected of being the most important components sealing the intercellular space and regulating the paracellular transportation pathway. Claudins form the protein strands [see 1.3.2] of the TJs that connect to claudin-proteins of neighboring cells (47). Experimental studies in cells devoid of claudin and transfected with different claudin-isoforms revealed that they are all capable of building bridges to equal isoforms localized at adjacent cells (homophilic adhesion), but some of them are additionally able to connect to other claudin-isoforms (heterophilic adhesion). Furthermore, it has been shown that selection and combination of different subtypes affect paracellular substance transport: Some claudins establish the basis for paracellular permeability by creating pores, allowing small substances to pass, while others decrease paracellular permeability by tightening the intercellular space. Hence, the variety of different claudins may enable epithelial cells to control paracellular absorption. At present, 24 different claudin-proteins are known in eukaryotes (48) and therefore, the combination possibilities for TJ assembly - and probably different TJ function - seem to be numerous. (49,50)

1.3.1.3 Junctional Adhesion Molecule

JAMs show extracellular components that resemble structures of immunoglobulins and may be involved in the transmigration of leucocytes across epithelial or endothelial cell layers. Furthermore, by connecting to TJ-scaffolding proteins, they contribute to the structural assembly of TJs and the maintenance of cell polarity. (37)

1.3.1.4 Peripheral Proteins at Tight Junctions

Peripheral TJ proteins form cytoplasmatic plaques at the inner surface of the cell membrane that interact with transmembrane proteins and structures of the actomyosin cytoskeleton. Besides their function as scaffolding proteins, they comprise signaling molecules and transcription factors, contributing to the various non-barrier functions of TJs. Peripheral proteins localized at these submembranous plaques include the membrane-associated guanylate kinase (MAGUK) proteins - called ZO-1, -2 and -3 (= Zonula occludens) – and a more heterogeneous group including cingulin or symplekin. MAGUK

proteins seem to be indispensable in the recruitment of TJ-forming proteins and for the correct linkage of various claudins into TJ strands. (51)

1.3.2 Ultrastructural Characteristics of Tight Junctions

In 1963, Farquhar and Palade first used ultra-thin electron microscopy to examine the intercellular space of adjacent epithelial cells (29). Within the TJ area, they described an extreme narrowing of the intercellular gap and *a variable number of intimate cell-cell contacts*. Subsequent analysis by freeze fracture electron microscopy revealed a wire mesh-like network at the membrane's internal fracture plane [Figure 6], consisting of ***fibrils*** or ***strands*** that correspond to the complex system of linked TJ integral membrane proteins [see 1.3.1]. These strands are thought to provide the physical barrier between the apical and the lateral side of the cell membrane. (27,51,52)

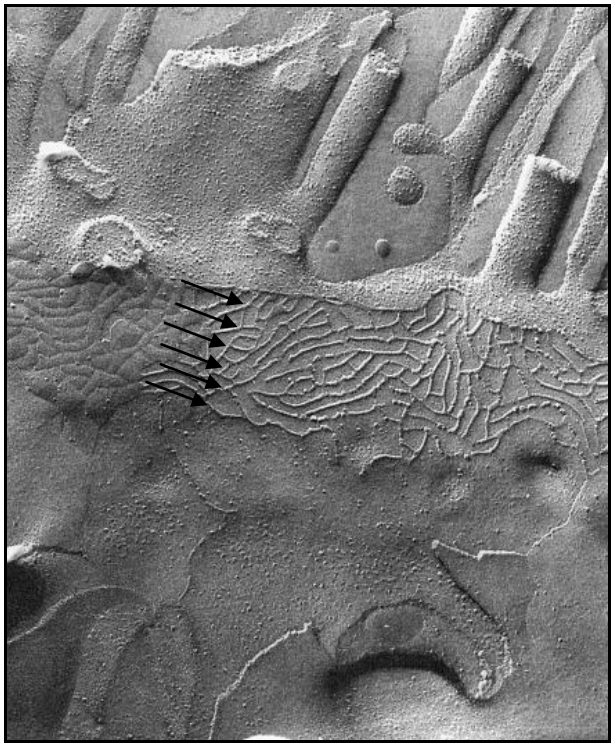

Figure 6. 'Freeze Fracture Electron Microscopy' of intestinal epithelial TJs. The numerous anastomosing strands (arrows) form a complex network. [adapted from (26)]

In ***transmission electron microscopy*** [Figure 7], TJs appear as sites of narrowed intercellular gaps close to the lumen, at the base of the striated border (microvilli). At high magnifications, it becomes obvious that in the TJ area, the outer leaflets of the neighboring cell membranes approach each other and fuse to form a joint line, the *intermediate* - or *fusion* – line [Figure 7B]. Within the TJ area, the characteristic picture of the **three-layered** cell membrane (two electron-dense lipid layers with a less electron-dense intermediate layer) is replaced by a **five-layered** structure that is formed by the two inner leaflets of the cell membranes (electron-dense), the fusion line (electron-dense) and two

less electron-dense intermediate layers [Figure 7B]. The intercellular space is obliterated within these areas. The fusion line cannot be tracked throughout the overall length of TJs, but rather seems to be a discontinuous series of spots. This discontinuity appears to be the transmission-electron-microscopic correlate of the mesh-like network observed in freeze-fracture electron microscopy, where the transmembrane proteins create links to their counterparts of neighboring cells. (29,32)

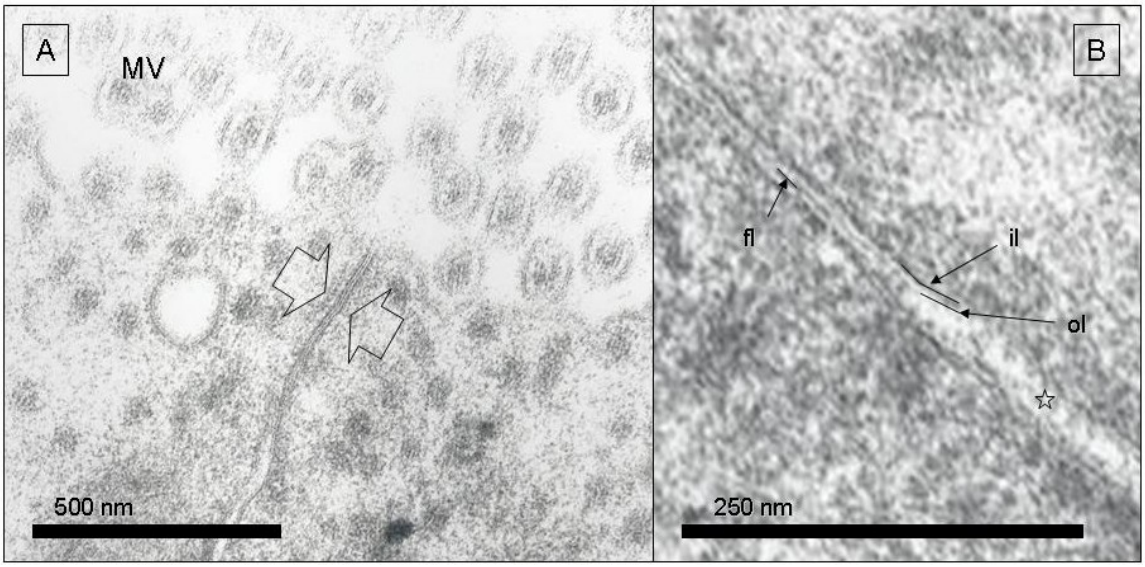

Figure 7. 'Tight Junction between 2 Enterocytes' A: The TJ (in-between the two arrows) is situated close to the luminal surface of the enterocytes and surrounded by a slight condensation of cytoplasmatic material. MV = microvilli. B: The discontinuous fusion line (fl) represents the fused outer leaflets (ol) of the adjoining cell membranes, where the intercellular space is obliterated. il = inner leaflet; open star = intercellular space.

1.4 Selective Paracellular Permeability

As stated above, TJ cell-cell connections not only represent barriers against uncontrolled *paracellular* solute uptake, but also show the ability to permit restricted uptake for selected substances. The term ***selective permeability*** is used to describe this mechanism of *discrimination between solutes on the basis of size and charge* (53). A huge variability of barrier [or permeability] properties in different tissues or conditions, ranging from almost complete tightening of the paracellular transportation pathway to forming paracellular pores for specific ions or solutes, was described. (53,54)

Two different components of selective permeability can be distinguished:

1) Pore Pathway:

   This is a pathway with high capacity for solutes less than 4 Å in diameter. Since this pathway serves for the uptake of most of the small electrically charged solutes

(primarily ions), its performance can be measured as the transepithelial electrical resistance (TER). The degree and charge selectivity of this pathway is regulated by ***TJ protein composition***, since ion conductance across epithelial layers can be experimentally manipulated by expressing or removing specific claudins. (34)

2) Leak Pathway:

Solutes larger than 4 Å can also penetrate intact TJs, which is suspected to take place via temporary breaks in the usually continuous TJ complex. This non-pore or leak pathway does not exhibit charge discrimination and does not affect the function of the pore pathway. It seems to be highly sensitive to any form of ***cellular injury*** and ***alterations of the actomyosin cytoskeleton*** linked to the TJ complexes. In particular, it is suspected that contraction of the actomyosin ring exerts mechanical tension to the TJ which results in a dilatation of the TJ gap. (34,51)

Formation and maturation of TJ structure and function takes place along the ***crypt-villus axis*** of the intestinal layer. In healthy individuals, substance permeation at the apical part of the villus is restricted to solutes smaller than 6 Å, allowing passive transport via solvent drag for small molecules (such as monosaccharides). Following the layer to the crypts, the permeation of larger molecules with cross-sectional diameters of even 50 or 60 Å is permitted (55). These *functional alterations* are coupled with *morphological modifications* of TJs along the crypt-villus-axis. For instance, the ***number of strands*** in the TJ area [Figure 6] seems to increase during cell migration from the crypt to the villus (24).

In summary, there seems to be a correlation between the architecture of TJ strand network – including TJ strand counts, the depth and width of the intercellular space in the TJ area - and the permeability or barrier property of different epithelia (54).

1.4.1 Tight Junction Dynamics affects Permeability – the Regulation of Paracellular Permeability

During the past 20 years, observations of altered paracellular solute permeability in different locations and under different circumstances created the idea of highly dynamic and modifiable TJs (39). Nowadays, solute traffic in-between epithelial cells is considered a *selective and dynamic process*, which is permitted in some, but complicated in others; depending on a vast amount of factors affecting permeability. These include humoral or neuronal signals, inflammatory mediators, the composition of chyme in the intestinal

lumen and a variety of cellular pathways that can be exploited by some sort of bacteria (40).

For example, after ingestion of a glucose-rich diet, the transcellular sodium-glucose cotransport is initiated which, in turn, reversibly increases tight junction permeability for small solutes as glucose. Simultaneously, barrier properties for larger molecules are maintained. In other circumstances, paracellular permeability of larger molecules is primarily affected, e.g. after the oral application of different pharmaceuticals. A very important role thereby can be attributed to the ***actomyosin cytoskeleton***: Initiation of the Na^+-glucose cotransport leads to a mechanistic modulation of the actin cytoskeleton which is, as already mentioned, linked to the TJ transmembrane components via scaffolding proteins and therefore, expected to cause the alterations in TJ permeability (56). Many other parameters, including proinflammatory cytokines (e.g. TNF-α or IFN-γ) or noninvasive bacteria, are also thought to alter paracellular permeability via the cytoskeleton-tight junction pathway. (39,57)

1.4.2 Measurement of Paracellular Permeability in vivo

The non-invasive assessment of intestinal permeability in humans can be realized by the oral administration of non-metabolized small probes as test substances whose detection in the urine allows conclusions regarding their intestinal uptake. Intestinal cells normally do not exhibit specific transporters for these solutes so that they cross the epithelial layer mainly via the paracellular pathway and alterations in this system will affect their appearance in the urine.

Indeed, movement in-between cells, especially across the intestinal epithelial layer, is reliant on several factors:

- The differences in concentration of test substances on both sides of the layer
- The total surface area
- The time the substance stays in the intestine
- The intrinsic properties of the barrier (i.e. TJ function)

Furthermore, intestinal epithelia show different permeability properties depending on the solutes' size, charge, shape and solubility, so that selection of the probes should be

considered very carefully. Usually, test substances share some characteristic features: They have cross-sectional ***diameters between 5 and 15 Å***, are ***water-soluble***, ***non-toxic***, ***non-charged***, ***not metabolized*** or ***sequestered*** once they permeated the epithelial layer. Under normal circumstances, they do not penetrate the epithelial layer, and if so, they are quantitatively cleared by the kidney into the urine. Preferably, the probes should not be naturally present in the urine. The most frequently used substances include *polyethylene glycol 400* (PEG 400) with a cross-sectional diameter of 5.3 Å, *mannitol* - a sugar alcohol with a diameter of 6.7 Å -, *lactulose*, a larger sugar with a cross-sectional diameter of 9.5 Å and ^{51}*Cr-EDTA*, a radioactive chromium labeled ethylenediaminetetetraacetic acid (cross-sectional diameter of approximately 11 Å). Furthermore, the disaccharide *sucrose* (1.5 Å, i.e. saccharose) can be used to assess permeability properties of the gastro-duodenal area since it is rapidly degraded by sucrose-isomaltase distal to the duodenal region. In a similar way, the other test substances mentioned (except ^{51}Cr-EDTA) are degraded by the bacterial flora of the large intestine and therefore, represent permeability of the gastric and small intestinal region. (58,59)

1.4.2.1 The Principle of the Differential Urinary Excretion of Ingested Test Substances

Given that the utilization of single test substances led to invalid results – by reason of uncontrollable influence of pre- and post-mucosal factors [Table 4] -, the implementation of combined test probes and the formation of differential urinary excretion ratios became necessary: When a non-hydrolyzed *larger molecule* (e.g. lactulose) and a *smaller one* (e.g. mannitol) are ingested together, possible alterations affect excretion in urine of both substances equally. Therefore, by generating the differential urinary excretion ratio (i.e. lactulose/mannitol) for a defined time (usually 5 hours), most of the problems associated with the use of a single test substance are overcome. Therefore the urinary excretion ratio becomes *a specific index of intestinal permeability* (33).

Premucosal Factors:
Completeness of ingestion
Gastric and intestinal dilution
Gastric emptying
Intestinal transit
Bacterial degradation

Unstirred water layer
Digestion hydrolysis
Postmucosal Factors:
Intestinal blood flow
Metabolism
Tissue distribution
Renal function
Timing and completeness of urinary collection
Bacterial degradation

Table 4. 'Factors affecting the Urinary Excretion of Test Substances' [adapted from (33)]

1.5 The Effects of Liver Disease on the Gastrointestinal System

1.5.1 Portal Hypertension (PH)

There are two peculiarities concerning hepatic blood circulation: First, there is the portal venous system, a formation of blood vessels connecting two systems of capillary beds and carrying blood from most parts of the digestive tract (small and large intestines, pancreas, spleen) to the liver. Therefore, this blood is rich in nutrients, but shows - because of the preceding capillary bed - a reduced perfusion and oxygen partial pressure (pO_2) (60). Secondly, there are additional blood vessels directing arterial blood to the liver, by way of the proper hepatic artery. The mixture of the two systems takes place in the sinusoids of the liver - narrow channels between the densely-packed hepatocytes -, where the exchange of substances takes place. The hepatic veins collect blood from the sinusoids via central veins and, in succession, drain into the inferior vena cava. (9)

However, portal venous pressure depends on both transhepatic blood flow and flow resistance along this route (5). Thus, an increase in vascular resistance, as well as an increase in blood flow through the portal veins affects portal pressure, which in healthy individuals ranges from 1 to 5 mmHg. In the setting of cirrhosis, the development of portal hypertension (PH) nearly always occurs, constituting the main initial factor for a variety of cirrhosis-associated complications. Secondary to *scarring, narrowing and compression of the hepatic sinusoids* (14), the outflow of the blood from the portal system to the hepatic veins is suppressed. To assess the severity of PH, the hepatic venous pressure gradient –

i.e. the difference between the wedged and the free hepatic venous pressure - can be measured. An increase to values above 5 mmHg permits diagnosis of PH; an increase > 10 mmHg is termed clinically significant PH and constitutes a prerequisite for the development of varices and ascites. (60-62)

Besides structural alterations, a functional imbalance between vasoconstrictive and vasodilative components seems to play an additional role in the pathogenesis of PH. Vessel diameter is the result of a complex interaction between *vasodilative agents* such as nitric oxide (NO), glucagon, bile acids, TNF-α or carbon monoxide, and *vasoconstrictors* including endothelin-1 (ET-1) or cyclooxygenase-derived prostaglandins. Among these substances – whose concentrations are altered in patients with cirrhosis -, ***NO*** is considered the most important vasodilator (60). It relaxes vascular smooth muscles and is normally released by endothelial cells depending on the wall shear stress caused by current blood flow (5). In the event of cirrhosis, there is not only a decrease in NO levels, but also a reduction of the activity of endothelial NO-synthetase (eNOS) and a hyporesponsiveness to systemic NO in the sinusoidal area. Moreover, the production and response to vasoconstrictors, mainly ET-1, seem to be increased maintaining and aggravating the increased vascular tone in the vessels of a cirrhotic liver.

In the setting of cirrhosis, ***hepatic, splanchnic and systemic circulation are affected in different ways***. Particularly noticeable are observations of *different availabilities of **NO** in the intrahepatic circulation with preserved production in the presinusoidal area and impaired production in the sinusoidal/postsinusoidal area* (60,63). Due to higher concentrations of NO in the splanchnic & portal venous bed, resistance in this area is reduced which contributes to an increase in blood inflow and the retention of blood in the portal area.

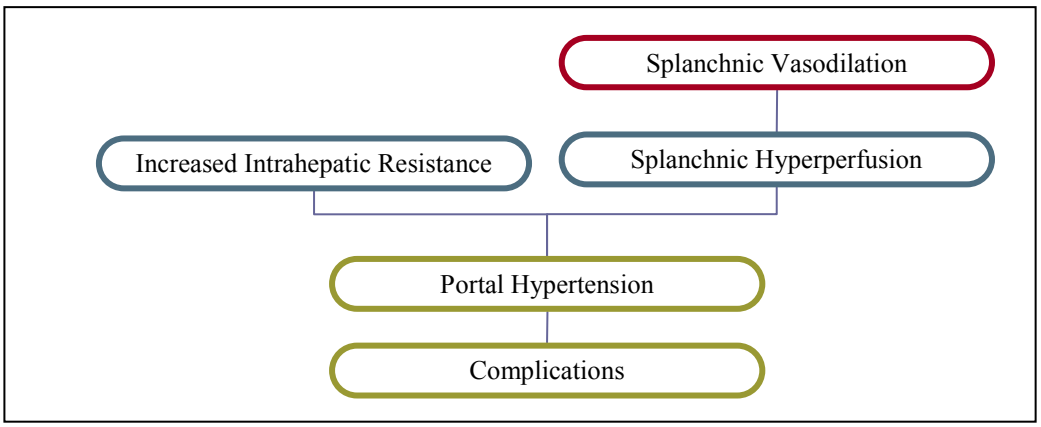

Figure 8. 'Pathogenesis of Portal Hypertension' [adapted from (63)]

However, PH leads to the formation of **collateral circulations** that connect high-pressure portal blood vessels to the low-pressure systemic circulation. Therefore, a large fraction of portal blood bypasses the liver circulating through porto-systemic shunts. As a result, many substances (toxins such as ammonia; hormones such as glucagon and many vasoactive agents) that are normally removed by hepatocytes now find their way to the systemic circulation, playing an important role in the development of hepatic encephalopathy or cardiovascular changes. The formation of collaterals occurs in sites of vascular juncture between the portal and the systemic system, for instance in the gastro-esophageal transition area (which results in the development of esophageal and upper gastric varices) or within the abdominal wall between the umbilical and superficial gastric vein (forming the so-called *caput medusae*). (60) Additionally, the formation of varices places the patient at high risk of portal hypertensive gastrointestinal hemorrhage (60).

1.5.2 Portal Hypertensive Gastropathy and Duodenopathy

An association between chronic liver disease and macroscopic abnormalities of the gastrointestinal epithelium was early assumed after the implementation of upper gastrointestinal endoscopy in the routine evaluation of varices in cirrhotic patients. Today, the lesions frequently observed in patients with PH are summarized as *portal hypertensive gastropathy* (PHG). The diagnosis of PHG is made endoscopically and usually, two different degrees of severity are identified [according to the NIEC (64)]: mild and severe PHG (64,65). Mild PHG is characterized by a 'snake-skin' appearance with 'mosaic-like pattern', consisting of *multiple erythematous areas, rectangular or diamond-shaped, outlined by a delicate white or yellowish network* (64). In patients with severe PHG, characteristic 'red marks' are present: *red lesions of variable diameter, flat or slightly protruding into the lumen of the stomach* (64) that represent stigmata of bleeding and are also described as 'cherry red spots'. Moreover, areas of diffuse hemorrhagic mucosal changes (66) can also be an expression of severe PHG. The mucosal lesions in patients with PH are most pronounced in the fundus and the body of the stomach (64), but similar alterations are observed throughout the whole gastrointestinal tract; consequently named portal hypertensive duodenopathy, intestinopathy, colonopathy or, in general, enteropathy (PHE).

Although the duodenum is accessible via upper gastrointestinal endoscopy, ***portal hypertensive duodenopathy (PHD)*** is by far not as well investigated as its counterpart located in the stomach (67). However, in contrast to the characteristic lesions seen in PHG,

duodenal alterations seem to be non-specific and include erythema, erosions, ulcers, teleangiectasia, duodenal varices, exaggerated villous patterns and mixed lesions. *Barakat et al.* (67) examined the duodenal mucosa of 105 patients with portal hypertension and detected PHD-associated macroscopic lesions in more than half of them. Furthermore, PHD was significantly higher in patients suffering from severe gastropathy and can also be the cause of gastrointestinal bleeding [in 9.5% of patients (67)].

1.5.2.1 Portal Hypertensive Enteropathy on Light Microscopy

By means of light microscopy, *McCormack et al.* (65) observed *dilated submucosal veins* and *vascular ectasia* in gastric mucosa of cirrhotic patients, which was thought to result from congestion due to PH. Similar histological changes were also found in duodenal biopsies and surprisingly not only in patients with macroscopic lesions, demonstrating that a macroscopically intact mucous membrane might already be confronted with the effect of PH or that further mechanisms might be involved in the pathophysiology of PHE (67). Furthermore, *capillary angiogenesis* mainly in the subepithelial area and *increased apoptosis* was described by *Barakat et al.* in 2007, referring to another theory of epithelial damage on the basis of insufficient oxygen supply (67). Other histological features seen in duodenal mucosa of cirrhotics include a *decreased villus to crypt ratio* with a consecutive diminution of the total absorptive surface (68), a *distension of the inter-enterocytic space* (69), *mucosal edema* of the lamina propria, *extravasation*, *fibromuscular proliferation,* and *a thickened muscularis mucosae* (67,68). In studies regarding chronic alcoholics with liver disease, an *increase in goblet cells, inflammation of the lamina propria* and a *loss of epithelium at the tips of the villi* were additionally observed (70). Thereby, direct effects of alcohol on gut mucosa might play an important role. All these changes are thought to lead to an increased susceptibility to injury from gastric and bile acids, non-steroidal anti-inflammatory drugs or alcohol. (66)

1.5.3 Ultrastructural Alterations in Small Intestine Mucosa of Cirrhotic Patients

Studies regarding ultrastructural characteristics of gastrointestinal mucosa (such as TJ structure) in cirrhotics are scarce and have given contradictory results (69-71). In 2002, *Such et al.* (69) analyzed the duodenal epithelium of cirrhotic patients and reported an enlarged intercellular space in the lower part of enterocytes on light microscopy, but observed no alteration in TJ structure on electron microscopy. In contrast, *Bhonchal et al.* described a widened intercellular junction, but, examined duodenal biopsy specimens of

chronic alcoholics with liver disease, who additionally suffer from direct toxic effects of alcohol on gut mucosa (70). Besides, they observed an increased number of rough endoplasmatic reticulum and increased & dilated mitochondria in small intestinal mucosa of chronic alcoholics. In 2007, a Chinese group (71) compared electron-microscopical characteristics of duodenal mucosa in cirrhotics with healthy controls and described a ***widening of the gaps of TJs***. Furthermore, they observed alterations regarding enterocytes' nuclei (karyopyknosis and karyorrhexis) and mitochondria (tumefactions). Distorted and shortened microvilli were found in all 3 studies.

1.5.4 Bacterial Translocation (BT)

Patients suffering from chronic liver disease have increased susceptibility to severe infections that occur mostly without any apparent focus of infection (72) and deteriorate the prognosis of patients significantly (73,74). It has been shown that bacteremia – the presence of bacteria in the blood - is 6 times more prevalent in patients with cirrhosis than in a non-cirrhotic control group (75) and among cirrhotics who acquire bacterial infections, mortality is increased about four-fold (76). One of the most dreaded infectious complications in chronic liver disease is spontaneous bacterial peritonitis (SBP), which is – in most cases – caused by bacteria that are normally present in the gut, such as Enterococcus faecalis, Escherichia coli or Klebsiella pneumonia (17). Furthermore, the risk of infection and especially of SBP caused by these microorganisms is substantially reduced after intestinal decontamination with antibiotics (77). These findings emphasize a gut origin of bacterial infections and led to the formation of the hypothesis of ***bacterial translocation (BT)***: intact intestinal bacteria, as well as bacterial wall constituents reach the mesenteric lymph nodes (MLN) through the epithelial mucosa and move from there to the systemic circulation (2). In order to assess the prevalence of this phenomenon in the setting of chronic liver disease, *Cirera et al.* examined MLNs of cirrhotics undergoing laparotomy either for liver transplantation or hepatic resection because of liver cancer (77). Enteric microorganisms were grown in MLNs in about 10% of all patients, with a higher incidence in Child's C (30.8%) than in Child's A (3.4%) cirrhosis. In an animal study, *Llovet et al.* (78) have shown that bacterial strains isolated from MLNs are genetically identical to strains causing SBP in cirrhotic rats. Therefore, the translocation of bacteria to the MLN and the consecutive systemic distribution was suggested one of the main steps leading to bacterial infection, especially SBP, in cirrhotic patients (77).

The function of the intestinal barrier and therefore, the prevention of BT, depends on three important factors: the normal intestinal flora (microbiome, i.e. the ecologic barrier), the enterocytes & their cohesion via intercellular junctions (the mechanical barrier) and immune cells responsible for the secretion of IgA or phagocytosis of microorganisms (immune barrier) (2). However, a clear etiopathogenetic mechanism underlying the development of BT is still the subject of intense research. Currently, there are several factors suspected of playing an important role in the pathogenesis of bacterial infections in cirrhosis:

1.5.4.1 Increased intestinal permeability

Intestinal permeability has been shown to increase in patients with cirrhosis, especially in patients with *alcoholic background* (79), *ascites* (73,80) or *severe septic complications* (17). In general, cirrhotics show significantly higher permeability values compared with healthy controls, as assessed *in vivo* either by the ^{51}Cr-EDTA permeability test (81) or the lactulose/mannitol test (16,82) [see 1.4.2]. In addition, the severity of intestinal permeability dysfunction seems to be associated with the stage of cirrhosis classified according to the Child-Pugh score (16,80-82). Since the gut seems to be 'leaky' also in patients with PH without hepatic dysfunction (83), and cirrhotics with ascites tend to have a more marked dysfunction of intestinal barrier than patients without ascites (80), there is some evidence that the congestive process and its concomitant effects facilitate the increase of intestinal permeability. This is also reflected in the improvement of disturbed intestinal permeability after treatment with transjugular intrahepatic portosystemic shunt (TIPS) in patients with portal hypertension (84).

Trying to reveal the underlying molecular mechanisms, scientists early stumbled over the abovementioned ***nitric oxide (NO)*** (79,85): Nitric oxide, an important cellular signaling molecule and powerful vasodilator agent, contains a single unpaired electron that implies high chemical reactivity and explains the short lifetime of NO (86). Indeed, its synthesis in the intestines has shown to be increased in patients with chronic liver disease and to play not only a key role in the onset of PH (82), but also in the generation of reactive nitrogen & oxygen species (RNS/ROS, e.g. peroxynitrite). The gastrointestinal tract has been shown to be susceptible to the effects of ROS & RNS, and enterocytes function hereby seems to be modified, including alterations in intestinal permeability. A modulation of the mucosal cytoskeleton (that is linked to the junctional complex) is suspected to be one of the

underlying pathophysiological mechanisms by which NO influences barrier function. (69,87)

Moreover, toxic effects of ethanol and its metabolites (like acetaldehyde) are suspected to affect intracellular signal-transduction pathways leading to an increase in paracellular permeability for macromolecules (82). In 2000, *Banan et al.* showed that ethanol exposure to Caco-2 monolayers also increases expression of NO synthetase and the subsequent production of NO. These findings were associated with a disruption of the microtubule cytoskeleton and an increased intestinal permeability, emphasizing the strong connection between NO, cytoskeleton and intestinal barrier function (87). However, alterations in permeability caused by alcohol consumption seem to be transient and return to normal at least two weeks after the cessation of drinking (79).

1.5.4.2 Impaired Defense Mechanisms

BT might be a physiologic phenomenon that occurs also in healthy individuals, without severe consequences, as long as the integrity of the body's defense mechanisms is preserved. However, all components of the immune system, including *mucosal* (secretory immunoglobulins), *cell-mediated* (macrophages, T-cells etc.) and *humoral immunity* (plasma immunoglobulins) seem to be involved in the prevention of bacterial translocation (88). In the setting of cirrhosis, several defense mechanisms have been shown to be impaired, including humoral and cellular components: A decreased phagocytic activity of reticuloendothelial cells – most of the RES activity is located in the liver - has been shown, as well as a reduced opsonic activity of serum and ascitic fluid due to low hepatic synthesis of complement factors; this is especially seen in patients with SBP (72). Recently, it has been demonstrated that neutrophil dysfunction (increased resting oxidative burst and decreased phagocytotic and killing capacity) in patients with decompensated cirrhosis is associated with increased susceptibility to infection and other complications (18,89).

Epithelial goblet cells secrete mucus containing immunoglobulin A (IgA) which, on the one hand, neutralizes toxins and other microbial products and, on the other hand, binds to bacteria, thereby preventing their adhesion and multiplication in the intestinal lumen (74). In the setting of advanced cirrhosis, reduced secretion of IgA contributes to the increased adhesion of bacteria on the intestinal surface and the consecutive increased susceptibility for infectious complications (2).

In addition, PH decreases bacterial clearance by the hepatic reticulo-endothelial system via the formation of porto-systemic shunts (17), which facilitates the systemic distribution of gut-derived bacteria.

1.5.4.3 Altered small Bowel Motility and Bacterial overgrowth

Furthermore, other intestinal features are observed to change in patients with cirrhosis: Altered small bowel motility leading to a delayed intestinal transit time has been shown in these patients depending on the degree of liver dysfunction (72,73). *Thalheimer et al.* evaluated oro-caecal transit time via lactulose breath test in seven cirrhotics compared with healthy controls and detected a delayed intestinal transit time in six of them (73). The underlying decrease in intestinal motility facilitates the overgrowth of bacteria in the gut lumen, which is very frequent in patients with chronic liver disease (one-third of patients with cirrhosis secondary to alcohol (72,90)) and related to the severity of liver disease (91). In fact, small intestinal bacterial overgrowth (SIBO) is not only characterized by an increased number of bacteria in the small bowel – most experts consider diagnosis of SIBO with the finding of $\geq 10^5$ colony-forming units per milliliter of proximal jejunal aspiration -, but also by an abnormal type of bacteria (74). Overgrowth of aerobic Gram-negative bacteria has been closely associated with the development of BT and bacterial infections in cirrhotics, emphasized by the finding that reduction of Gram-negative intestinal bacilli with oral antibiotics substantially decreases the incidence of SBP in patients with cirrhosis (92).

The underlying processes of delayed intestinal motility are still the subject of intense discussion, but are suspected to be associated with various mechanisms such as stimulation of sympathetic neurons, increased synthesis of NO and intestinal oxidative damage (92). Beta-adrenergic blockade with propranolol (that is also used in the prophylaxis of variceal hemorrhage) has been observed to accelerate intestinal transit and decrease SIBO & BT in rats with advanced cirrhosis (93).

1.5.5 Beyond Bacterial Translocation

The integrity of the intestinal epithelial barrier not only plays an important role in the prevention of bacteria to translocate, but also - more general -, in the absorption of a huge variety of substances. Therefore, it seems appropriate to enlarge the extent of possible effects caused by impaired intestinal function beyond overt infection. The mechanisms underlying BT seem to be involved in the maintenance and the progress of liver disease,

emphasized by the finding that even patients without cirrhosis (but proven liver disease) exhibit altered intestinal function, especially increased intestinal permeability (82). Moreover, epidemiologic studies have revealed that only 30% of chronic alcoholics develop cirrhotic remodeling of the liver (85), suggesting that one or more additional factors are required for chronic liver injury to occur. Bacterial wall constituents like **endotoxins (a lipopolysaccharide, LPS)** are suspected of being such factors and have been detected in the blood from portal veins of chronic alcoholics with cirrhosis (94). They are believed to transpose the intestinal epithelial barrier and accumulate in the liver, where they can cause an activation of Kupffer cells that, in turn, results in an increased production of pro-inflammatory cytokines including TNF-α and, again, NO-derived substances & ROS/RNS (72,95). Both cytokines and reactive oxygen (or nitrogen) species have been shown to feed inflammation and fibrosis of the liver (82) and therefore, maintain the progression of liver disease.

However, the definition of BT was extended to include the permeation of bacterial products such as endotoxins, bacterial DNA or antigens (***non-viable bacterial translocation***) (92). Besides 'promotion' of liver damage, in the setting of both porto-systemic shunting and impaired clearance by the liver, these substances are also delivered to the systemic circulation (endotoxemia). The capability of endotoxins and other bacterial products to initiate the cytokine cascade – including the release of pro-inflammatory cytokines and the production of NO – leads to a consequent **pre-activation status of the immune system** in these patients, even in the absence of evident bacterial infection (96). Therefore, an immunological response similar to that produced by viable microorganisms can be promoted (74). *Francés et al.* have proven that cirrhotics with bacterial DNA in both serum and ascitic fluid show a more pronounced production of basal cytokines (without stimulation) by monocytes and macrophages compared to patients without detectable bacterial DNA (97).

In fact, viable and non-viable BT not only influences down-streamed organs, but also *the intestine itself*. The loss of integrity of gut barrier function results in the contact of microorganisms and toxic products with immune cells and thus, contributes to an intestinal inflammatory response that exerts immediate effects in the mucosal wall such as the overstimulation of macrophages & other immune cells, and their production of inflammatory cytokines & NO (2).

In summary, cirrhosis behaves like a chronic inflammatory disease in which the immune system is permanently stimulated by bacteria and bacterial products of intestinal origin (74). Bacteria themselves might not need to transpose the epithelial intestinal barrier, since translocation of toxic products from the gut and the release of pro-inflammatory substances might be responsible for both the progression of liver disease and the onset of complications in patients with cirrhosis (2).

1.6 Hypothesis and aims

Although the presence of several morphological abnormalities on light microscopy of small intestinal mucosa in cirrhotic patients is already well documented, the relevance of these changes in the pathogenesis of BT is still the subject of intense discussion. With regard to electron microscopy, former studies are scarce and have shown several, sometimes inconsistent, alterations [see 1.5.3]. Therefore, the aim of this study was to assess correlations between morphological changes in duodenal mucosa of cirrhotics (by means of light and electron microscopy) and functional alterations (by means of an orally administered permeability test and the detection of bacterial & fungal DNA in the plasma of patients). Since TJs are the rate-limiting barrier of the paracellular pathway, and the gut barrier has been shown to be more permeable to substances using this pathway in cirrhosis, we focused on the structure of TJs and expected to find structural correlates for functional changes. In fact, it has been shown that NO is able to dilate TJs in cultured epithelial cells (98), and NO levels are increased in the splanchnic area of patients with cirrhosis (82).

We hypothesize that increased intestinal permeability is caused by ultrastructural changes of TJs, particularly an increase in TJ-gap width which can be evaluated by transmission electron microscopy. Furthermore, we expect the pathophysiological process to occur via a contraction of the perijunctional actomyosin ring, which is reflected by a rise in electron-density of the perijunctional actomyosin complex (PAC). An increase in gastrointestinal permeability leads to higher excretion rates of sucrose and a higher ratio of lactulose/mannitol compared to healthy individuals. The final stage of BT – bacterial constituents present in the systemic circulation – can be detected by the measurement of bacterial DNA in plasma of the cirrhotic patients.

1.6.1 Specific aims

- To investigate morphological alterations of small intestinal mucosa (especially of TJs) in patients with cirrhosis via light and electron microscopy
- To correlate morphological changes
  - with the severity of liver disease according to the Child-Pugh score
  - with alterations in gastro-intestinal permeability, assessed by the sucrose/lactulose/mannitol test
  - with the appearance of bacterial products in the blood of patients, using a molecular test for bacterial and fungal DNA

2 Material and Methods

2.1 Overview

Consecutive patients with cirrhosis referred to the Medical University of Graz, undergoing upper gastrointestinal (GI) endoscopy as part of their routine work-up, were enrolled. After signing informed consent, patients were investigated in a two-day trial: On the first day, blood collection (for detection of bacterial/fungal DNA) and upper gastrointestinal endoscopy (to obtain three biopsy specimens from the ***distal duodenum***) was performed. On the second day, an orally administered permeability test (sucrose/lactulose/mannitol test) took place. In addition, blood collection, endoscopy and permeability test were performed in age-matched healthy controls (who underwent esophagogastroduodenoscopy for clarification of upper abdominal symptoms, but without pathologic findings in the duodenum) to compare the results. Control patients were recruited at the Department of Internal Medicine (Medical University of Graz).

An overview of the study design for the patient group is given by Figure 9; similarly, also the control patients were examined.

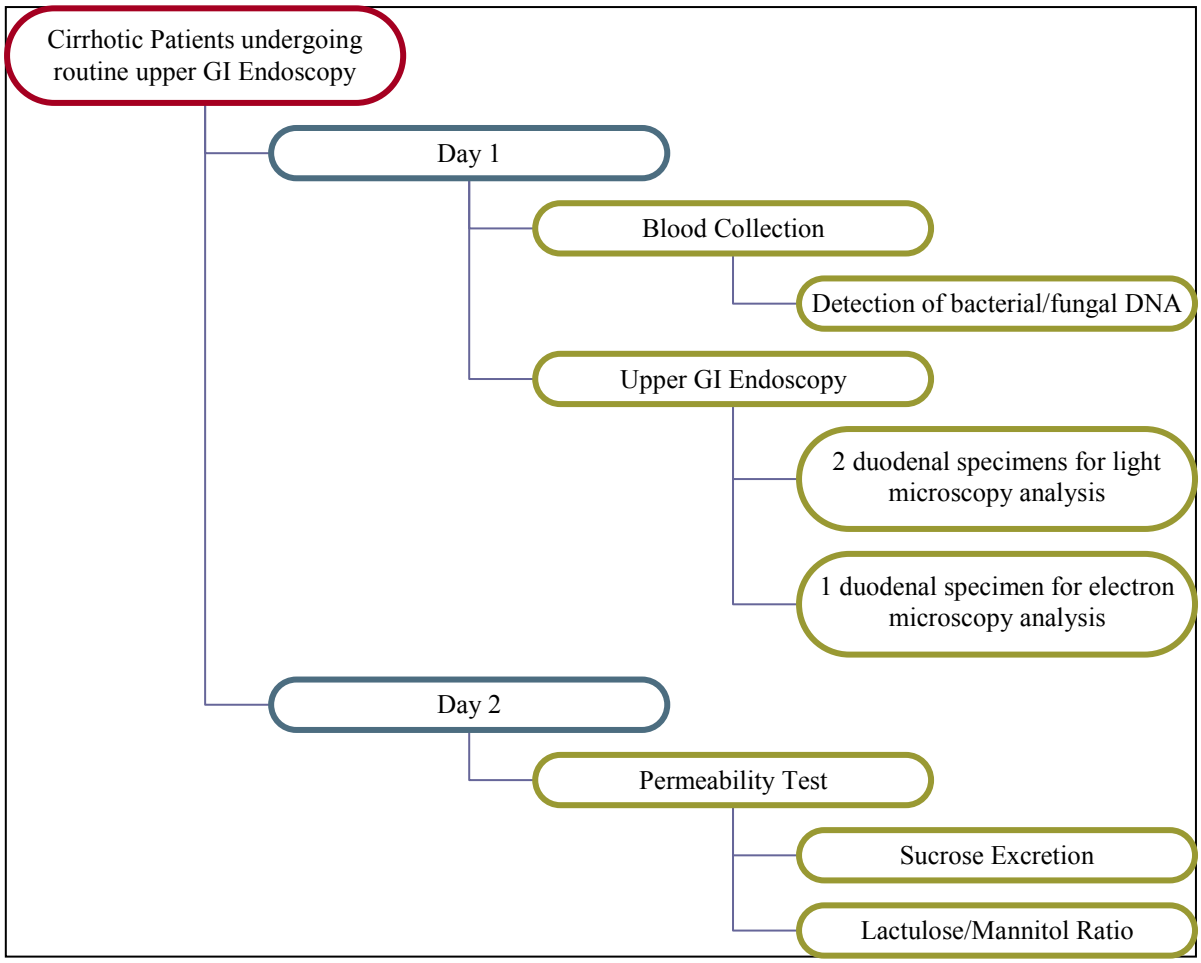

Figure 9. 'Study Workflow' for cirrhotics

2.2 Patient Selection

Consecutive patients with cirrhosis were enrolled, including inpatients (medical ward) and outpatients (liver clinic). Diagnosis of cirrhosis was confirmed either by liver biopsy or typical clinical findings such as portal hypertension (esophageal varices, spider naevi, hepatic ascites, palmar erythema, splenomegaly, hepatic encephalopathy and/or reduced platelets), reduced hepatic synthetic function (impaired coagulation, low albumin) and typical findings in ultrasound examination (increased echogenicity, irregular appearing areas). The severity of liver dysfunction was evaluated by calculating the Child-Pugh score [see 1.1.3] according to clinical and laboratory parameters obtained on the day of upper gastrointestinal endoscopy and blood collection (day 1). To compare differences in-between the cirrhosis group, patients were classified as *early-stage (Child's A)* and *advanced (Child's B and C)* cirrhotics.

Routine laboratory procedure included measurement of hemoglobin, MCV, differential blood count, coagulation (INR PT, aPTT, fibrinogen), renal function parameters

(creatinine, blood urea nitrogen, uric acid), electrolytes (Na, K), LDH, liver function parameters (AST, ALT, CHE, AP, GGT, bilirubin), total protein, albumin, cholesterol, alpha-fetoprotein (AFP), triglycerides, blood sugar levels, and CRP.

The presence and severity of ascites were assessed by using abdominal ultrasound. Depending on its degree, it was graded into no (no evidence of ascites), mild (only detectable by ultrasound) and massive (massive volume of ascites detected by distension of abdomen) ascites.

Hepatic encephalopathy was graded on a scale from 0 to IV depending on the level of consciousness, intellectual function and neurological abnormalities [Table 5].

Grade	Level of Consciousness	Intellectual Function	Neurological Abnormalities
0	normal	normal	normal
I	lack of awareness change in personality day/night reversal	short attention span easy forgetfulness	slight tremor asterixis
II	lethargy unsuitable behavior	loss of orientation	asterixis abnormal reflexes
III	asleep but arousable confused	loss of interpersonal communication	abnormal reflexes
IV	unarousable	absent	Babinski/clonus decerebrate

Table 5. 'Grading of Hepatic Encephalopathy' [from (99)]

The following inclusion and exclusion criteria were defined for the patient group:

2.2.1 Inclusion Criteria

- Adult patient with age > 18 years
- Cirrhosis of any etiology and severity (Child's A, B & C)
- Assignment for upper gastrointestinal endoscopy
- Informed consent

2.2.2 Exclusion Criteria

- Recent alcohol abuse within the last 2 weeks before examination
- Patients with a low platelet count (< 50,000/µl) or a prothrombin time (PT) < 50%

- Patients with low serum fibrinogen (< 210 mg/dl)
- Patients who received medication with impact on gastric permeability or gastric motility within the last 2 weeks before examination (e.g. NSAIDs, anticholinergics, metoclopramide, loperamide), except non-selective beta-blockers for prophylaxis of variceal bleeding
- Patients who received medication that affects gastrointestinal bacteria within the last 2 weeks (e.g. antibiotics, probiotics), except for SBP prophylaxis
- Patients with known gastrointestinal (e.g. Crohn's disease) or renal disease (creatinine > 1.5 mg/dl)
- Patients with acute or chronic infection within the last 2 weeks
- Patients with high-grade hepatic encephalopathy (grades II – IV)
- Patients with hepatorenal syndrome
- Patients suffering from therapy-resistant ascites
- Recent esophageal hemorrhage (within the last 6 weeks)
- Patients suffering from hepatocellular (HCC) or cholangiocellular carcinoma (CCC)
- Pregnancy

Since ethanol and its metabolites exert toxic effects on intestinal epithelia, patients with recent alcohol abuse within the last two weeks before examination were excluded (gut mucosa is said to regenerate within two weeks) (33,79). Furthermore, all cirrhotics taking medication with possible impact on gastrointestinal motility (anticholinergics, metoclopramide etc.), permeability (NSAIDs etc.) or bacterial growth (antibiotics, probiotics etc.) except for non-selective β-blockers (e.g. propranolol for treatment of portal venous pressure) were excluded. Since patients with liver disease regularly suffer from bleeding tendency and additional duodenal biopsy specimens was collected during upper GI endoscopy, patients had to present with a platelet count > 50,000/µl and a prothrombin time > 50%. The presence of renal or gastrointestinal diseases like Crohn's or hepatorenal syndrome could distort the results of the permeability test and therefore, was considered an exclusion criterion.

2.3 Control Group

Age-matched control patients were recruited at the Department of Internal Medicine (Medical University of Graz) and routinely underwent upper gastrointestinal endoscopy in

the work-up of unspecific epigastric complaints or as a follow-up examination after the treatment of gastritis. In general, control patients were selected according to similar exclusion criteria as cirrhotics have been, but, did not suffer from any liver disease or any other condition possibly leading to portal hypertension When upper GI endoscopy was negative for ulcerations or erosions (i.e. intact mucosa), biopsy specimens were obtained from ***distal duodenum*** and examined using light and electron microscopy. After that, control patients were invited to participate in the permeability test (day 2).

2.4 Upper Gastrointestinal Endoscopy

Upper gastrointestinal endoscopy was performed by experienced investigators at the Endoscopic Unit of the Department of Internal Medicine (Medical University of Graz). Additionally to the biopsy specimens collected in the course of their underlying disease – i.e. gastric biopsies for checking *Helicobacter pylori* status or gastritis; duodenal biopsies for clarification of celiac disease, mostly in control patients -, three specimens were obtained from ***distal duodenum*** using standard biopsy forceps. The first specimen was fixed in glutaraldehyde for subsequent electron-microscopic analysis; two other specimens were fixed in formalin for further staining and light-microscopic examination.

According to the Baveno I consensus conference, esophageal varices were classified into two grades – small and large – either by semiquantitative morphological description or by quantitative measurement of variceal size with a suggested cut-off diameter of 5 mm (100). Presence of gastric varices, portal hypertensive gastro- and/or duodenopathy was recorded whenever appropriate.

2.5 Permeability Test

Intestinal permeability was assessed *non-invasive*ly in the participants by measuring the urinary excretion of orally administered test substances on the second day of examination [see 1.4.2]. We decided to utilize the sucrose/lactulose/mannitol test for the evaluation of both the small intestinal (i.e. the lactulose/mannitol ratio) and the gastric (i.e. the sucrose excretion) permeability values. The sucrose/lactulose/mannitol test was similarly performed by *Wyatt et al*. to assess permeability alterations in patients with Crohn's disease (101). Furthermore, this test was already applied and established in a previous trial conducted at the liver unit of the Medical University of Graz.

Following the *principle of differential urinary excretion of test substances* [see 1.4.2.1], *mannitol* – a sugar alcohol with a diameter of 6.7 Å - was administered together with *lactulose* - a larger disaccharide (cross-sectional diameter of 9.5 Å) - and the urinary lactulose/mannitol excretion ratio was generated to overcome the uncontrollable influence of pre- and post-mucosal factors. On the one hand, there is mannitol, a monosaccharide not metabolized *in vivo,* whose urinary excretion after intravenous administration is reported to lie between 67 and 100% (33). Even though the human body produces small endogenous amounts of mannitol, its quantity is too low to crucially distort urinary excretion values if at least 1 g of mannitol is ingested (33). On the other hand, there is lactulose, an artificial disaccharide consisting of fructose and galactose that is, in healthy individuals, not digested or absorbed in the intestine. Both mannitol and lactulose are degraded by the bacterial flora of the large intestine when the test solution enters the caecum and thus, the lact/man ratio can be regarded as permeability estimators of the gastric and small intestinal region (58,59).

Furthermore, the disaccharide *sucrose* (1.5 Å, consisting of glucose and fructose, also known as saccharose) was administered to assess permeability properties of the gastroduodenal area, since sucrose is rapidly degraded by sucrose-isomaltase distal to the duodenal region. The additional administration of sucrose has been reported to exert no effect on the measurement of intestinal permeability with lactulose and mannitol.

Patients were fasted overnight. Apart from the collection of a sample of the sucrose/lactulose/mannitol solution (1 ml) for subsequent analysis of its concentrations, a sample of urine (1 ml) was collected prior to the ingestion of the test solution. The patient was asked to drink a solution of 100 ml water containing ***20 g sucrose, 10 g lactulose and 5 g mannitol***. Urine was then collected over 5 hours while fasting was continued for 4 hours after study start. The urine volume collected at 5 hours was measured and 1-ml aliquots were frozen immediately at -80°C without preservative for subsequent analysis by high performance liquid chromatography. Excretion values were presented as a *percentage of totally ingested amounts*. Intestinal permeability was estimated from the lactulose/mannitol ratio in the 5-hr urine sample (percentage of lactulose excreted in the urine (%L) to percentage of mannitol excreted in the urine (%M)), gastric permeability from the urinary sucrose excretion ratio in the 5-hr urine sample (%S).

Normal values are depicted in Table 6.

		Normal Value
%L	percentage of lactulose excreted in the urine to total ingested lactulose	≤ 0.440
%M	percentage of mannitol excreted in the urine to total ingested mannitol	≤ 27.80
%S	percentage of sucrose excreted in the urine to total ingested sucrose	≤ 0.230
%L/%M	lactulose/mannitol ratio (percentage of excreted lactulose to percentage of excreted mannitol)	≤ 0.0300

Table 6. 'Normal Values of Lactulose-, Mannitol- and Sucrose-Excretion'

2.6 Light Microscopy

For light microscopy, three-µm thick sections were prepared from formalin-fixed and paraffin-embedded biopsy specimens and stained with hematoxilin-eosin. For electron microscopy, semi-thin sections were stained with toluidine blue. Immunohistochemistry with antibodies against activated caspase-3 was used to detect apoptotic cells.

All slides were analyzed according to the criteria summarized in Table 7.

Villus/crypt ratio (H&E stain)	Score 0: ≥3:1 Score 1: <3:1
Total villi count (H&E stain)	(absolute number)
IEL/100 epithelial cells (H&E stain)	intraepithelial lymphocytes per 100 enterocytes (in high-power fields)
Goblet cells/100 epithelial cells (toluidine stain)	(in high-power fields)
Distended intercellular space between enterocytes *(Number of villi with distended intercellular space)* (H&E stain)	(at the tips of the villi) Score 0: absent (<1/3 of all villi in the slide) Score 1: moderate (1/3 to <2/3 of villi) Score 2: severe (≥2/3 of villi)
Vacuolization of the cytoplasm *(Number of villi with vacuolated enterocytes)* (H&E stain)	(at the tips of the villi): Score 0: absent (<1/3 of all villi in the slide) Score 1: moderate (1/3 to <2/3 of villi) Score 2: severe (≥2/3 of villi)
Dilatation of Gruenhagen's space (number of villi with a dilatation of the subepithelial space) (H&E stain)	(in relation to total number of villi)

Denudation of Villi (H&E stain)	(in relation to total number of villi)
Apoptotic Ratio (caspase-3 antibody staining)	Standardized number of apoptotic cells (in relation to mean villi count)
Number of areas with barely stainable ('pale') cells (toluidine stain)	(in relation to number of villi)
Edema of the lamina propria (H&E stain)	Score 0: absent Score 1: present
Inflammation of the lamina propria (H&E stain)	Score 0: leucocytes absent Score 1: leucocytes present
Fibrosis of the lamina propria (toluidine stain)	Score 0: absent Score 1: present
Extravasation (toluidine stain)	Score 0: absent Score 1: present
Capillary Congestion & Dilatation (toluidine stain)	capillary profiles (sections of vessels) in 3 villi & mean diameter of 3 capillaries in those villi

Table 7. 'Scoring Criteria for Light Microscopy'

2.7 Electron Microscopy

Following fixation in 2.0% glutaraldehyde in 0.1M phosphate (pH 7.2) buffer, specimens were post-fixed in 1.0% osmium tetroxide, dehydrated in ethanol, and embedded in resin for sectioning. Two ultrathin sections (70–80 nm) were placed, one section per grid, on 200 mesh copper grids. These were contrast-stained with lead citrate and uranyl acetate for examination via transmission electron microscopy (TEM).

Electron micrographs of patient and control group were analyzed for differences in ultrastructural characteristics, with special emphasis on TJ morphology. At least 15 ***TJ complexes*** were identified in every section and photographed with a magnification of 28,500. Only TJs located along the side or at the tips of the villi were evaluated (since TJs situated in the crypts seem to be less tight [see 1.4]). For subsequent stratification, it was listed if TJs were located in healthy areas (1), in epithelial areas with perishing cells (2) or a distended intercellular space in the basal parts of enterocytes (3). The width of TJ-gaps was measured using ImageJ, a public domain image-processing program. Furthermore, the ***density of the PAC*** in relation to the density of the microvilli (to eliminate picture-related differences caused by slide thickness, printer properties etc.) was measured.

Besides, ***height and width of enterocytes' microvilli*** were measured and compared between cirrhotics and non-cirrhotics. Other observations included ***number & size of mitochondria***, alterations in ***nuclei*** and the presence of ***apoptotic and/or necrotic features***.

2.8 Detection of bacterial/fungal DNAs by Molecular Testing

Immediately after blood sampling for routine labor on the first day of examination, 1x6 ml blood was additionally collected in EDTA tubes from the same access and kept frozen at -20° C until assay.

The LightCycler^{R} Septi*Fast* Test M^{GRADE} was designed to detect microorganisms that cause approximately 90% of all blood stream infections. While microbiological methods detect viable microorganisms, this test detects viable and non-viable microorganisms and free microbial DNA as well. The target species are listed in the Septi*Fast* Master List (Table 8).

Gram (-)	Gram (+)	Fungi
Escherichia coli	Staphylococcus aureus	Candida albicans
Klebsiella (pneumoniae/oxytoca)	Coag.-neg. Staphylococci	Candida tropicalis
Serratia marcescens	Streptococcus pneumoniae	Candida parapsilosis
Enterobacter (cloacae/aerogenes)	Streptococcus spp.	Candida glabrata
Proteus mirabilis	Enterococcus faecium	Candida krusei
Pseudomonas aeruginosa	Enterococcus feacalis	Aspergillus fumigatus
Acinetobacter baumannii		
Stenotrophomonas maltophilia		

Table 8. 'Species detected by the LightCycler^{R}Septi*Fast*TestM^{Grade},

These species were detected as positives using the LightCycler^{R} Septi*Fast* Test M^{GRADE} during internal studies and/or clinical trials. Some of these species are those which are most frequently treated inadequately: *Enterococcus app.; E. coli; Candida spp..; Klebsiella spp.*. More than one species in one specimen may be detected; thus, the real-time PCR-result is an additional tool to facilitate an early clinical judgment.

The LightCycler^{R} Septi*Fast* Test M^{GRADE} is based on 3 major processes:

- Specimen preparation with mechanical lysis and purification of DNA

- Real-time PCR amplification of target DNA in 3 parallel reactions (Gram positive bacteria, Gram negative bacteria, Fungi) and detection by specific hybridization probes

- Automated identification of species and controls

The feasibility of the Septi*Fast* test has already been confirmed in pilot experiments in 15 patients with acute-on-chronic liver failure (ACLF) or sepsis performed by assistants of the Molecular Diagnostics Laboratory, Institute of Hygiene, Microbiology and Environmental Medicine in Graz.

2.9 Ethical Considerations

An application for this study has been filed at the Ethics Committee of the Medical University of Graz. Informed consent was obtained in accordance with the declaration of Helsinki for all participants fulfilling inclusion criteria. All study-related blood sampling was performed within routine blood collections. The risk of administering small amounts of sugars in the course of the sucrose/lactulose/mannitol test was negligible. Furthermore, the risk associated with the collection of gastric and duodenal mucosal specimens (3 additional biopsy samples) was diminished by the surveillance of coagulation parameters prior to endoscopic examination.

2.10 Statistics

Data collection was performed with Microsoft Office Excel 2003; further data analysis with statistical tools was conducted using SPSS 20. Quantitative variables are presented as means, standard deviation (SD), median, maximum, minimum and range. Normal distribution was tested by using the Kolmogorov-Smirnov test. Mean and standard deviation are used for normal distributed variables, whereas the median is used for non-normal distributed variables. Qualitative variables are presented as absolute and relative frequencies. Differences in-between two groups were assessed using the student's t-test for independent samples if variables were normally distributed and if variances of the two populations were assumed to be equal. The equality of variances in different samples was assessed by using the Levene's test; if the result revealed inequality of variances, Welch's t-test was applied. Furthermore, Mann-Whitney U test was performed if variables were not normally distributed or if number of cases was less than 10.

To estimate possible correlations between two values, Pearson's product-moment coefficient was used if variables were parametric; if not, Spearman's rank correlation coefficient was calculated. Furthermore, to compare the counts of categorical responses between two independent groups, the Chi-Square test was performed; if cells have expected count less than 5, Fisher's exact test was used.

The significance level was set at 5%.

3 Results

3.1 Study Cohort

Between March 2011 and November 2012, 15 consecutive cirrhotics admitted to the liver clinic of the Medical University of Graz and 13 healthy controls were included. Three patients with liver disease had to be ruled out, either because of recent alcohol abuse (one patient) or non-compliance (two patients); similarly, three control patients were excluded after pathological upper GI endoscopy (one patient had duodenal erosions) or light microscopy (one patient presented with celiac disease, the other one with acute duodenitis). In summary, *12 cirrhotic patients* and *10 healthy controls* were included in the study.

3.1.1 Cirrhotic Patients

The clinical parameters of the study cohort are summarized in Table 9.

	Variable	Count	Column N %
gender	male	9	75
(n = 12)	female	3	25
etiology	ASH	9	75
(n = 12)	cryptogenic	2	17
	AIH	1	8
Child-Pugh class	Child's A	7	59
(n = 12)	Child's B	4	33
	Child's C	1	8
ascites	no ascites	6	50
(n = 12)	mild	3	25
	massive	3	25

hepatic encephalopathy	no HE	11	92
(n = 12)	grade I	1	8
	grade II	0	0
	grade III	0	0
	grade IV	0	0

Table 9. 'Clinical Parameters of Cirrhotics'

In further clinical examination, nevus araneus (7 patients; 58%), caput medusae (3 patients; 25%), jaundice & palmar erythema (2 patients each; 17%), and glossitis & facial erythema (1 patient each; 8%) were also detected.

Table 10 gives an overview of import characteristics and laboratory values of cirrhotics:

Variable	Valid N	Mean	Standard Deviation	Median	Maximum	Minimum	Range
age (years)	12	56	11	59	69	26	43
height (m)	12	1.74	.09	1.76	1.85	1.58	.27
weight (kg)	12	78	7	79	86	65	21
BMI (kg/m²)	12	25.9	3.0	24.9	32.8	22.9	9.9
Child-Pugh Score	12	7	2	6	13	5	8
Hb (g/dl)	12	12.6	2.4	13.2	15.4	7.9	7.5
MCV (fl)	12	92	10	92	116	76	40
leucocytes (G/l)	12	5.4	1.5	5	9.2	3.5	5.7
neutrophil granul. (%)	12	62	10	65	73	43	30
thrombocytes (G/l)	12	131	55	119	246	39	207
PT (%)	12	65	23	63	105	30	75
INR	12	1.39	.37	1.30	2.30	.98	1.32
aPTT (sec)	12	38.0	6.7	38.2	49.5	26.5	23
fibrinogen (mg/dl)	12	255	65	273	328	113	215
Na+ (mmol/l)	12	137	6	139	142	124	18
K+ (mmol/l)	12	4.3	.5	4.2	5.1	3.6	1.5
creatinine (mg/dl)	12	.91	.18	0.92	1.18	.59	.59
BUN (mg/dl)	12	30	9	28	46	19	27

uric acid (mg/dl)	12	6.3	1.3	6.2	9.3	4.6	4.7
LDH (U/l)	12	221	90	188	460	115	345
AST (U/l)	12	52	26	47	122	26	96
ALT (U/l)	12	29	7.3	28	42	18	24
GGT (U/l)	12	221	382	67	1331	25	1306
AP (U/l)	12	106	54	82	224	63	161
CHE (U/l)	12	4678	2450	4721	8075	1556	6519
total bilirubin (mg/dl)	12	2.25	2.82	1.27	10.78	.31	10.47
Total serum protein (g/dl)	12	7.8	.5	7.8	8.5	6.6	1.9
albumin (g/dl)	12	3.9	.5	4.0	4.7	2.7	2.0
cholesterol (mg/dl)	12	165	51	158	283	104	179
triglycerides (mg/dl)	12	104	70	70	227	37	190
glucose (mg/dl)	12	103	18	103	145	70	75
CRP (mg/l)	12	5.1	4.9	3.2	14.8	.9	13.9

Table 10. 'Characteristics of Cirrhotic Patients'

Six patients were recruited at the medical ward (inpatients; 50%) and the examinations were performed in the course of their hospital stay. Five of them (42%) were admitted to hospital for evaluation of orthotopic liver transplantation (OLT), one of them because of catheterization of liver veins for measurement of HVPG. In the other six patients (50%), examinations were performed on an outpatient basis.

Further diagnoses in the cirrhosis group included: vitamin D deficiency (5 patients; 42%), arterial hypertension (5 patients; 42%; 4 patients suffered from essential arterial hypertension, 1 from secondary hypertension due to renal artery stenosis), hypercholesterolemia, hyperuricemia and hypothyroidism, (2 patients each; 17%); colonic diverticula, colonic polyps, hypoferric anemia, type 2 diabetes mellitus, osteoporosis and polyneuropathy (1 patient each; 8%). In the course of the examinations, in one patient, a neuroendocrine tumor in the stomach (type III carcinoid) was detected (8%).

Furthermore, one patient with Child's B cirrhosis (7 points) had history of ***spontaneous bacterial peritonitis*** (SBP) and therefore, was prophylactically treated with fluoroquinolone antibiotics. Notably, this patient suffered additionally from insulin-dependent diabetes mellitus (IDDM) and could not participate in the permeability test.

Another patient (Child-Pugh class A, 6 points) was treated with transjugular intrahepatic portosystemic shunting (TIPS) in August 2011.

With regard to *medication*, the majority of cirrhotics were taking non-selective beta-blockers for the treatment of portal hypertension and gastro-esophageal varices (7 patients; 58%). It is already proven that administration of non-selective beta-blockers ameliorates gastrointestinal permeability and leads to a decrease in bacterial translocation (102). Eight cirrhotics were using proton-pump inhibitors (67%), five were taking antimineralocorticoid agents (spironolactone) and vitamine D analogues (42%), three patients used lactulose (25%), two patients folic acid, phytomenadione, levothyroxine, allopurinol, benzodiazepines or vitamine E analogues (17%) and angiotensin-converting-enzyme inhibitors, $beta_1$-selective blockers, angiotensin-II-receptor antagonists, anticonvulsants, antidepressants, ursodeoxycholic acid, oral anticoagulants, insulin, fluoroquinolone antibiotics, azathioprine and vitamine B analogues were taken by one patient each (9%).

When patients were using lactulose (n = 3), they did not take it in the morning of the permeability test (day 2), but postponed it after the completion of urine collection.

3.1.2 Control Patients

10 control patients were recruited at the Endoscopic Unit of the Medical University of Graz. Most of them were female (9 patients; 90%); their mean age was 49 years (SD 13). Table 11 presents the main characteristics of the control group:

Variable	Valid N	Mean	Standard Deviation	Median	Maximum	Minimum	Range
age (years)	10	49	13	47	70	29	41
height (m)	10	1.66	0.08	1.64	1.81	1.60	0.21
weight (kg)	10	75	9	75	90	60	30
BMI (kg/m²)	10	27.0	4.9	25.6	35.2	20.2	15.0
Hb (g/dl)	9	13.0	1.0	13.4	14.2	10.6	3.6
MCV (fl)	9	87	6	87	95	74	21
leucocytes (G/l)	9	6.6	1.5	6.2	9.6	5.0	4.6
neutrophil granul. (%)	9	58	7	59	74	50	24
thrombocytes (G/l)	9	253	35	257	301	182	119
PT (%)	9	100	10	103	111	87	24

INR	8	1.00	.06	1.00	1.08	0.94	.14
aPTT (sec)	9	29.4	2.3	29.7	31.9	26.1	5.8
fibrinogen (mg/dl)	8	356	67	366	445	242	202
Na+ (mmol/l)	9	141	2	141	144	139	5
K+ (mmol/l)	9	4.0	.2	4.1	4.5	3.7	.8
creatinine (mg/dl)	9	.80	.16	.77	1.16	.60	.56
BUN (mg/dl)	9	28	9	28	44	16	28
uric acid (mg/dl)	8	4.8	1.1	4.4	6.2	3.2	3.0
LDH (U/l)	9	172	27	169	233	132	101
AST (U/l)	9	21	6.2	19	37	16	21
ALT (U/l)	9	21	15	16	60	15	45
GGT (U/l)	9	30	47	14	155	10	145
AP (U/l)	8	55	14	60	69	29	40
CHE (U/l)	2	9161	826	9161	9745	8577	1168
total bilirubin (mg/dl)	8	.56	.32	.50	1.17	.26	.91
total serum protein (g/dl)	7	7.1	.4	7.3	7.4	6.4	1.0
albumin (g/dl)	7	4.4	.2	4.4	4.6	4.2	.4
cholesterol (mg/dl)	7	228	40	232	283	152	131
triglycerides (mg/dl)	7	140	45.8	119	222	96	126
glucose (mg/dl)	9	92	22	92	135	56	79
CRP (mg/l)	9	4.4	4.3	3.1	14.4	.6	13.8

Table 11. 'Characteristics of Control Patients'

Two of the control patients had hepatic steatosis (20%), as assessed via abdominal ultrasound examination, but only one patient demonstrated slightly elevated liver values (AST 37 U/l; ALT 60 U/l; GGT 155 U/l; other values within the normal range). Seven of them (70%) additionally suffered from essential arterial hypertension, and therefore, were taking antihypertensive drugs - mostly beta-blockers ($beta_1$-selective agents; 5 patients, 50%) and also imidazoline-derivates (1 patient; 10%), angiotensin-II-receptor antagonists (1 patient; 10%) or calcium-channel blockers (1 patient; 10%). Moreover, four of the patients had repeatedly elevated serum cholesterol levels (40%; two of them were using HMG-CoA reductase inhibitors), four patients had a history of depression (all of them were taking selective serotonin reuptake inhibitors; 40%), three of the controls were taking

benzodiazepines (30%) and two of them antipsychotics (phenothiazine; 20%). Proton pump inhibitors were already taken by five controls (50%), either due to already diagnosed gastroesophageal reflux disease (1 patient; 10%) or upper GI complaints like heartburn or upper abdominal pain (4 patients; 40%). Rare diseases and medication included coronary heart disease, osteoporosis, rheumatoid arthritis, asthma, secondary Raynaud's, hashimoto's thyroiditis; acetylsalicylic acid, levothyroxine, metamizole and tramadol (1 patient each; 10%).

3.1.3 Comparison of the Study Groups

Cirrhotic and control group were tested for structural equality in important features. With regard to demographic parameters, the two groups did not differ in features like age or BMI [Table 12]. Notably, in the control group, 9 females and only one male were recruited, whereas the cirrhotic group consisted of 9 males and 3 females.

The comparison of patients on the basis of their BMI was performed to exclude a potential effect of obesity on intestinal permeability; however, no patient was malnourished or severely obese based on the BMI values. Control group and cirrhosis group did not differ from each other.

Value	Asymp. Sig. (2-tailed)
age	*.147*
BMI	*.489*

Table 12. 'Comparison of Demographic parameters'

Furthermore, *laboratory findings* were compared between the two study groups.

As expected, most of the liver values and coagulation parameters **differed significantly** between the two groups. Furthermore, uric acid (value in cirrhotic patients higher than in controls) and cholesterol concentrations (value in cirrhotic patients lower than in controls) differed significantly.

Value	Asymp. Sig. (2-tailed)	Value	Asymp. Sig. (2-tailed)
total bilirubin	.008	*thrombocytes*	.000
total protein	.005	*PT*	.003
AST	.000	*INR*	.003
ALT	.004	*aPTT*	.002
GGT	.001	*fibrinogen*	.006
AP	.001	*albumin*	.018

CHE	.028	*uric acid*	.013
leucocytes	.028	*cholesterol*	.010
creatinine	.109	*BUN*	.776
Hb	.887	*LDH*	.075
MCV	.177	*triglycerides*	.151
neutrophil granulocytes	.269	*blood sugar level*	.126
sodium	.110	*C-reactive protein*	.749
potassium	.316		

Table 13. 'Comparison of the two study groups' (in all characteristics, Mann-Whitney U test was performed, since values were either not normal distributed or N < 10); Asymp. Sig. = asymptotic significance

3.2 Upper Gastrointestinal Endoscopy

Upper gastrointestinal endoscopy was performed in five cirrhotic patients (42%) in the course of their evaluation for OLT; in another four patients (33%), gastroesophageal varices were already diagnosed and esophago-gastro-duodenoscopy was carried out as a follow-up examination. Three cirrhotics (25%) were screened for the first time in search of varices. Five cirrhotics (42%) already underwent banding of esophageal varices.

In the control group, upper gastrointestinal complaints were the main indication for endoscopy (six patients presented with epigastric pain, 60%; two patients with heartburn, 20%). In one patient (10%), gastroesophageal reflux disease (GERD) was already diagnosed and a follow-up examination was performed. In another control patient, a Nissen fundoplication for the treatment of GERD was carried out in 2007. Table 14 summarizes the endoscopic findings of the cirrhotic patients:

Variable		Count	Column N %
esophageal varices	no varices	5	42
(n = 12)	small	6	50
	large	1	8
portal hypertensive gastropathy	PHG present	9	75
(n = 12)	no PHG	3	25
scars as a result of banding	scars	3	25
(n = 12)	no scars	9	75

gastritis	gastritis present	3	25
(n = 12)	no gastritis	9	75
erosions in the stomach	erosions present	2	17
(n = 12)	no erosions	10	83
Gastroesophageal reflux disease	GERD present	1	8
(n = 12)	no GERD	11	92

Table 14. 'Upper GI Endoscopic Findings in the Cirrhotic Group'

Upper gastrointestinal alterations were more likely present in patients with advanced cirrhosis; therefore, all of the patients with Child's B and Child's C cirrhosis (advanced stage, n = 5) presented with PHG and four of them with esophageal varices, whereas in the Child's A group (early stage; n = 7), three patients didn't suffer from PHG and four patients had no esophageal varices.

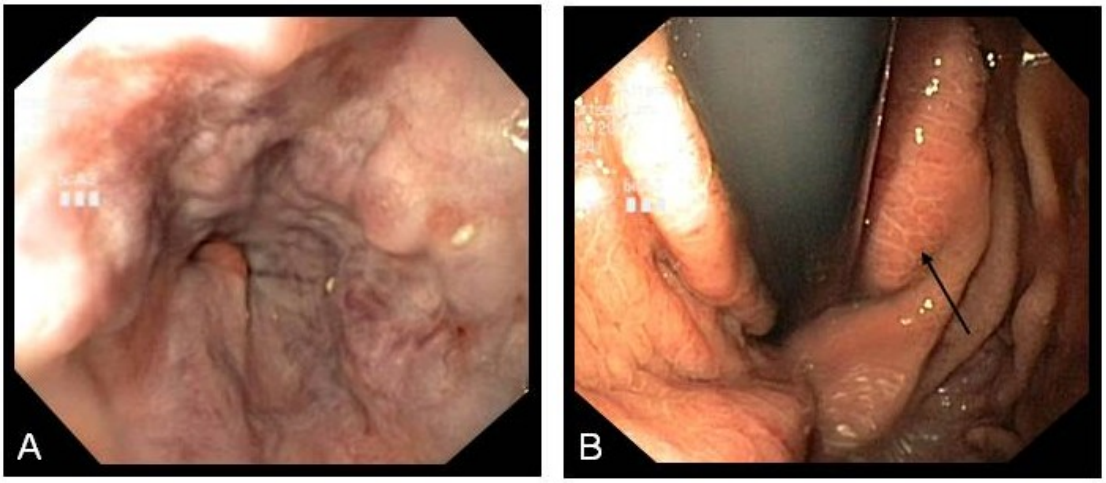

Figure 10. 'Upper GI findings in cirrhotic patient 04 (Child's B)' A: Along the distal 5cm of the esophagus, 3-4 variceal strands, up to 5 mm in size, with cherry red spots were detected. B: In the fundus of the stomach, prominent mucosal folds with mosaic like patterns (arrow) were present (portal hypertensive enteropathy).

In the control group, seven individuals (70%) presented with gastroesophageal reflux disease (6 patients with reflux esophagitis, one patient with non-erosive reflux disease), in four patients (40%) erythematous gastritis was detected and gastric fundic gland polyps (Elster's polyps) were seen in one patient (10%). In another control patient (10%), no pathology was detected.

3.3 Permeability Test

The sucrose/lactulose/mannitol test was successfully finished in 10 cirrhotics and 4 healthy individuals. Pathological results in *gastric permeability* (i.e. percentage of sucrose excretion) were observed in two out of ten cirrhotics (20%), whereas all of the controls showed normal values (0%). Notably, in one control patient, Helicobacter pylori infection was found in the course of his evaluation. Although in 2001, *Fukuda et al.* showed that existence of H. pylori is associated with increased permeability for sucrose (103), this individual showed normal %sucrose excretion.

Gastric permeability values of healthy controls and cirrhotics are summarized in Table 15.

						Mann- Whitney U test		
		N	*Median*	*Min.*	*Max.*	*Mean Rank*	*Mann-Whitney U*	*Asymp. Sig. (2-tailed)*
%S	no cirrhosis	4	.055	.040	.080	6.5	16	**.569**
	cirrhosis	10	.070	.030	.490	7.9		

Table 15. 'Comparison of %Sucrose Excretion' between Healthy Controls and Cirrhotic Patients

With regard to the *lactulose/mannitol ratio*, three pathological results were obtained in the cirrhotic group (30%) - two in advanced (Child's B and C) and one in early-stage cirrhosis (Child's A). In the control group, all participants had normal intestinal permeability values.

						Mann- Whitney U test		
		N	*Median*	*Min.*	*Max.*	*Mean Rank*	*Mann-Whitney U*	*Asymp. Sig. (2-tailed)*
%L/%M	no cirrhosis	4	.0033	.0000	.0060	4.0	6	**.048**
	cirrhosis	10	.0165	.0030	.1050	8.9		

Table 16. 'Comparison of %Lactulose/%Mannitol Ratio' between Healthy and Cirrhotic Patients

While on the one hand, lactulose excretion increased in patients with cirrhosis (mean value 0.244%, SD 0.094 in cirrhosis versus 0.038%, SD 0.015 in healthy individuals; Mann-Whitney U test: asymp. Sig. (2-tailed): 0.089), mannitol excretion decreased in cirrhotics (mean value 9.32%, SD 3.41% in cirrhosis versus 11.22%, SD 1.78%; Mann-Whitney U test: asymp. Sig. (2-tailed): 0.258).

Differences between *early-stage* and *advanced cirrhotics* are depicted in Table 17.

						Mann- Whitney U test		
		N	*Median*	*Min.*	*Max.*	*Mean Rank*	*Mann-Whitney U*	*Asymp. Sig. (2-tailed)*
%L/%M	early	6	.0165	.0036	.0523	5.50	12	**1.000**
	advanced	4	.0228	.0025	.1047	5.50		
%S	early	6	.070	.030	.440	5.25	10.5	**.748**
	advanced	4	.085	.030	.490	5.88		
%L	early	6	.165	.050	.800	6.17	8	**.394**
	advanced	4	.090	.020	.870	4.50		
%M	early	6	10.21	9.34	15.24	7.50	0	**.011**
	advanced	4	6.87	3.59	7.49	2.50		

Table 17. 'Comparison of %Lactulose/%Mannitol ratio, %Sucrose, %Lactulose and %Mannitol Excretion' between early-stage and advanced cirrhotics

Although the lactulose/mannitol ratio increased in advanced when compared with early-stage cirrhotics, the difference was not statistically significant. The percentage of mannitol excretion in healthy individuals was similar to the value observed in early-stage cirrhotics; only at an advanced stage (Child's B and C), mannitol excretion decreased significantly.

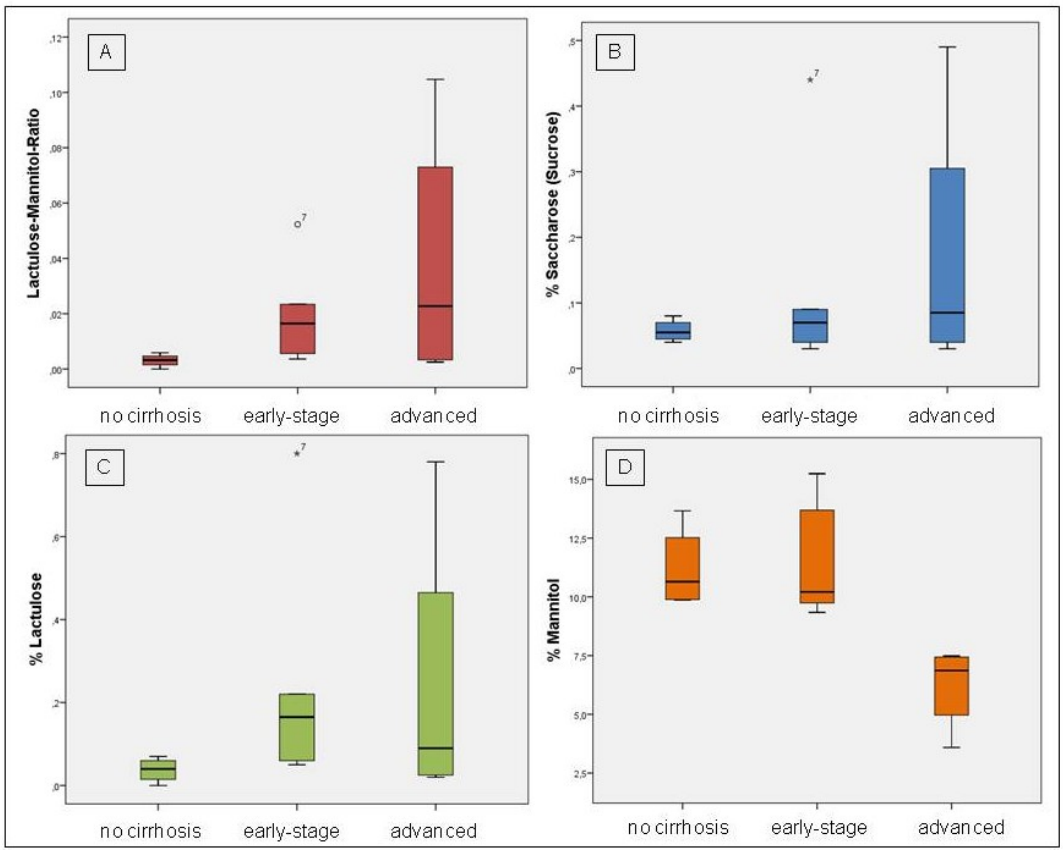

Figure 11. 'Comparison of %Lactulose/% Mannitol ratio (A)**, %Sucrose** (B, i.e. Saccharose)**, %Lactulose** (C) **and %Mannitol Excretion** (D)**'** between healthy patients, early-stage and advanced cirrhotics

With regard to Figure 11, *patient number 7* appears in most illustrations as outlier; this patient (Child-Pugh class A, 6 points, alcoholic cirrhosis) previously suffered from decompensated cirrhosis with massive ascites & esophageal hemorrhage and therefore, was treated with TIPS. As a consequence, with the decrease in PH and the disappearance of his ascites, the Child-Pugh score improved. However, it seems as if mechanisms deteriorating gut barrier were not affected to the same degree by TIPS.

To assess a possible correlation between the severity of liver disease and the worsening of epithelial barrier function, the %Lact/%Man ratio was correlated with the Child-Pugh score; the same test was also applied to the percentage of sucrose excretion. Table 18 summarizes the obtained results:

		number	Correlation Coefficient	Sig. (2-tailed)
Pearson Correlation	***%Lact/%Man ratio*** ***Child-Pugh Score***	10	.733	**.016**
Pearson Correlation	***%Sucrose excretion*** ***Child-Pugh Score***	10	.585	**.076**

Table 18. 'Correlation between %Lact/%Man ratio & Child-Pugh Score and %Sucrose Excretion & Child-Pugh Score' using the Pearson's product-moment coefficient

3.4 Light Microscopy

3.4.1 Differences in Architecture

In healthy individuals, the villus-to-crypt ratio in the distal duodenum usually amounts to ≥3:1. In the control group, only 1 individual with a decreased villus/crypt ratio was observed (10%), whereas in the setting of cirrhosis, 4 patients presented with shortened villi (36%; one patient (Child's B) was not evaluated).

			Fisher's Exact Test
Variable	*cirrhotics (n=11)*	*control (n=10)*	*Exact Sig. (2-sided)*
decreased villus/crypt ratio	4 (36%)	1 (10%)	**.311**

Table 19. 'Comparison of the Villus/Crypt Ratio' between cirrhotics and controls; the difference did not reach statistical significance

However, the villus-to-crypt ratio was more likely disturbed in patients with advanced cirrhosis: 3 out of 4 Child's B & C cirrhotics (75%), in comparison with 1 early-stage cirrhotic (14%) and 1 healthy control (10%), presented with a decrease in villi height [Figure 12]. Comparing healthy controls and early-stage cirrhotics with advanced cirrhotics, the difference became statistically significant (**p-value: 0.028;** Fisher's exact test).

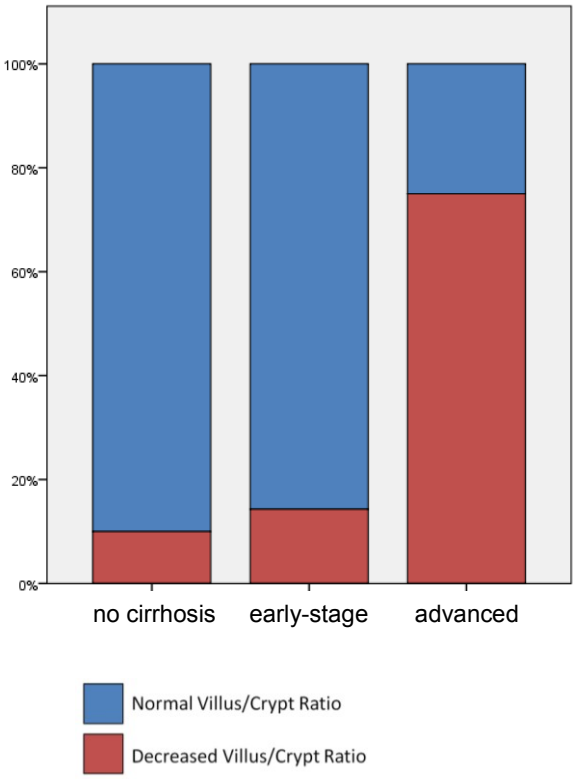

Figure 12. 'Increase in Relative Frequency of Decreased Villus/Crypt Ratio' between healthy controls, early-stage and advanced cirrhotics

Besides flattening of the duodenal villi, they simultaneously seemed to increase in width; this phenomenon was also more likely observed in patients with advanced liver disease.

Figure 13 compares architecture of duodenal mucosa in healthy and cirrhotic patients:

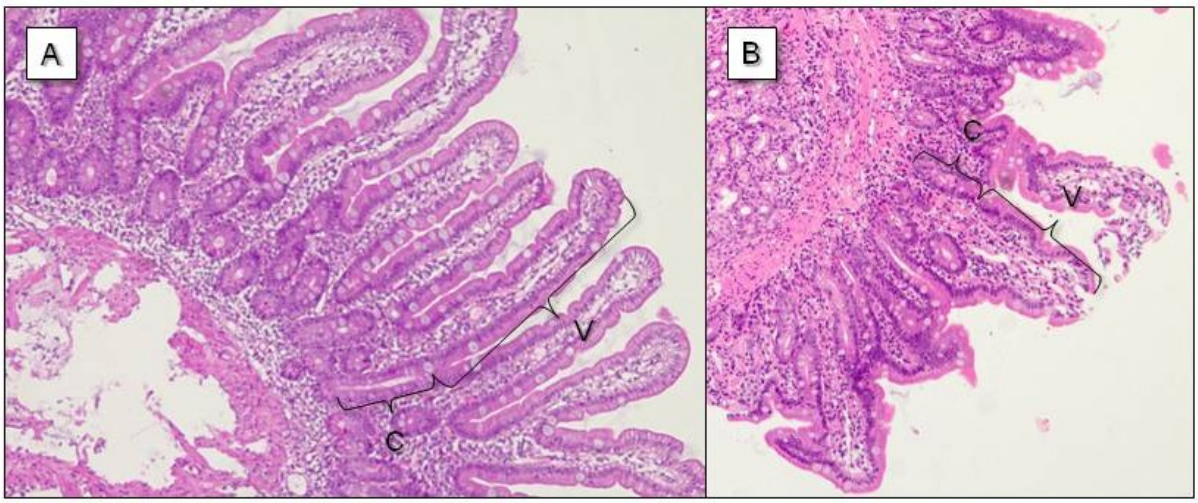

Figure 13. 'Histological Sections of Duodenal Mucosa' in healthy controls (A) and decompensated cirrhotics (B). Note the presence of flattened and broadened villi in the patient suffering from cirrhosis (Child's C, 13 points) leading to a decreased villous/crypt ratio. V = villi; C = crypt (H&E stain. 40x)

Furthermore, the total number of villi was counted in every slide and compared between healthy controls and cirrhotic patients:

					Welch's t-test		
		N	*Mean*	*Std. Deviation*	*T*	*Sig. (2-tailed)*	*Mean diff.*
total villi count	controls	10	**40**	16	-3.626	**.003**	-20
	cirrhosis	12	**20**	8			

Table 20. 'Total Villi Count'

3.4.2 Changes in Cellular Composition of the Intestinal Epithelium

No difference was observed in appearance of intraepithelial lymphocytes (IEL) between cirrhotic and healthy participants. Thereby, interpretation of IEL count was complicated, since in two of the control patients – in those with high-ranked counts – Helicobacter pylori was found during routine evaluation. However, in earlier studies, increase in IEL was more likely observed in patients who recently consumed alcohol, whereas all of our cirrhotics quit drinking for several weeks.

We observed a slight increase in number of goblet cells in cirrhotics as compared to healthy controls. However, the difference did not reach statistical significance.

Changes in epithelial cellular composition are presented in Table 21.

				Mann- Whitney U test		
		N	*Median*	*Mean Rank*	*Mann-Whitney U*	*Asymp. Sig. (2-tailed)*
IEL /100 enterocytes	no cirrhosis	10	16	14.3	32	**.064**
	cirrhosis	12	11	9.2		
goblet cells /100 enterocytes	no cirrhosis	10	5	8.7	32	**.063**
	cirrhosis	12	9	13.8		

Table 21. 'Changes in Epithelial Cellular Composition'

3.4.3 Changes at the Villous Tips

At the tips of the villi, ***distension of the intercellular space (DIS)*** was observed as described in previous studies of cirrhotic patients (69,104). On light microscopy, this phenomenon was particularly observed in the lower (basal) portion of enterocytes, whereas at the luminal border, epithelial cells seemed to stay closely attached to each other. To

quantify these alterations in our biopsy specimens, villi with DIS in the epithelium were counted and set in relation to the total number of villi in every slide. The relative frequencies of villi with DIS were compared in Table 22:

					Welch's t-test		
		N	*Mean*	*Std. Deviation*	*T*	*Sig. (2-tailed)*	*Mean diff.*
Percentage of villi with distended intercell. space	controls	10	**43.6%**	14.3	-2.136	**.047**	-17.8
	cirrhosis	12	**61.4%**	24.3			

Table 22. 'Number of Villi with Distended Intercellular Space'

In fact, even in control patients, DIS was observed in 43.6% of villi, especially in those patients with the *highest number of medication* (especially benzodiazepines and antidepressants). Both groups of drugs are suspected to affect gastrointestinal motility and permeability (33,85) and therefore, might also be related to the high incidence of light-microscopic findings in the control group. Notably, 5 controls were taking antidepressants and/or benzodiazepines (this is considered one of the limitations of the study).

Applying the scoring criteria determined in chapter 2.6, eight out of ten control patients (80%) presented with score 1. In the setting of cirrhosis, 61.4% of villi featured DIS, distributed among six patients with score 2 (50% of patients), four patients with score 1 (33%) and two patients with score 0 (17% of patients). Surprisingly, the two patients with score 0 suffered from advanced cirrhosis.

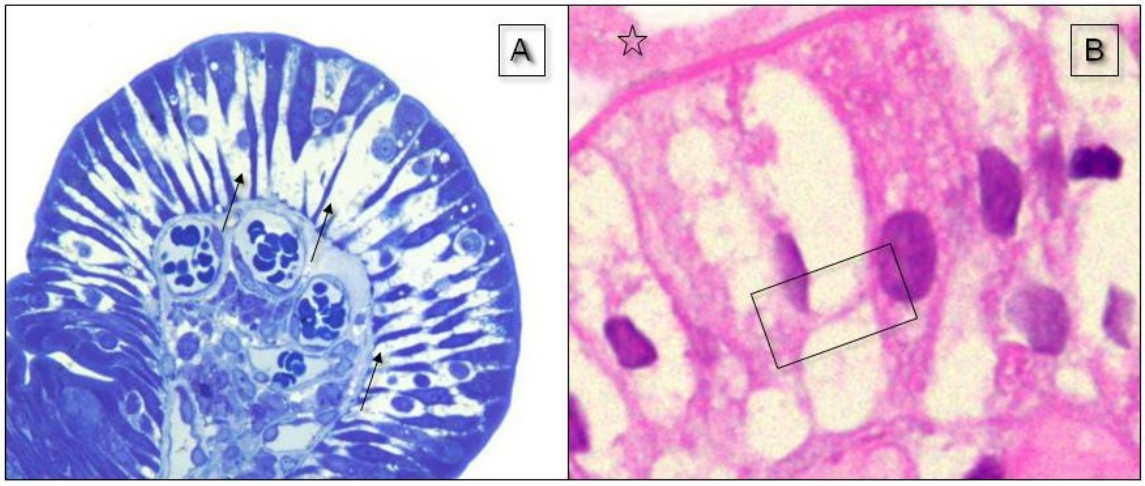

Figure 14. 'Villi with Enterocytes separated by a Distended Intercellular Space' in the lower portion of the cell. A: The arrows mark the inter-enterocytic space. (toluidine blue stain. 200x); B: Note the presence of ties in-between separated enterocytes (open box), where desmosomes try to preserve cell-cell connection [see Figure 26A], open star = intestinal lumen (H&E stain. 400x)

Furthermore, ***vacuolization of the cytoplasm*** was observed especially in enterocytes covering the villous tips. To evaluate this phenomenon, a similar approach to that used in the quantification of distended intercellular spaces was chosen.

					Welch's t-test		
		N	*Mean*	*Std. Deviation*	*T*	*Sig. (2-tailed)*	*Mean diff.*
percentage of villi with vacuolated enterocytes	no cirrhosis	10	**12.3%**	7.72	-3.260	**.006**	-27.8
	cirrhosis	12	**40.1%**	28.3			

Table 23. 'Number of Villi with Vacuolated Enterocytes'

Performing the Welch's t-test, a statistically significant difference was observed. In healthy individuals, no participant obtained a score other than 0 (100%), whereas in cirrhosis, 4 patients had score 1 (33% of cirrhotics) and two patients had score 2 (17% of cirrhotics).

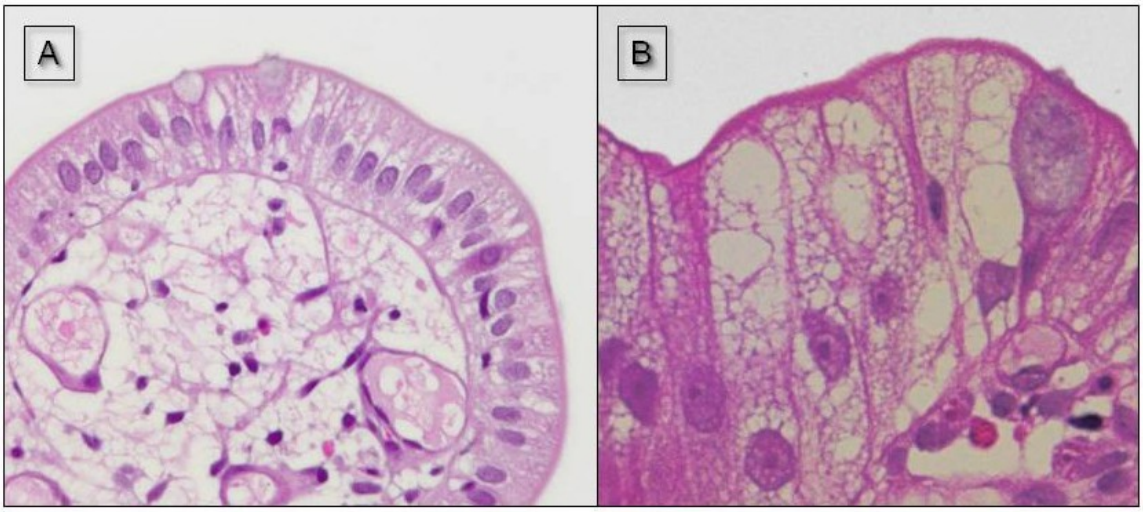

Figure 15. 'Enterocytes with Vacuolated Cytoplasm' covering the villous tips in cirrhotic patients (H&E stain. 400x)

Furthermore, detachment of the epithelium from the lamina propria (i.e. ***dilatation of Gruenhagen's space***) and appearance of ***denuded villi*** was investigated in both study groups. Villi with preserved epithelial integrity, but presence of subepithelial blebs (dilatation of Gruenhagen's space [Figure 16A]) on the one hand, and denuded villi (with desquamated enterocytes [Figure 16B]) on the other hand were counted and set in relation to the total number of villi in every slide. Table 24 compares the relative frequencies between the two study groups:

					Welch's t-test		
		N	*Mean*	*Std. Deviation*	*T*	*Sig. (2-tailed)*	*Mean diff.*
percentage of villi with dilatation of Gruenhagen's space	no cirrhosis	10	9.5%	6.1	-2.485	**.023**	-9.4
	cirrhosis	12	18.9%	11.3			

				Mann-Whitney U test		
		N	*Median*	*Mean Rank*	*Mann-Whitney U*	*Asymp. Sig. (2-tailed)*
percentage of denuded villi	no cirrhosis	10	18.2%	8.5	30	**.048**
	cirrhosis	12	29.8%	14		

Table 24. 'Denudation of Villi'

In cirrhotic patients, both dilatation of Gruenhagen's space and denudation of villi were observed more frequently when compared to healthy controls.

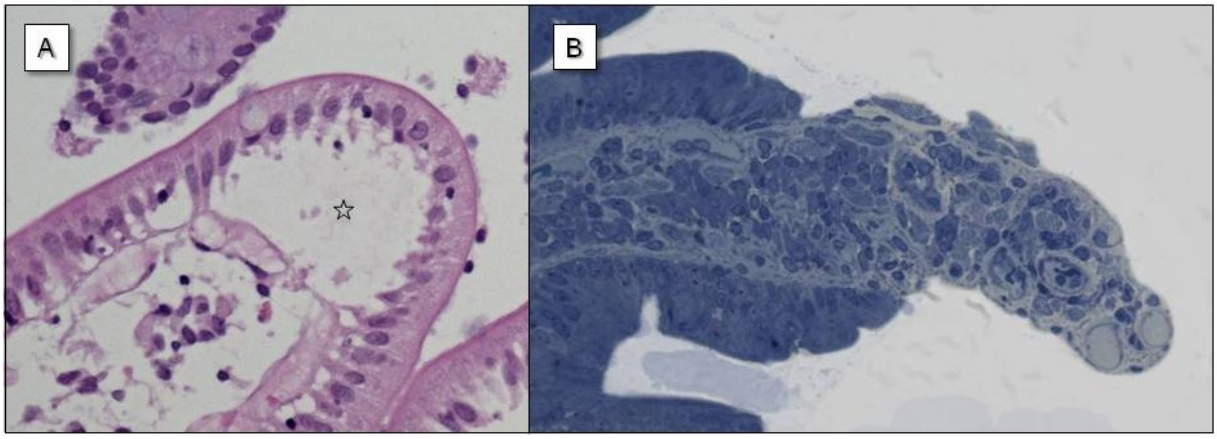

Figure 16. 'Denudation of Villi in Cirrhotic Patient' A: The epithelium is detached from the basement membrane (open star, dilatation of the Gruenhagen's space). B: Duodenal villi after loss of epithelium; A: H&E stain, 400x; B: toluidine blue stain, 200x

3.4.3.1 Correlation with Permeability Values

Trying to correlate the extent of villi affected by *DIS* and the mean *lactulose/mannitol-excretion ratio*, a slight tendency, but no statistically significant result was obtained (**p-value: 0.116**; Spearman's rank correlation coefficient: 0.440; N=14).

In contrast, the *urinary excretion ratio of lactulose/mannitol* significantly increased with the appearance of *denuded villi* (**p-value: 0.005)**:

		number	Correlation Coefficient	Sig. (2-tailed)
	%Lact/%Man ratio			
Pearson Correlation	***Percentage of Denuded Villi***	14	.706	**.005**

Table 25. 'Correlation between %Lact/%Man ratio & Percentage of Denuded Villi' using the Pearson's product-moment coefficient

Figure 17 depicts the obtained results:

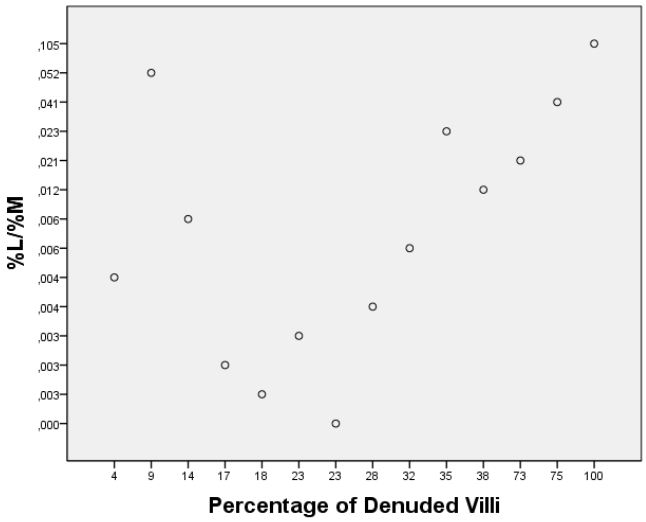

Figure 17. '%L/%M correlated with the Percentage of Denuded Villi'

3.4.4 Apoptotic Ratio

To a certain extent, ***apoptosis*** at the villous tips is considered a physiologic event. Labeling of apoptotic cells with caspase-3 antibodies was observed in most patients (10 of 12) and controls (7 of 10). Since cirrhotics presented with a highly reduced number of villi, the total count of apoptotic cells was set in relation to the number of villi in every slide and multiplied with the mean number of villi observed in all biopsy specimens (= 29 villi).

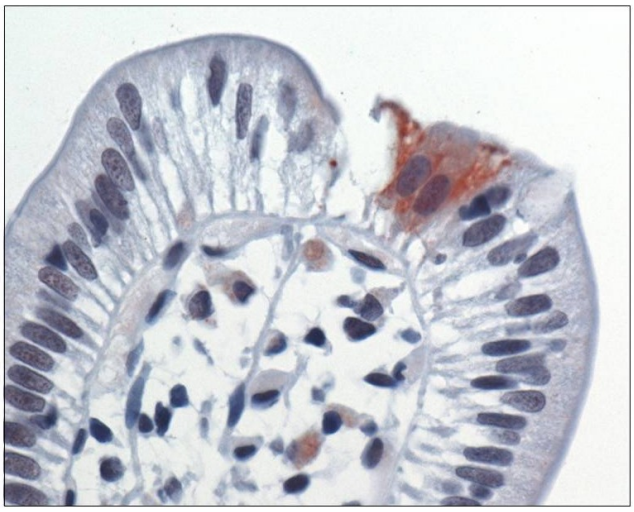

Figure 18. 'Apoptotic Cells at a Villous Tip'
Anticaspase-3 Stain (brown-colored cells), 400x

Table 26 shows that comparison between the two study groups revealed a marked tendency, but did not reach statistical significance:

				Mann- Whitney U test		
		N	*Median*	*Mean Rank*	*Mann-Whitney U*	*Asymp. Sig. (2-tailed)*
Apoptotic cell count *(projected to the mean number of villi)*	no cirrhosis	10	**1.4**	8.7	32	**.063**
	cirrhosis	12	**3.5**	13.8		

Table 26. 'Comparison of Apoptotic Cell Count between Healthy Controls and Cirrhotics'
Asymp. Sig. = Asymptotic Significance

3.4.5 'Pale Cells' at the Villous Tips

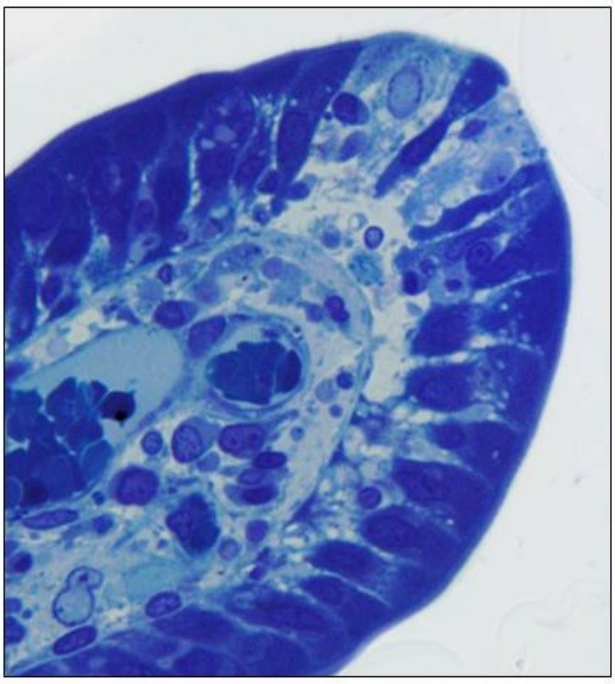

Figure 19. 'Weakly stained ('pale') Cells'
(toluidine blue stain. 400x)

In toluidine-stained slides, enterocytes that appeared extremely pale with swollen nuclei were observed at the tips of some villi [Figure 19]. In the control group, only 2 patients (20%) presented with those ***'pale cells'*** at their villous tips; in patients with cirrhosis, the frequency of those cells was much higher: only 3 of 12 patients **did not** show this feature (all of them were Child's A cirrhotics), whereas in 9 patients (75%), they were detected.

Table 27 compares the percentage of villi presenting 'pale cells' between healthy controls and cirrhotic patients:

					Mann- Whitney U test		
		N	*Mean*	*Std. Deviation*	*Mean Rank*	*Mann-Whitney U*	*Asymp. Sig. (2-tailed)*
percentage of villi presenting pale cells	no cirrhosis	10	6.9%	18.1	8.35	28.5	**.026**
	cirrhosis	12	19.4%	18.3	14.13		

Table 27. 'Villi hosting Pale Cells'

Within the control group, the total number of pale cells counted was 23, whereas in the setting of cirrhosis, 73 of those enterocytes were detected.

Furthermore, the percentage of villi presenting pale cells was increased in patients with higher stages of cirrhosis:

Figure 20. 'Child-Pugh Score and Percentage of Villi Presenting Pale Cells'

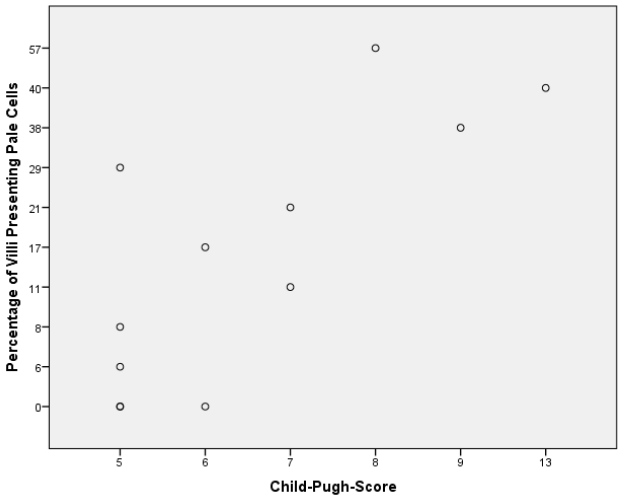

Using the Pearson's product-moment coefficient, a statistically significant result was obtained correlating the Child-Pugh Score with the percentage of villi with pale cells.

		number	Correlation Coefficient	Sig. (2-tailed)
Pearson Correlation	***Percentage of Villi Presenting Pale Cells***	12	.674	**.016**
	Child-Pugh Score			

Table 28. 'Correlation between Percentage of Villi presenting Pale Cells and Child-Pugh Score'

3.4.6 Alterations in the Lamina Propria

Within the lamina propria, ***edema, fibrosis*** and ***inflammation*** were assessed. In all of them, the frequency was higher in patients with cirrhosis than in control subjects. Table 29 gives an overview of the statistical results.

			Fisher's Exact Test
Variable	*cirrhotics (n=12)*	*control (n=10)*	*Exact. Sig. (2-sided)*
Edema	8 (67%)	2 (20%)	**.043**
Fibrosis	8 (67%)	2 (20%)	**.043**
Inflammation	4 (33%)	0 (0%)	**.096**

Table 29. 'Alterations observed in Lamina Propria' Absolute and relative frequencies are given.

The differences regarding edema and fibrosis [Figure 21] were statistically significant. If present, the inflammatory infiltrate consisted predominantly of lymphocytes and mononuclear cells.

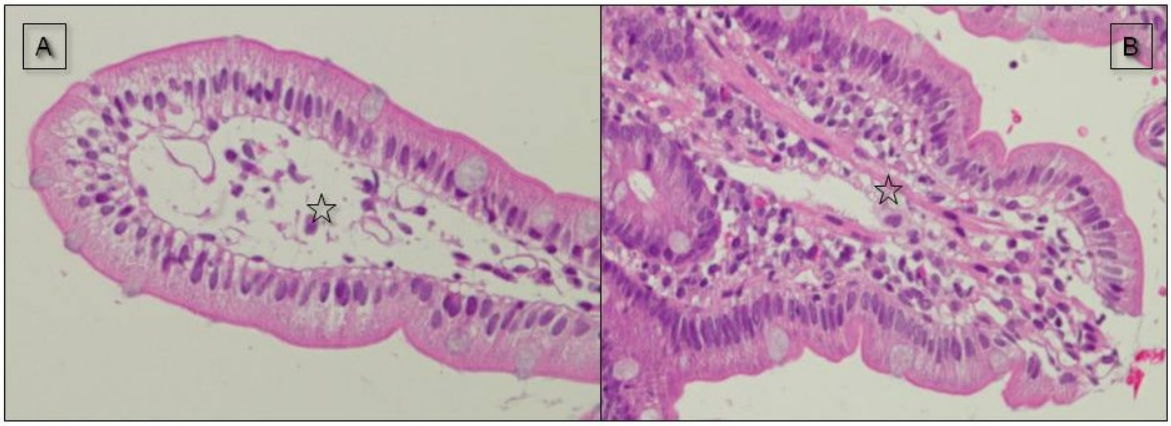

Figure 21. 'Edema (A, open star) **and Fibrosis** (B, open star)**'** of the lamina propria (H&E stain. 200x)

Extravasation, defined as free erythrocytes in the lamina propria, was observed in three cirrhotics (25%), and only in one healthy individual (10%):

			Fischer's Exact Test
Variable	*cirrhotics (n=12)*	*control (n=10)*	*Exact Sig. (2-sided)*
Extravasation	3 (25%)	1 (10%)	**.594**

Table 30. 'Extravasation' Absolute and relative frequencies are given.

3.4.7 Vascular Abnormalities

Vascular changes were evaluated in 3 villi of each sample: First, the number of ***capillary profiles*** within the villi was counted; furthermore, the ***diameter of the capillaries*** was measured at 3 locations with the highest vascular diameter using ImageJ. The mean diameter was calculated then [Figure 22].

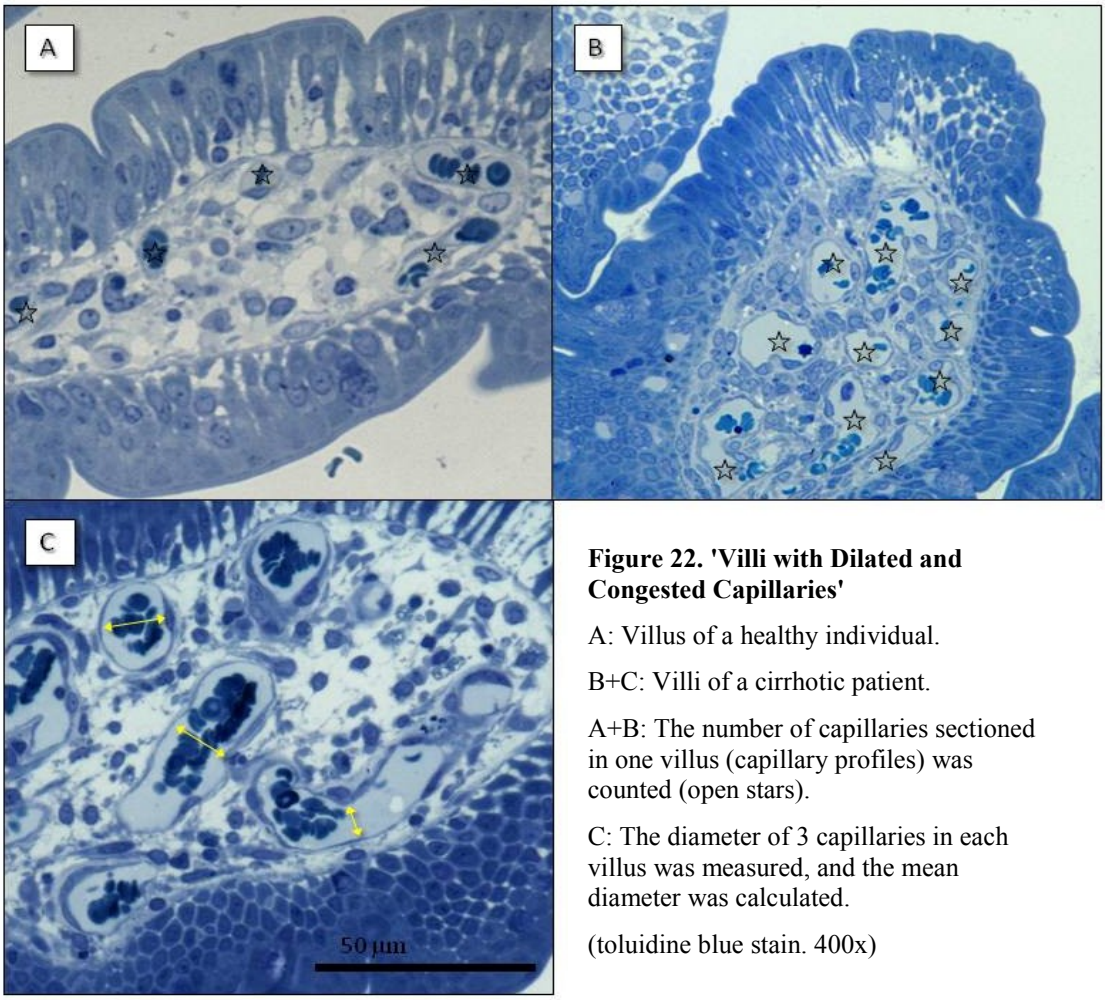

Figure 22. 'Villi with Dilated and Congested Capillaries'

A: Villus of a healthy individual.

B+C: Villi of a cirrhotic patient.

A+B: The number of capillaries sectioned in one villus (capillary profiles) was counted (open stars).

C: The diameter of 3 capillaries in each villus was measured, and the mean diameter was calculated.

(toluidine blue stain. 400x)

In healthy individuals, the median number of capillary profiles counted was 15, whereas in cirrhotics, at least 19 profiles were observed in 3 villi. The difference did not reach statistical significance:

					Student's t-test		
		N	*Mean*	*Std. Deviation*	*T*	*Sig. (2-tailed)*	*Mean diff.*
number of capillary profiles *(in 3 villi)*	controls	10	16.9	7.6	-.779	**.445**	-2.3
	cirrhosis	12	19.2	6.1			

Table 31. 'Comparison of Number of Sectioned Capillaries' in 3 villi

In terms of vessel diameter, the difference between the two study groups was statistically significant. The results are summarized in Table 32.

					Student's t-test		
		N	*Mean*	*Std. Deviation*	*T*	*Sig. (2-tailed)*	*Mean diff.*
mean vessel diameter (µm)	no cirrhosis	10	4.65	0.69	-7.659	**.000**	-4.13
	cirrhosis	12	8.77	1.58			

Table 32. 'Comparison of Mean Capillary Diameter'

There was also a significant difference (p-value: **0.007**; Mann-Whitney U test) in mean capillary diameter between early-stage (7.82µm; SD 1.08; n = 7) and advanced cirrhosis (10.12µm; SD 1.13; n = 5). The highest values were observed in the three patients with *massive ascites* (indicating high portal venous pressure); the lowest values were observed in patients without signs of portal hypertension [Figure 23].

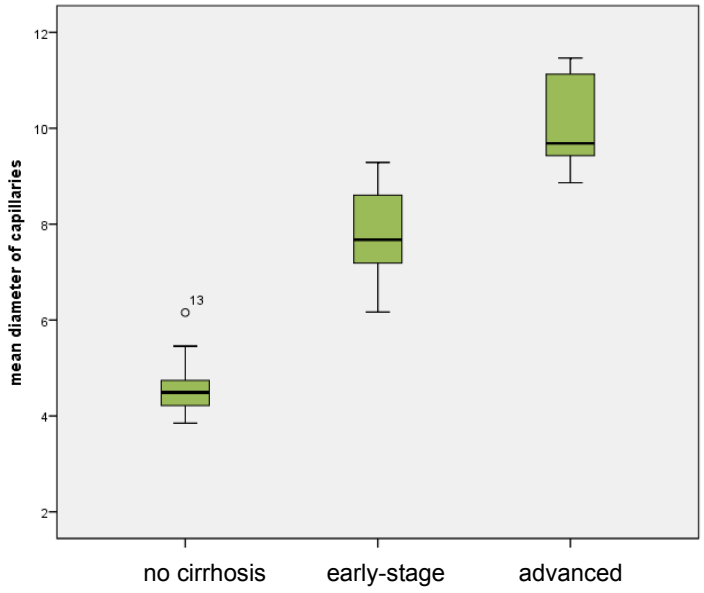

Figure 23. 'Boxplot: Comparison of mean vessel diameter [µm]' between healthy controls, early-stage and advanced cirrhotics

Correlating the mean capillary diameters – as a correlate of portal hypertension – with the lactulose/mannitol excretion ratio, a tendency, but no significant result was obtained:

		number	Correlation Coefficient	Sig. (2-tailed)
Pearson Correlation	***%Lact/%Man ratio***	14	.489	**.076**
	Mean Capillary Diameter			

Table 33. 'Correlation between %Lact/%Man ratio & Mean Capillary Diameter' using the Pearson's product-moment coefficient

3.5 Electron Microscopy

3.5.1 Alterations in Epithelial Architecture

Alterations in duodenal epithelial architecture of cirrhotics were already assessed and quantified in the previous chapter [see 3.4.1]; this section deals with their ultrastructural correlates.

Most of the enterocytes in healthy controls were positioned closely together; their numerous microvilli were densely packed:

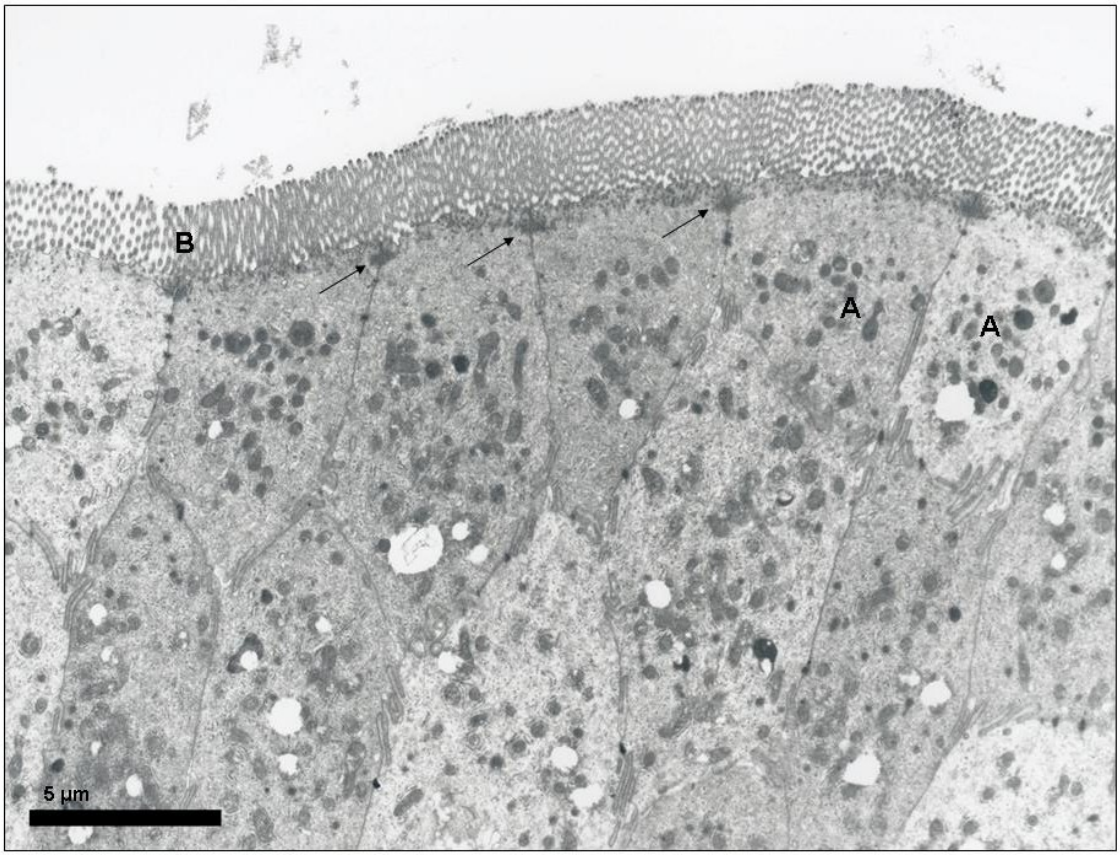

Figure 24. 'Duodenal Epithelial Lining of Control' There are narrow intercellular spaces between enterocytes (A) with a brush border (B) counting of numerous tall microvilli. Arrows point at junctional complexes consisting of tight junctions, intermediate junctions and spot desmosomes. Bar line: 5 µm

As already described on light microscopy, ***distension of the intercellular space (DIS)***, particularly in the lower portion of enterocytes with preserved cell/cell-contacts at the luminal side (in relatively low magnification) was observed more frequently in cirrhotic patients. This phenomenon was more pronounced at the tips & half way down along the sides of the villi [Figure 25].

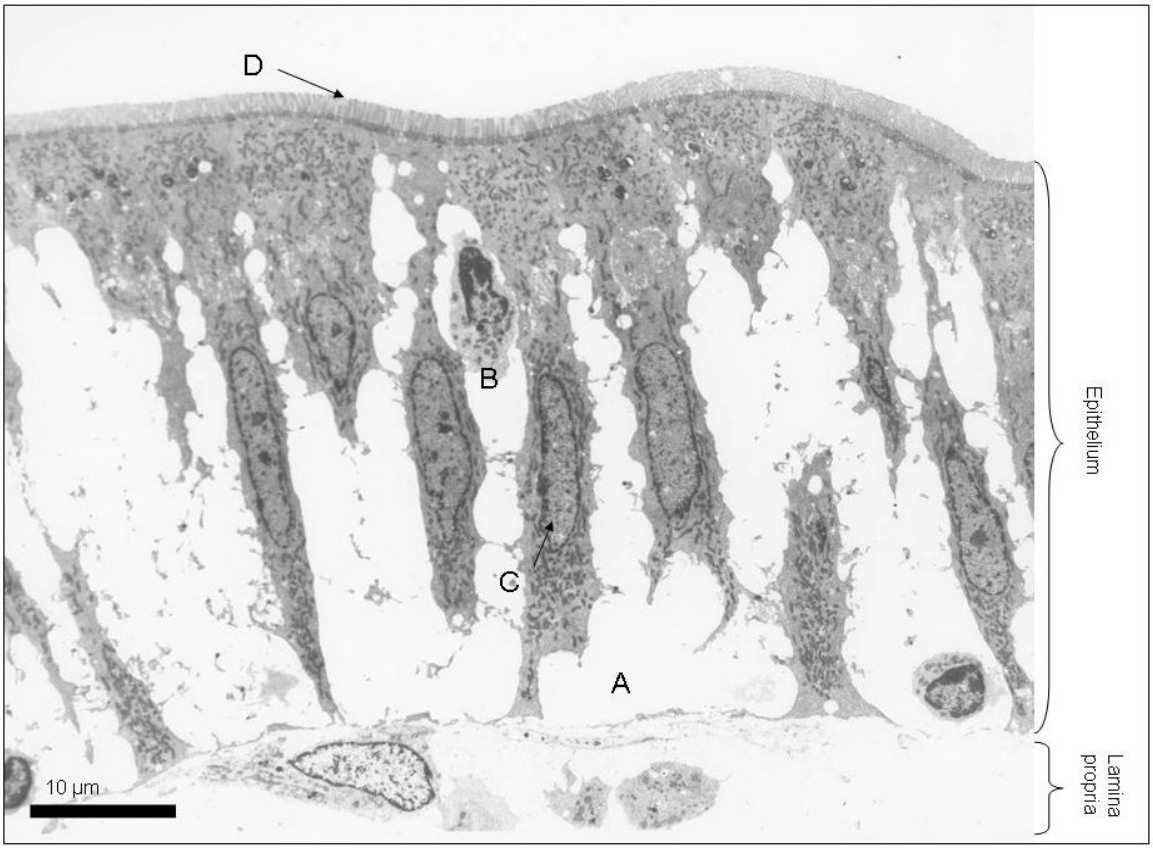

Figure 25. 'Columnar Epithelium of a Cirrhotic Patient' (Child's B, 8 pts). The enterocytes are separated by a dilated extracellular space (A) that is more evident in the basal portions of cells. The microvilli (D) appear less high compared with control patients. B:IEL; C: nucleus of an enterocyte; bar line: 10 µm

In the lower portion of enterocytes, cytoplasmatic strands connecting two neighboring cells were observed; higher magnification of these areas revealed spot desmosomes trying to keep the contact between adjacent enterocytes [see Figure 26A]. In Figure 26B, the transitional region between the basal epithelium and the lamina propria is depicted in a villus with DIS. The anchorage of enterocytes in the basement membrane seems markedly heavy so that sometimes, residues of the cells stay attached to the membrane.

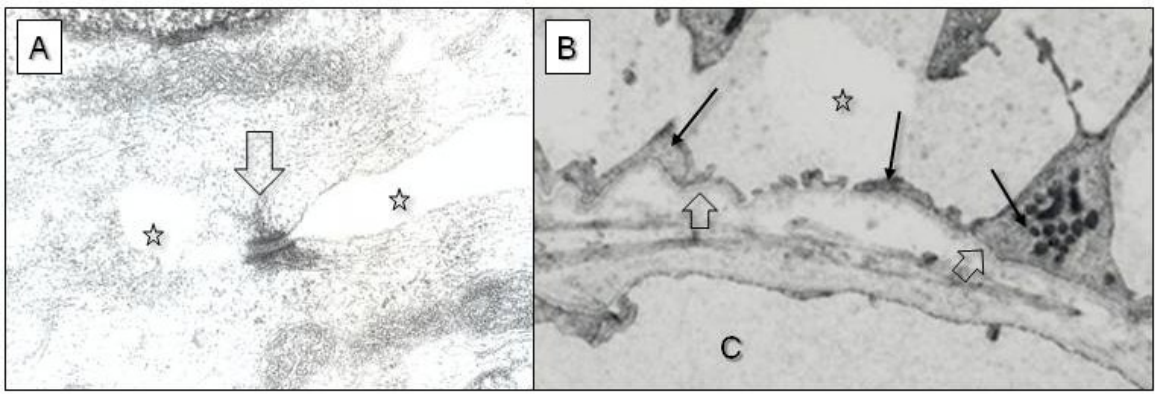

Figure 26. 'Spot Desmosome (A) and Anchorage in the Basement Membrane (B)' A: Desmosome (open arrow) tries to maintain the intercellular connection; open star = DIS. **B:** Anchorage of enterocytes in the basement membrane. Arrows: residues of enterocytes, open arrows = lamina densa of the basement membrane, C = lumen of dilated capillary; open star = DIS

3.5.2 Characteristics of Perishing Cells

Ultrastructural analysis of 'pale cells' (in toluidine-blue staining [see 3.4.5]) at the villous tips showed evidence of ***necrosis*** including *swelling of cytoplasm & nuclei* and *disruption of plasma membrane & organelles* [Figure 27].

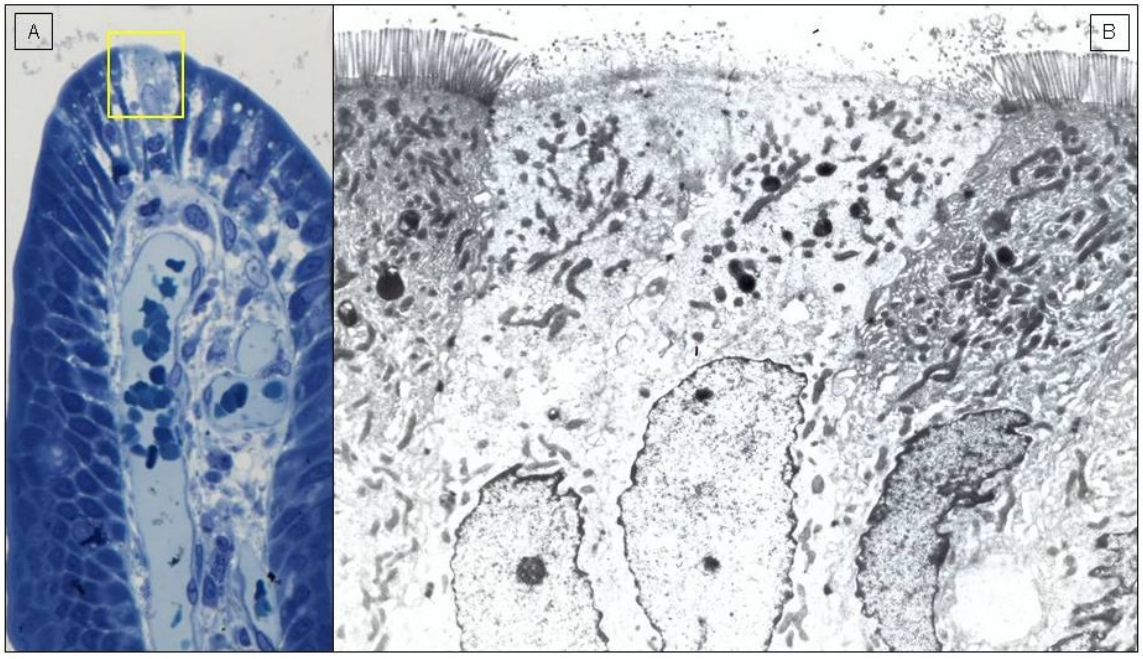

Figure 27. 'Pale Cells covering the Villous Tips exhibit Features of Necrosis' in Electron Microscopy. A: toluidine-blue staining; B: Electron micrograph of area within the box in figure A. The cells show nuclear swelling, distorted & rarified microvilli and disruption of the plasma membrane.

Furthermore, enterocytes with characteristics of ***apoptosis*** were detected: *chromatin condensation, cytoplasmatic vacuolization, cell shrinkage* and *formation of apoptotic bodies* were found in some enterocytes covering the villi of cirrhotic patients [Figure 28].

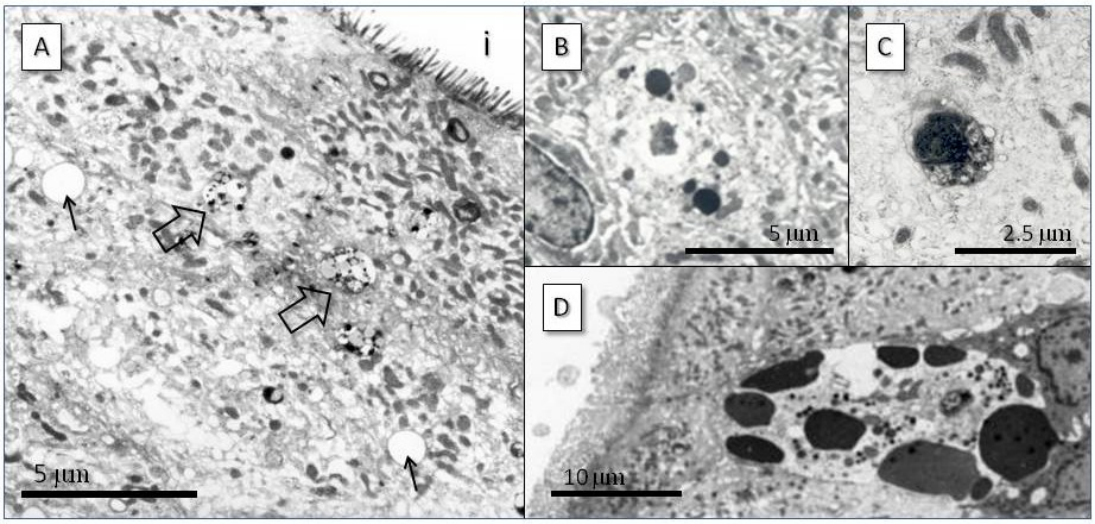

Figure 28. 'Apoptotic Features of Enterocytes' A: Autophagic vacuoles (open arrows) and cytoplasmic vacuoles (arrows, probably lysosomes); i = intestinal lumen. B: apoptotic bodies. C: chromatin condensation. D: Formation of apoptotic bodies.

3.5.3 Vacuolization of the Cytoplasm

Increased presence of vacuoles filled with homogenous content was observed in cells featuring both apoptotic and necrotic features [see Figure 29]. Indeed, it seems as if the appearance of these vacuoles was somehow linked to the disruption of the microvilli, since they were already present in cells with slightly disrupted microvilli, just underneath the luminal cell border, and even more when microvilli were totally disrupted.

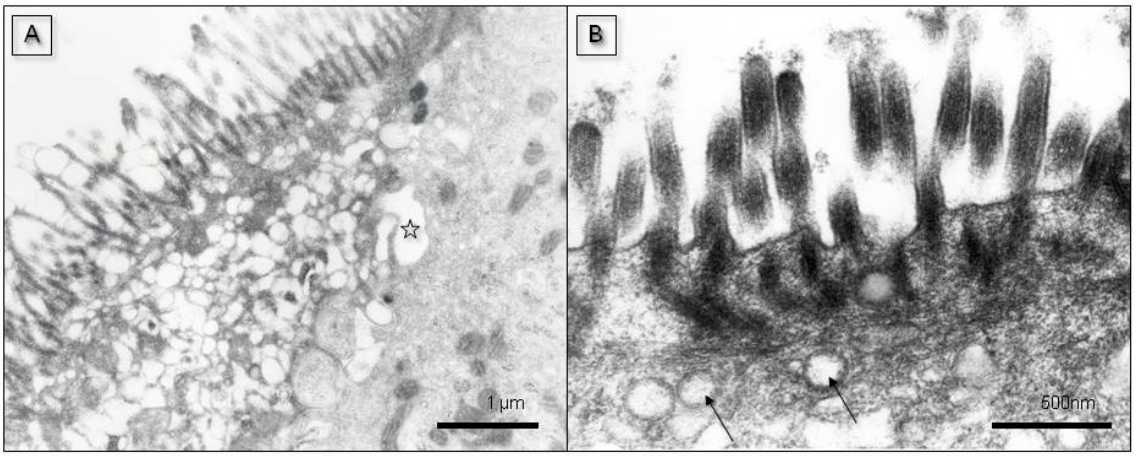

Figure 29. 'Increased Presence of Vacuoles' A: Cell crowded with vacuoles and distorted microvilli. In the right corner, a 'healthy' enterocytes is depicted. The open star marks the distended intercellular space. B: Vacuoles (arrows) just underneath distorted microvilli.

3.5.4 Tight Junctions

In every study participant, at least 15 TJ complexes were photographed.

At first sight, TJs from patients with chronic liver disease exhibit similar ultrastructural characteristics when compared with healthy controls [Figure 30].

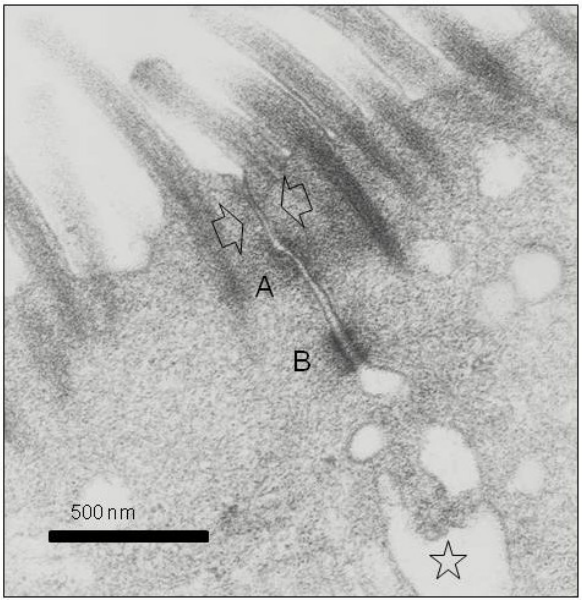

Figure 30. 'TJ complex of a Cirrhotic Patient' (Child's B, 8 points). Bar line: 500nm

The two arrows point to the TJ, A marks the adherens junction, B a spot desmosome. In the area underneath the junctional complex, the extracellular space is clearly dilated (open star). Furthermore, microvilli appear less high when compared with healthy control patients [see 3.5.5].

Subsequently, images of TJ complexes were analysed using an image processing program (ImageJ). The width in-between the inner leaflets of the enterocytes' cell membranes in the TJ area (***TJ-gap width***) was measured as depicted in Figure 31.

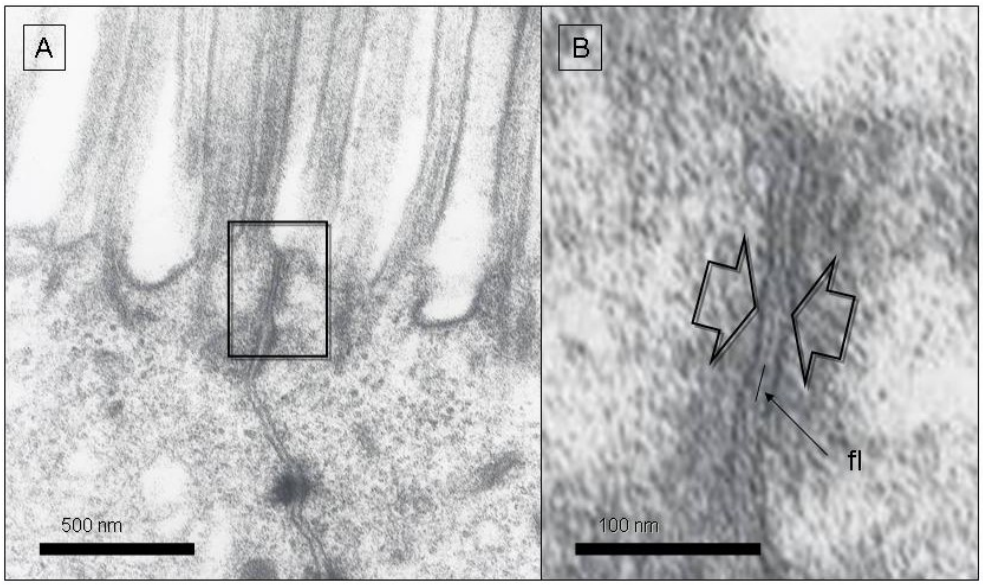

Figure 31. 'Electron Micrograph from Normal Intestinal Villi' A: The junctional complex - situated at the luminal border of the enterocytes' lateral surface - is pictured. (Bar line: 500nm). Figure B shows a higher magnification of the area in the square of figure A, the TJ complex. The TJ-gap width - i.e. the area in-between the two inner leaflets of the cell membranes (arrows) - was measured and analyzed. (fl = fusion line; bar line: 100nm)

First of all, the mean width of TJ gaps in healthy controls, in ***epithelial areas with neither a distended intercellular space nor perishing cells***, was measured and set as ***reference value***. Then, this value was compared with the mean TJ-gap width of ***cirrhotic patients***, divided into 3 groups:

(a) TJ-gap width between enterocytes of **'healthy' epithelial areas** (without distended intercellular spaces or perishing cells)

(b) TJ-gap width between enterocytes of **epithelial areas with distended intercellular spaces**

(c) TJ-gap width between **perishing enterocytes** (less electron-dense cells featuring either apoptotic or necrotic features)

All in all, 245 evaluable TJs were measured. Table 34 shows in which areas the individual TJs were located.

	'healthy' areas	*areas with distended intercellular space*	*areas with perishing cells*	Total Number
Cirrhosis	55	75	10	140
No Cirrhosis	102	2	1	105
Total Number	157	77	11	*245*

Table 34. 'Tight Junctions and their Areas of Origin' (absolute frequencies)

In the cirrhosis group, TJ complexes in healthy epithelial areas and areas with distended intercellular spaces were found and measured in all patients; TJs in areas with perishing cells were only detected in four patients. In the control group, only TJs in 'healthy' areas were able to be evaluated, since TJs in epithelial areas with DIS or perishing cells were only pictured in one patient each. Table 35 gives an overview of the mean values observed:

		Mean	*Std. Deviation*	*Median*
Control group	TJ-gap width in 'healthy' epithelial areas [nm]	10.45	.463	10.56
Cirrhosis group	TJ-gap width in 'healthy' epithelial areas [nm]	10.25	1.789	10.38
Cirrhosis group	TJ-gap width in epithelial areas with DIS [nm]	11.71	1.060	11.56
Cirrhosis group	TJ-gap width in epithel. areas with perish. cells [nm]	12.47	2.388	12.55

Table 35. 'Values of TJ-gap width'

No difference was observed in TJ-gap width of enterocytes found in 'healthy' epithelial areas, between cirrhotic and control patients.

Comparing the reference value of TJ-gap width (healthy controls, 'healthy' areas) with mean values observed in epithelial areas with DIS of cirrhotic patients, the following results were obtained:

					Welch's t-test		
		N	*Mean*	*Std. Deviation*	*T*	*Sig. (2-tailed)*	*Mean diff.*
Width of TJ gaps [nm]	Healthy areas (control group)	10	10.45	.463	-3.715	**.002**	-1.26
	Areas with DIS (cirrhosis group)	12	11.71	1.060			

Table 36. 'Comparison of TJ-gap width' between the reference value and TJ-gap width measured in epithelial areas with DIS of cirrhotic patients

With regard to the ***cirrhosis group***, no difference was observed either in 'healthy' epithelial areas or in areas with DIS between early-stage (Child-Pugh class A) and advanced cirrhotic patients (Child-Pugh classes B and C).

		Mean	*Std. Deviation*	*Median*	*p-value*
Early-stage Cirrhotics	TJ-gap width in 'healthy' areas [nm]	10.03	2.26	10.56	**.685**
Advanced Cirrhosis	TJ-gap width in 'healthy' areas [nm]	10.57	.95	10.18	
Early-stage Cirrhosis	TJ-gap width in areas with DIS [nm]	11.59	1.26	11.05	**.570**
Advanced Cirrhosis	TJ-gap width in areas with DIS [nm]	11.88	.80	11.87	

Table 37. 'Comparison of TJ-gap width within the cirrhosis group' in healthy areas and areas with DIS. Mann-Whitney U test was performed; asymptotic significance is given.

Furthermore, the reference value of healthy controls was compared with mean TJ-gap width observed in areas with perishing cells; those cells were defined as cells with less electron-density and apoptotic or necrotic features [Figure 27 & Figure 28].

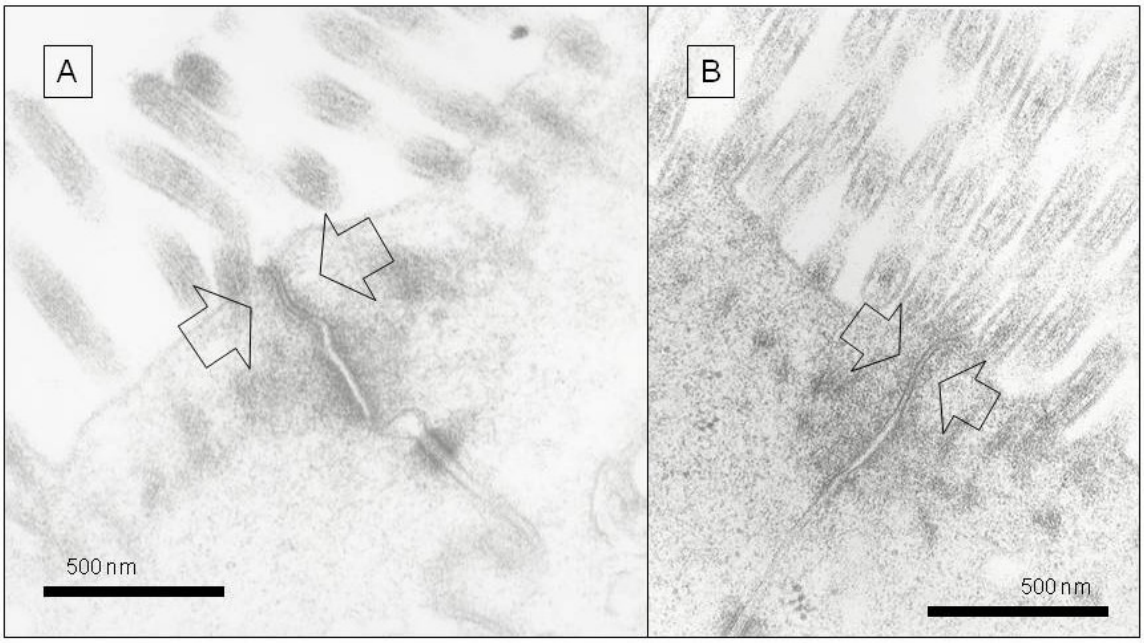

Figure 32. 'TJ in-between two Perishing Cells (A, cirrhotic patient) **and TJ between Healthy Enterocytes** (B, control)**'**

TJ-gaps in-between perishing enterocytes were detected and measured in 4 cirrhotic patients and one healthy control. The results are depicted in Table 38.

						Mann-Whitney U test	
		N	*Mean*	*Std. Deviation*	*Median*	*Mean Rank*	*U*	*Asymp. Sig. (2-tailed)*
Width of TJ gaps [nm]	Healthy areas (control group)	10	10.45	.46	10.56	6.3	8	**.037**
	Areas with perish. cells	5	12.67	2.15	12.55	11.4		

Table 38. 'Comparison of TJ-gap width' observed in healthy epithelial areas of controls (reference value) and areas with perishing enterocytes

A statistically significant difference was observed. Figure 33 depicts the observed results.

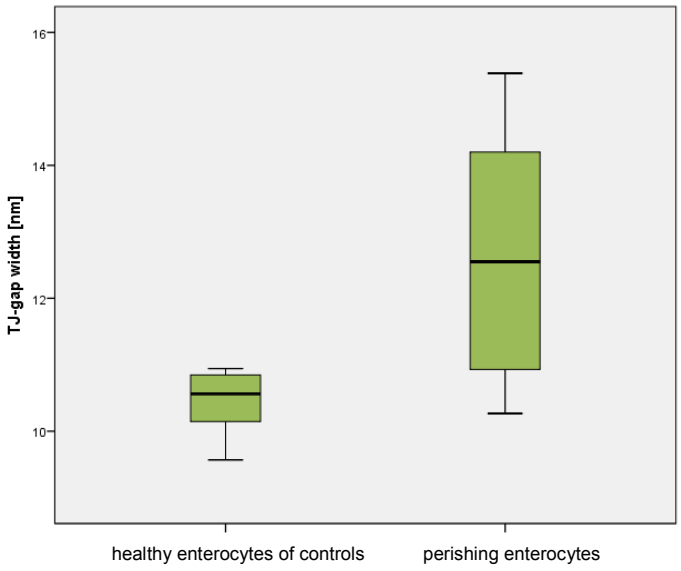

Figure 33. 'Boxplot: Differences in TJ- gap width' of healthy enterocytes (controls) and perishing enterocytes

3.5.4.1 Perijunctional Actomyosin Ring

The mean density of the perijunctional actomyosin complex (PAC) was measured in non-cirrhotic and cirrhotic participants. To eliminate disturbance variables such as slide thickness or printer-related effects, the obtained values were put in relation to the mean density of the microvillus located nearest to the TJ complex in the examined picture. Figure 34 gives an overview of the evaluation approach:

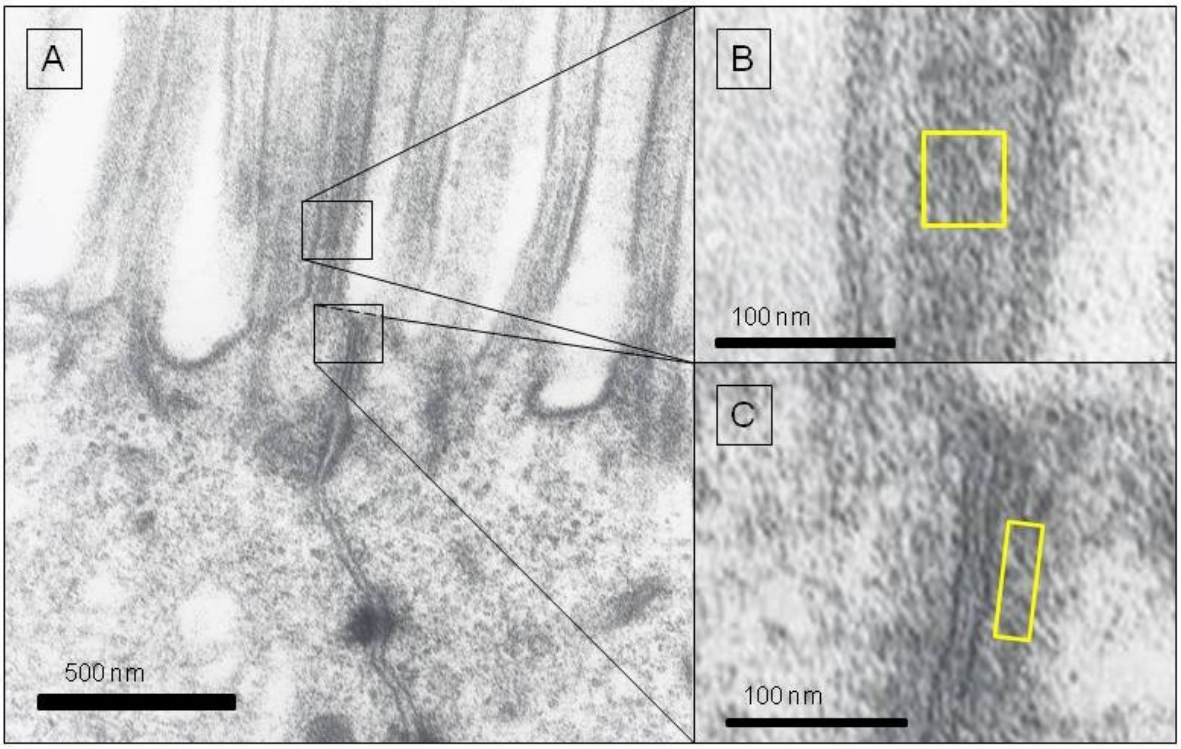

Figure 34. 'The Density of the Perijunctional Actomyosin Complex' A: To measure the density of the PAC, two areas of the picture were chosen: the microvillus located nearest to the TJ complex (figure B) and the TJ area itself (figure C). B: The density of the microvillus - more precisely of the bunches of actin filaments inside the microvillus, was measured to obtain a reference value. C: The area located just besides the TJ was then measured. This is where the actomyosin cytoskeleton is linked to TJ proteins. The space within the yellow rectangles was measured then.

Therefore, the mean density value of pixels within the yellow rectangles was measured as depicted in Figure 35:

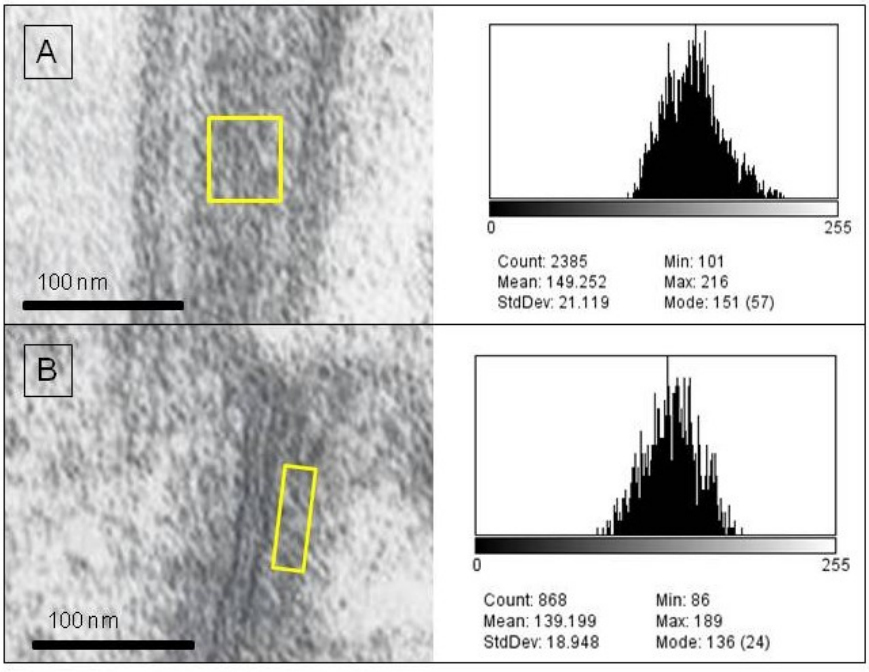

Figure 35. 'Measurement of the Mean Density using ImageJ'
ImageJ differentiates between 256 shades of gray, whereas 0 = black and 255 = white. A: The mean density of the bunches of actin filaments within the microvillus is 149; B: The mean density of the PAC in this picture is 139.

The PAC-density value of every image was set in relation the corresponding microvillus-density value and multiplied with the mean density value of all microvilli (=188, SD 22.2, n=341) to obtain the ***standardized PAC-density***.

Similarly as in the case of TJ-gap width, the standardized PAC-density of healthy controls, in epithelial areas without DIS or perishing enterocytes, was set as ***reference value*** and other density values were compared therewith. Comparing the reference value with the mean density of PACs in 'healthy' areas of cirrhotics, a *statistically significant difference* was observed:

					Student's t-test		
		N	*Mean*	*Std. Deviation*	*T*	*Sig. (2-tailed)*	*Mean diff.*
Density of PAC	Healthy areas (control group)	10	178	9.6	6.846	**.000**	25.9
	Healthy areas (cirrhosis group)	11	152	7.7			

Table 39. 'Comparison of the Mean Density of PAC' between non-cirrhotic and cirrhotic patients (both in healthy epithelial areas).

Furthermore, the reference value was compared with PAC-density measured in epithelial areas with DIS.

					Student's t-test		
		N	*Mean*	*Std. Deviation*	*T*	*Sig. (2-tailed)*	*Mean diff.*
Density of PAC	Healthy areas (control group)	10	178	9.6	3.982	**.001**	23.5
	Areas with DIS (cirrhosis group)	12	155	16.5			

Table 40. 'Comparison of the Mean Density of PAC' between healthy controls ('healthy' areas) and areas with DIS (distended intercellular space) in the cirrhosis group

Comparing patients within the cirrhosis group, no difference was observed between early-stage and advanced cirrhotics regarding both PAC-density of healthy areas and in epithelial areas with DIS.

Finally, PAC-density in areas with perishing cells of cirrhotics was compared with the reference value, whereas the most marked difference was observed.

						Mann-Whitney U test		
		N	*Mean*	*Std. Deviation*	*Median*	*Mean Rank*	*U*	*Asymp. Sig. (2-tailed)*
Density of PAC	Healthy areas (control group)	10	178	9.6	179	9.5	0	**.005**
	Areas with perish. cells (cirrhosis group)	4	141	11.4	141	2.5		

Table 41. 'Comparison of the Mean Density of PAC' between healthy controls ('healthy' areas) and areas with perishing cells in the cirrhosis group

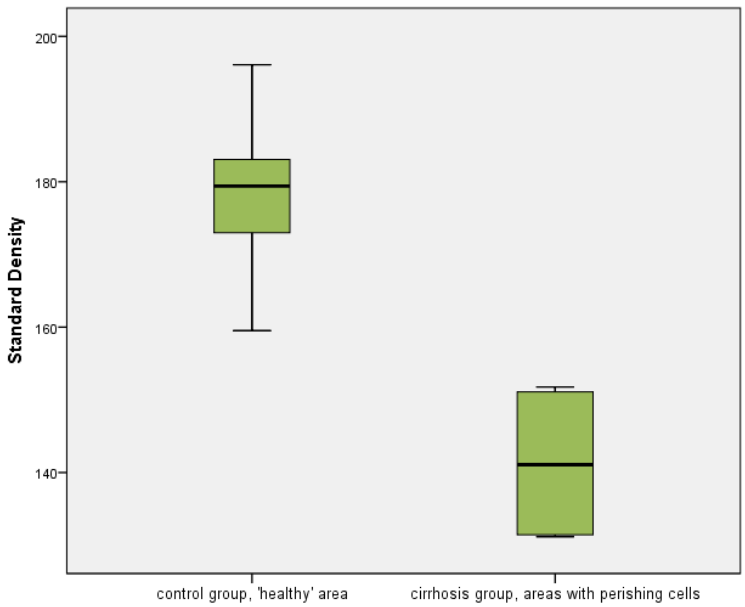

Figure 36. 'Standard Density Comparison' between 'healthy' areas (control group) and areas with perishing cells (cirrhosis group)

Figure 37 depicts the mean PAC-density of healthy enterocytes in non-cirrhotic patients (178; left side) and compares it to the mean density measured in perishing enterocytes (141; right side).

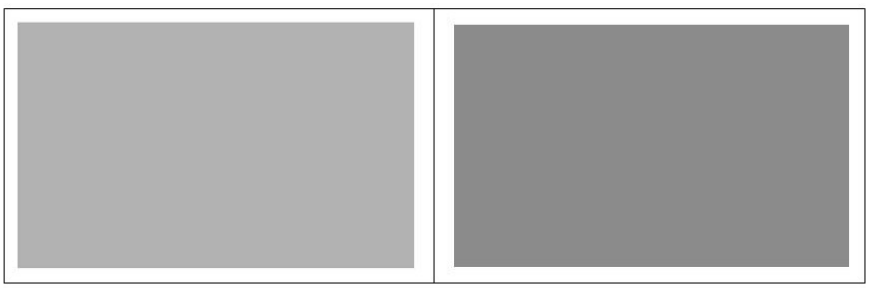

Figure 37.'Gray Value of PAC in Healthy Areas (left side) **and in Areas with Perish. Cells** (right side)**'**

3.5.5 Differences in Mitochondria

Electron microscopy in representative cases indicated an increase and dilatation of mitochondria, especially in enterocytes covering the villous tips. Furthermore, in perishing cells (less electron-dense), accumulation of secondary lysosomes with inhomogeneous content was found near swollen and injured mitochondria, referring to a mitochondrial origin of these structures. Figure 38 shows mitochondria of healthy enterocytes:

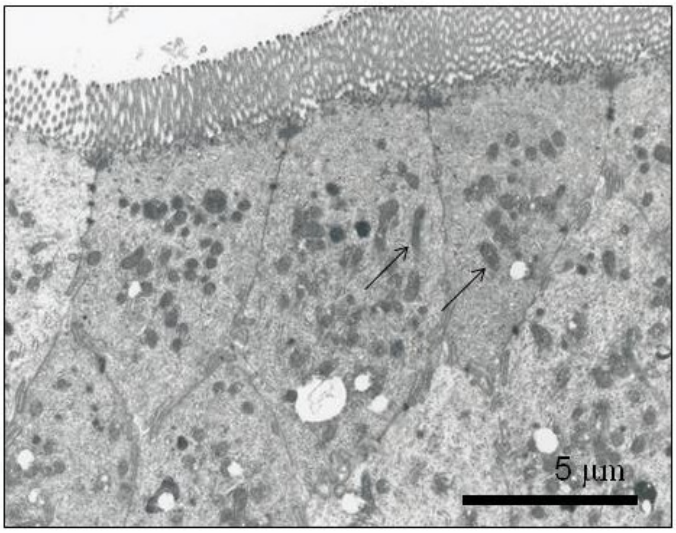

Figure 38. 'Mitochondria of Healthy Enterocytes (arrows)'

Figure 39 depicts mitochondria in cells located at the villous tips of cirrhotics:

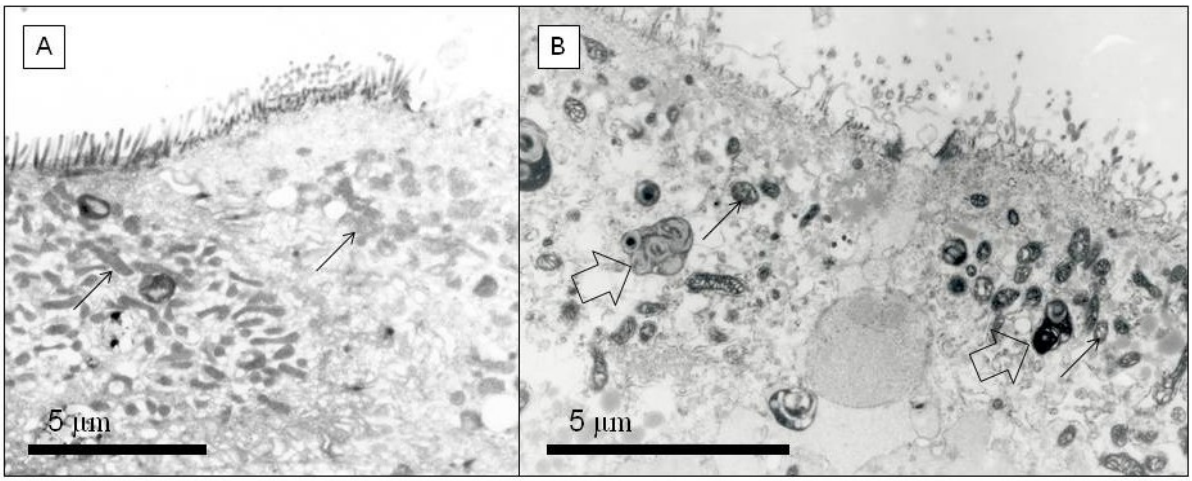

Figure 39 'Progression of Mitochondrial Injury to Autolysosomes' A: mitochondria of cirrhotic patient: the left cell shows an increase in mitochondria; the right, *perishing* enterocyte exhibits dilated mitochondria. B*: Perishing enterocytes* show large numbers of secondary autolysosomes, probably derived from mitochondria. (arrows = mitochondria, open arrows = autolysosomes)

3.5.6 Microvilli

In earlier studies, a decrease in the height/width ratio and distortion of enterocytes' microvilli were described (69,70). In our cirrhotic patients, *clearly* distorted microvilli were only observed in perishing cells located at the villous tips:

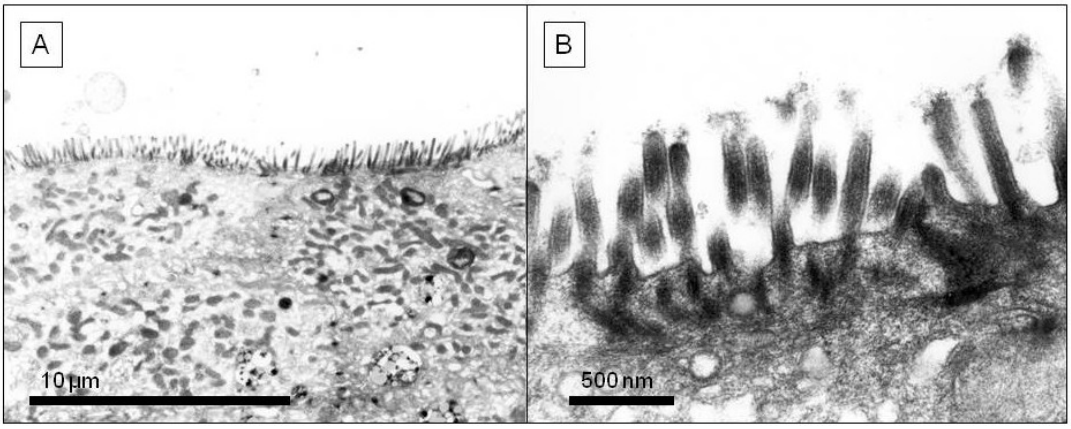

Figure 40. 'Distorted Microvilli in Perishing Cells of Cirrhotic Patients' A: Bar line: 10 µm; B: 500nm

Comparing the microvilli's height of perishing cells in cirrhotic patients with microvilli from healthy controls, the following results were obtained:

					Mann-Whitney U test		
		N	*Mean*	*Std. Deviation*	*Mean Rank*	*Mann-Whitney U*	*Asymp. Sig. (2-tailed)*
microvilli height [nm]	healthy cells (control group)	10	1579	209	10.5	0	**0.002**
	perishing cells (cirrhosis group)	5	713	104	3.0		

Table 42. 'Comparison of Microvilli Height' between healthy and perishing enterocytes. In 5 cirrhotics, microvilli height of perishing cells was measurable (totally 28 cell measured vs. 10 controls/34 cells).

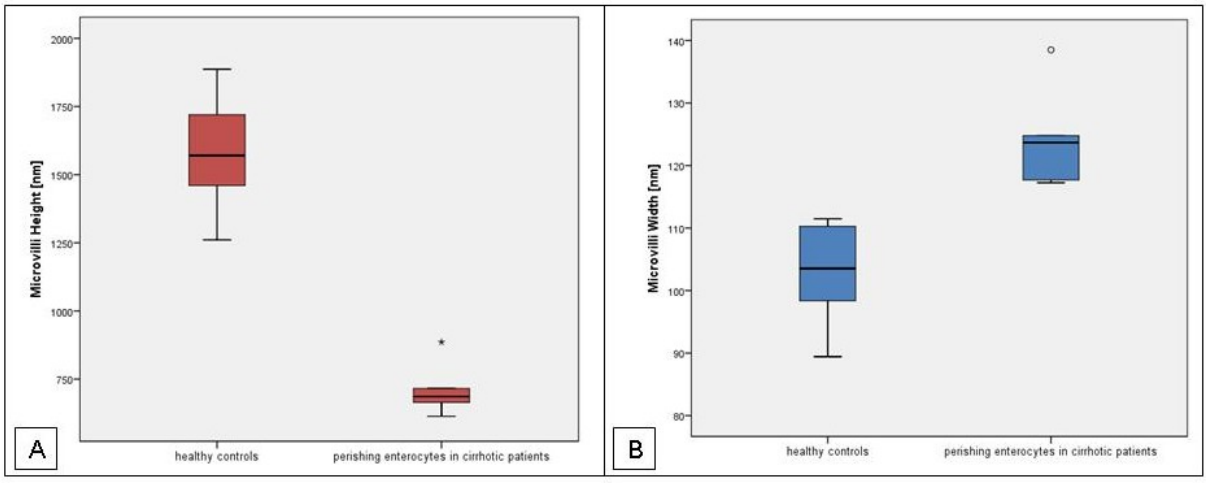

Figure 41. 'Boxplot: Comparison of Microvilli Height & Width' between healthy and perishing enterocytes

A statistically significant difference was also observed in the width of microvilli between healthy enterocytes of control patients and perishing enterocytes of cirrhotics. As shown in Figure 41, the height of microvilli decreased, whereas the width increased. Table 43 shows the statistical results regarding microvilli width:

						Mann-Whitney U test	
		N	*Mean*	*Std. Deviation*	*Mean Rank*	*Mann-Whitney U*	*Asymp. Sig. (2-tailed)*
Microvilli width [nm]	healthy cells (control group)	10	103	7.1	5.5	0	**0.002**
	perishing cells (cirrhosis group)	5	124	8.6	13.0		

Table 43. 'Comparison of Microvilli Width' between healthy and perishing enterocytes

Subsequently, microvilli of ***'intact' enterocytes*** were compared between healthy controls and patients with chronic liver disease. In the cirrhosis group, the brush border appeared less high and the individual microvilli less densely packed than in the control group. Figure 42 shows representative cases of microvilli in cirrhotic and healthy individuals.

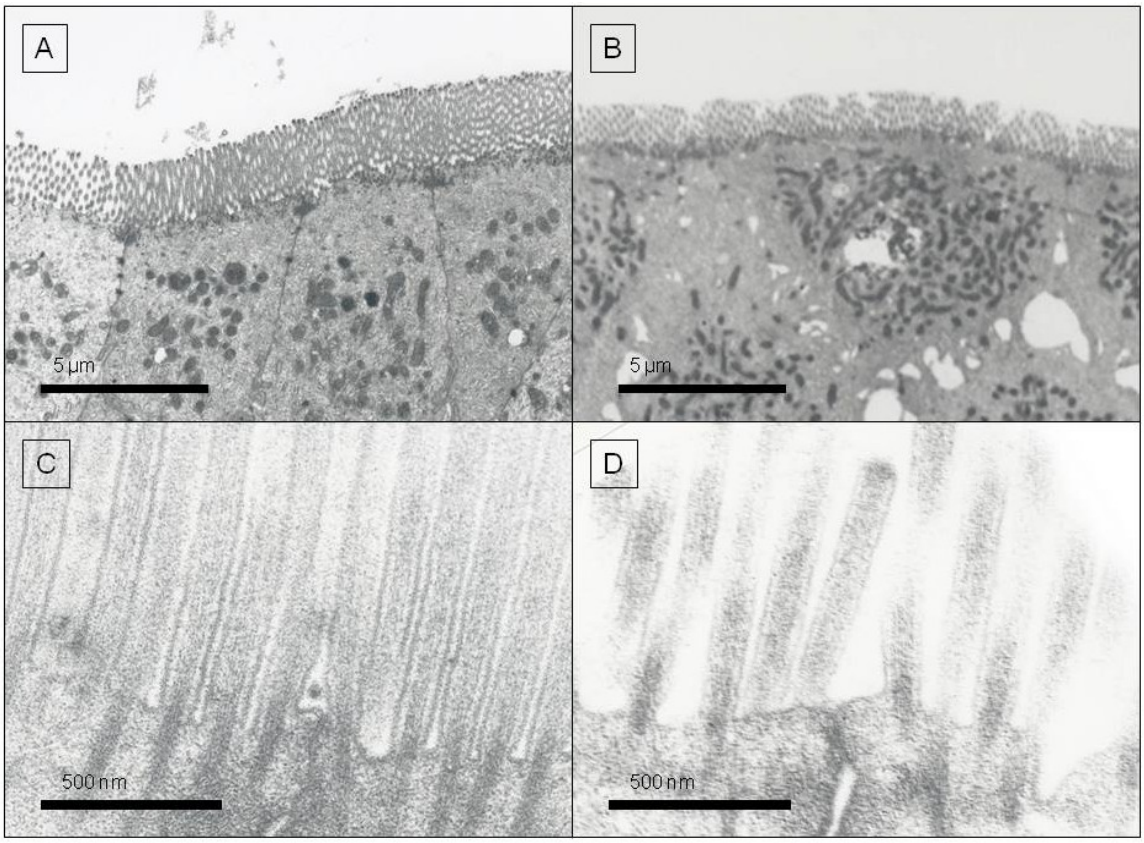

Figure 42. 'Brush Border in Control and Cirrhosis Patients' A, C: Microvilli of a healthy control; they stand close to each other. B, D: Microvilli of a cirrhotic patient; they seem shorter and less densely packed

Statistical analysis of the measured values revealed a significant decrease in the height of microvilli between control and cirrhosis patients that was not as pronounced as between healthy enterocytes and perishing cells.

					Student's t-test		
		N	*Mean*	*Std. Deviation*	*T*	*Sig. (2-tailed)*	*Mean diff.*
microvilli height [nm]	healthy cells no cirrhosis	10	1579	209	3.626	**0.002**	398.2
	healthy cells cirrhosis	10	1181	278			

Table 44. 'Comparison of Microvilli Height' between healthy enterocytes of control and cirrhosis patients

With regard to the width of microvilli, no difference was observed between healthy enterocytes from controls (mean = 103 nm; SD = 7; n = 10 patients) and cirrhotic patients (mean = 106 nm; SD 5; n = 12 patients).

3.6 Detection of bacterial/fungal DNAs

In summary, seven cirrhotic patients were examined for bacterial and/or fungal DNAs in peripheral venous blood. Five of them were cirrhotics with a Child-Pugh stage A (72%); one of them was Child-Pugh B (14%) and one Child-Pugh C (14%).

In *none of them*, bacterial or fungal DNA was detected.

4 Discussion

In summary, several ***morphological alterations*** in distal duodenal mucosa of cirrhotic patients were observed in both light and electron microscopy. Light-microscopic findings included distended intercellular spaces (in the basal parts of enterocytes), vacuolization of the cytoplasm & an increased number of 'pale cells' at the villous tips, increased number of denuded villi, edema & fibrosis of the lamina propria and larger capillary diameters in cirrhotic patients. Electron microscopy showed morphologically preserved cell/cell-connections at the enterocytes' luminal borders, but, an increased density of the perijunctional actomyosin complex, a slightly increased TJ-gap width in epithelial areas with DIS (in the lower parts of enterocytes) and in-between perishing enterocytes, shorter & rarified microvilli and accumulation of vacuoles in cells covering the villous tips as main findings in the cirrhosis group.

Differences in ***gastrointestinal permeability*** between cirrhotic patients and healthy individuals were consistent with results from previous studies, indicating an increase in small intestinal permeability for macromolecules (by means of the lactulose/mannitol ratio) and an increase in gastric permeability for sucrose. The lactulose/mannitol ratio significantly correlated with the Child-Pugh score and the number of denuded villi. Mannitol excretion was not impaired until decompensated cirrhosis was present, since mannitol uptake is more likely depending on total absorptive surface area than on integrity of the paracellular barrier (16) and light-microscopic analysis in this study revealed that duodenal villi suffer a loss in height only in advanced liver disease. Moreover, the wider distribution of excretion values especially in advanced cirrhotics [indicated by an increase in interquartile range; Figure 11ABC] in comparison with healthy individuals emphasizes the hypothesis that intestinal permeability is not increased in all patients with advanced liver disease and might be affected by additional factors. In fact, %L/%M excretion ratio was highly pathological in three patients: two (of four) advanced cirrhotics with massive ascites and esophageal varices (*patient 2*: Child's C, 13 points, massive ascites, small esophageal varices; *patient 4*: Child's B, 8 points, massive ascites, small esophageal varices) and in one early-stage cirrhotic treated with TIPS implantation (*patient 7*: Child's A, 6 points, no ascites, scars after variceal banding,). Similar considerations apply to sucrose excretion, where the three highest values were observed in the same patients, but only two results were pathological (*patient 2* and *7*).

4.1 Differences in Tight-Junction Ultrastructure

TJ-gap width of cirrhotic patients in epithelial areas without DIS or perishing enterocytes did not differ from the reference value ('healthy' areas of controls). In contrast, a widened TJ gap was observed in epithelial areas presenting with DIS and in-between perishing enterocytes. Despite the fact that a statistically significant difference was detected in both values (compared to the reference value), the clinical relevance seems discussible considering the poor difference and the maintained morphological integrity of TJs. However, correlating the lactulose/mannitol excretion ratio with the appearance of villi with DIS (and therefore also with the appearance of TJs with extended gap widths), a clear tendency, but no significant result was observed, probably owing to the small number of cases.

Since solutes used in the permeability test were larger than 4 Å (e.g. lactulose = 9.5 Å), they were suspected of transposing the TJ barrier via the ***non-pore pathway*** that has been

shown to react sensitive to ***cytoskeletal disruption*** and any form of ***cellular injury*** (34) [see 1.4]. In fact, increased permeability via the non-pore pathway seems to be mediated by an enhanced production of nitric oxide: increased NO synthesis was observed together with increased myosin light chain phosphorylation, causing a contraction of the actomyosin ring and alterations in TJ-barrier function (36,105). Hence, *Citi et al.* suggested a model where cortical tension induced by the actomyosin cytoskeleton mechanically influences the permeability of TJs. Increased paracellular permeability therefore is also suspected to result from a contraction of the perijunctional actomyosin ring, measurable by an increase in density of the PAC:

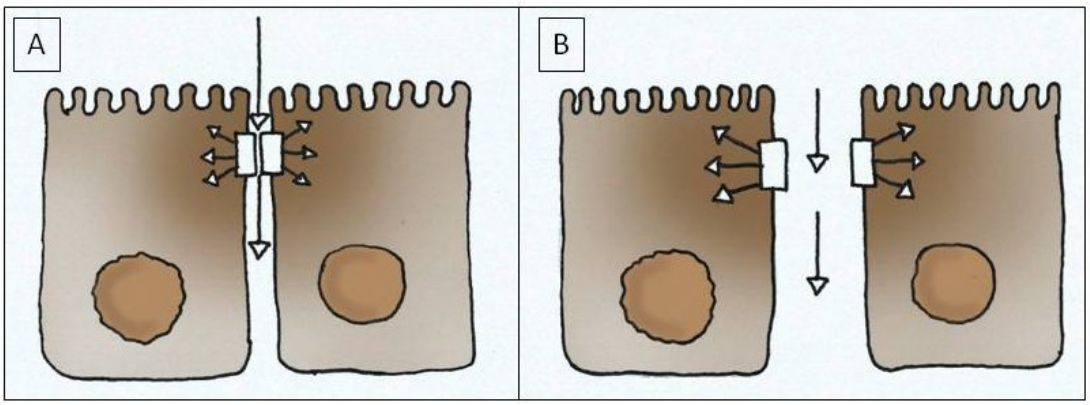

Figure 43. 'Schematic Representation of the Possible Influence of Alterations in the Junctional Actomyosin Ring on TJs' Barrier Function' Under normal circumstances, TJs are exposed to a physiologic 'tonic' contraction (A), but, when the actomyosin ring is contracted (B), the increased tension induces adjacent epithelial cells to spread apart and increase the gap width in the TJ area. Therefore, paracellular permeability might be increased. [adapted from (51)]

In contrast to TJ-gap width, mean density of PAC was not only increased in areas with DIS or perishing cells, but also in 'healthy' epithelial areas of cirrhotics. Comparing the reference value (control group, 'healthy' enterocytes) with values from areas with DIS or perishing cells, the difference was even more pronounced. Together with the gradual increase in TJ-gap width from *'healthy' epithelial areas* (located mainly at the bases and along the sides of the villi) via *epithelial areas with DIS* (located mainly along the sides of the villi and at the villous tips) to *areas with perishing enterocytes* (located at the villous tips), a stepwise process is suspected, whereby contraction of the PAC occurs prior to an increase in TJ-gap width, which is only affected when additional factors (like cellular injury) are present.

4.2 The Role of Portal Hypertension

Previous studies suggested PH (and its effects on intestinal mucosa) to represent an important connecting link between liver damage and altered intestinal function (65,67,68,80,83,84). In this study, dilated capillaries and edema of the lamina propria – as correlates of PH - were more frequently observed in the patient group when compared with healthy individuals. Furthermore, the influence of PH on intestinal permeability is emphasized by our findings, since the lactulose/mannitol excretion ratio showed a clear tendency to correlate with the mean diameter of capillaries in the lamina propria of cirrhotics.

In fact, some histological alterations were found ***especially at the villous tips*** including DIS in-between the enterocytes' lower portions and vacuolar degeneration of epithelial cells. Staining with caspase-3 antibodies suggested an augmented number of cells undergoing apoptosis at the villous tips, as it was already depicted in previous trials (67). In electron-microscopy analysis, cells in these areas presented with signs of apoptosis, but also, features of necrotic cell death were revealed. The 'pale cells' observed in toluidine-blue staining presented with necrotic features on electron microscopy and therefore, might indicate enterocytes in a necrotic or pre-necrotic state (106). However, since those epithelial changes were the most pronounced at the tips of the villi – where oxygen tension is lower than it is in arterial blood even under normal conditions (2) -, ***hypoxic injury of epithelial cells*** caused by altered blood flow in the splanchnic bed might contribute to this phenomenon. A decrease in oxygen concentration in intestinal mucosa of patients with PHE has been proven in studies using endoscopic reflectance spectrophotometry (107). Furthermore, similar histological changes as in this study were also observed in the small intestine of rats challenged with ischemia and ischemia/reperfusion injury (108). However, congestive and hypoxic conditions in the intestines are suspected of being involved in the ***synthesis of nitric oxide***, probably closing the gap between liver injury, portal hypertension, cytoskeletal alterations and TJ alterations.

Furthermore, besides alterations in oxygen supply, vascular shear stress, direct effects of alcohol or its metabolites, and the confrontation of immune cells with transposing bacterial products are currently discussed as factors contributing to an increased NO production in the intestines of cirrhotic patients. Apart from the induction of cytoskeletal alterations (directing towards the cytoskeleton-TJ axis), a surfeit of NO and the related generation of ROS/RNS are suspected to interfere with mitochondrial respiration and therefore, to

disrupt the energy balance of cells. (2,28,109). During their migration from the crypts to the villous tips, enterocytes of cirrhotic patients – injured by oxidative/nitrosative stress -, might increasingly and untimely undergo ***apoptosis*** (110), or, if energy stores do not suffice to enable controlled cell degradation, ***necrosis*** respectively (111,112). Therefore, the gradual increase of TJ-gap width and PAC-density from the bases to the tips of the villi [see 4.1] probably reflects the influence of increasing hypoxic injury along the crypt-villus axis on TJ ultrastructure.

4.2.1 Fluid Accumulation

On electron microscopy, increased presence of vacuoles underneath the luminal border was observed mainly in cells covering the villous tips [Figure 29]. Thereby, PH and splanchnic congestion seem to hinder the effluent of fluid and solutes to the liver and lead to their accumulation in the intestinal mucosa – even within enterocytes, which is probably reflected by the appearance of these vacuoles. Furthermore, fluid congestion might also contribute to the development of DIS and even denuded villi, by way of fluid-accumulation in the extracellular space, mechanical separation of the enterocytes at the villous tips and a weakening of their anchorage in the underlying layer. In fact, basolateral gaps similar to the DIS of our cirrhotics physiologically appear in the epithelium of the large intestines, where a vigorous resorption of water takes place (113). In toluidine-blue staining, we observed that the distended intercellular space was filled with some amorphous substance presenting the same dye-ability as it was seen within capillaries and lymph vessels [Figure 44]. Therefore, the appearance of DIS, the detachment of the epithelium from the lamina propria and the appearance of ***denuded villi*** might represent consecutive stages of epithelial damage caused by fluid accumulation in patients with cirrhosis. Due to the high incidence of denuded villi, the 'true' number of apoptotic and 'pale' cells might be underestimated in those patients. Reversely, increased cell-turnover and exfoliation of apoptotic/necrotic enterocytes at the villous tips are also suspected to contribute to the appearance of denuded villi in cirrhotic patients.

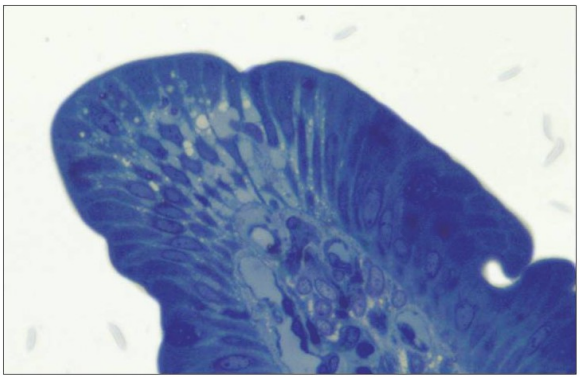

Figure 44. 'Villous Tip with DIS' The intercellular space is filled with some amorphous substance (toluidine-blue stain, 200x)

However, DIS and the consecutive induction of lateral tension could influence on the permeability of TJs, since it has been shown that mechanically applied lateral tension is capable of altering tight junction morphology (114). This is also consistent with our findings of increased TJ-gap widths in-between cells located in areas with DIS.

4.3 Viable and Non-Viable Bacterial Translocation

Previous studies have shown that bacterial DNA is often detectable in both serum and ascitic fluid of cirrhotic patients (92). Since bacterial DNA was not detected continuously in repeated measurements, but rather persisted for variable periods of time, BT was suggested to be a ***transient occurrence*** (92). Furthermore, bacteria and their products are eliminated much faster from the portal vein than from MLN (77) and therefore, testing blood samples only at one point – as it was performed in this study - may underestimate the prevalence of BT to MLN.

In fact, translocation of ***viable bacteria*** was early assumed to follow rather a transcellular than a paracellular pathway, unless there is physical damage to the epithelium (74,88). In this study, histological analysis of duodenal biopsy specimens revealed both increased appearance of perishing cells and increased presence of denuded villi. *Dickinson et al.* challenged rats with endotoxin and observed exfoliation of apoptotic cells at the tips of the villi; there, bacterial entry was demonstrated by use of confocal microscopy, ***emphasizing the theory of luminal bacteria to transpose the epithelial barrier in the area of perishing cells or denuded villi*** (115). Moreover, we showed that presence of denuded villi might also affect permeability for macromolecules, since the lactulose/mannitol excretion ratio significantly correlated with the appearance of those epithelial lesions in patients with cirrhosis.

Nevertheless, even if translocation of viable microorganisms seems unlikely to occur via slightly increased TJ-gap widths, TJ impairment is suspected to contribute to the uptake of smaller luminal content including toxins, antigens or bacterial products like LPS in diseases presenting with an impaired gut barrier function: *Gitter et al.* demonstrated that leaks in the epithelial barrier after administration of TNF-α were only about half based on the induction of apoptosis, whereas the other half of increased permeability was caused by ***degradation of tight junctions*** in non-apoptotic areas (116). Therefore, the role of TJ alterations in gut barrier dysfunction should not be underestimated.

4.4 The Circle of Bacterial Translocation

So far, a causal factor initiating the BT cascade and an exact sequence of events regarding BT and liver disease are not given. In the light of earlier findings, it rather seems as if the various alterations mutually influence each other and form a ***self-perpetuating circle***, which can be initiated at whatever point - liver, intestinal barrier or luminal content:

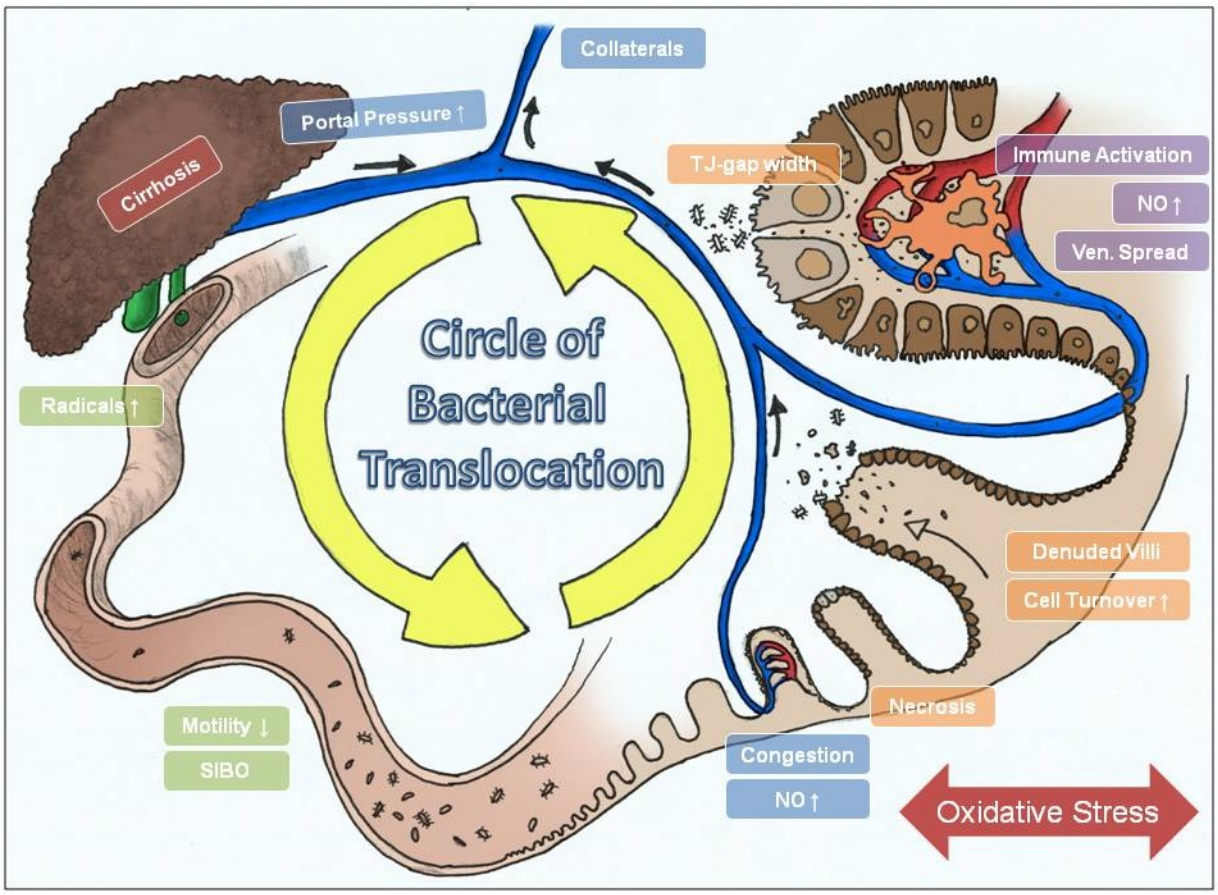

Figure 45. 'Schematic Representation of a *possible Circle of Bacterial Translocation*' Regardless of the etiology of cirrhosis, the progression of liver disease is usually associated with *portal hypertension, vascular congestion* and *shear stress* in the splanchnic bed [blue rectangles]. The consecutive *production of nitric oxide* and *oxidative/nitrosative stress* forces enterocytes to undergo *apoptosis & necrosis* and leads to a *contraction of the PAC* that, in advanced stages, affects *TJ-gap width*. Increased cell-turnover as well as the congestion of fluid within the epithelium (leading to a mechanical separation of enterocytes and a weakening of their anchorage in underlying layers) might explain the higher incidence of *denuded villi* in cirrhotics [orange rectangles]. Besides, oxidative/nitrosative stress might also originate in the injured liver and reach the intestinal lumen via bile flow. [green rectangles, see (117)]. *Decreased gut motility* and *overgrowth of selected bacteria* are regarded as additional factors influencing luminal composition and the intestinal epithelium [green rectangles]. However, toxins, antigens and bacterial products such as LPS are suspected to transpose the epithelial barrier within areas of increased TJ-gap width, perishing cells or denuded villi. Viable microorganisms might benefit from the exfoliation of epithelial cells from the villous tips. In the lamina propria, they are involved in the *activation of immune cells* (such as macrophages) and their production of pro-inflammatory cytokines &, again, NO [purple rectangles]. Finally, microorganisms as well as their products reach the vessel systems, the liver and - due to the development of collaterals - the systemic circulation. Since their accumulation in the liver aggravates *hepatic injury* and *cirrhotic remodeling*, ***the circle of bacterial translocation*** is completed. (2,17,28,34,36,39,57,65,67,68,70,72-74,79,82,85,87,88, 95,109,115,116)

In conclusion, it seems as if bacterial translocation in patients with cirrhosis is a multi-etiological phenomenon that still offers a variety of uncertainties. A wide range of structural alterations – on both the light- and electron-microscopic level – in small intestinal biopsy specimens of cirrhotics has been detected. Only the number of denuded villous tips correlated significantly with an increased lactulose/mannitol excretion ratio. Furthermore, a few other variables, including appearance of DIS and mean capillary diameters, showed a marked tendency to correlate with permeability values. Nevertheless, it remains unclear *to what an extent* the individual changes influence paracellular solute flux and whether the translocation of viable microorganisms and development of overt infection is linked to this process.

Further studies in larger cohorts of cirrhotic patients are needed to confirm our findings and to reach statistical significance in some indicated alterations. Furthermore, more reliable markers of viable and non-viable bacterial translocation (repeated assessment of bacteremia or the detection of bacterial products like LPS in the blood plasma) might help distinguish between different mechanisms facilitating those two phenomena.

5 References

(1) Dave M, Higgins PD, Middha S, Rioux KP. The human gut microbiome: current knowledge, challenges, and future directions. Transl Res 2012 Oct;160(4):246-257.

(2) Balzan S, de Almeida Quadros C, de Cleva R, Zilberstein B, Cecconello I. Bacterial translocation: overview of mechanisms and clinical impact. J Gastroenterol Hepatol 2007 Apr;22(4):464-471.

(3) Damman CJ, Miller SI, Surawicz CM, Zisman TL. The microbiome and inflammatory bowel disease: is there a therapeutic role for fecal microbiota transplantation? Am J Gastroenterol 2012 Oct;107(10):1452-1459.

(4) EASL European Association for the Study of the Liver. The Liver: Vital for Life. Available at: http://www.easl.eu/assets/application/files/19d80b59a26a03c_file.pdf. Accessed May, 2012.

(5) Klinke R, Pape HC, Silbernagl S. Physiologie. 5. Auflage ed. Stuttgart: Georg Thieme Verlag; 2005.

(6) ECDC European Centre for Disease Prevention and Control. Epidemiological Report on Communicable Diseases. EU statistical yearbook 2006-2007 2007 May.

(7) Statistik Austria. Jahrbuch der Gesundheitsstatistik 2006. Wien: Bundesanstalt Statistik Österreich; 2007.

(8) Rodés J, Benhamou J, Blei A, Reichen J, Rizzetto M. Textbook of hepatology: From basic science to clinical practice. 3rd edition ed. Malden, Mass: Blackwell; 2007.

(9) Denk H, Dienes HP, Trauner M. Leber und intrahepatische Gallenwege. In: Böcker W, Denk H, Heitz PU, editors. Pathologie. 3. Auflage ed. München: Elsevier; 2004. p. 755-798.

(10) Anthony PP, Ishak KG, Nayak NC, Poulsen HE, Scheuer PJ, Sobin LH. The morphology of cirrhosis. Recommendations on definition, nomenclature, and classification by a working group sponsored by the World Health Organization. J Clin Pathol 1978 May;31(5):395-414.

(11) Herold G. Innere Medizin. Eine vorlesungsorientierte Darstellung. 2009th ed. Köln: Herold Innere Medizin; 2009.

(12) Heidelbaugh JJ, Bruderly M. Cirrhosis and chronic liver failure: part I. Diagnosis and evaluation. Am Fam Physician 2006 Sep 1;74(5):756-762.

(13) Appenrodt B, Trebicka J, Sauerbruch T. Complications of liver cirrhosis. Dtsch Med Wochenschr 2011 Aug;136(31-32):1601-1604.

(14) Heidelbaugh JJ, Sherbondy M. Cirrhosis and chronic liver failure: part II. Complications and treatment. Am Fam Physician 2006 Sep 1;74(5):767-776.

(15) van Erpecum KJ. Ascites and spontaneous bacterial peritonitis in patients with liver cirrhosis. Scand J Gastroenterol Suppl 2006;(243)(243):79-84.

(16) Pascual S, Such J, Esteban A, Zapater P, Casellas JA, Aparicio JR, et al. Intestinal permeability is increased in patients with advanced cirrhosis. Hepatogastroenterology 2003 Sep-Oct;50(53):1482-1486.

(17) Campillo B, Pernet P, Bories PN, Richardet JP, Devanlay M, Aussel C. Intestinal permeability in liver cirrhosis: relationship with severe septic complications. Eur J Gastroenterol Hepatol 1999 Jul;11(7):755-759.

(18) Almeida J, Galhenage S, Yu J, Kurtovic J, Riordan SM. Gut flora and bacterial translocation in chronic liver disease. World J Gastroenterol 2006 Mar 14;12(10):1493-1502.

(19) P. Douschan, H. Olschewsky, R. Lipp, R. Stauber. Hepatoplumary Syndrome in Patients with Compensated Cirrhosis. Graz: Medizinische Universität Graz; 2012.

(20) Otto HF, Gabbert HE. Jejunum und Ileum. In: Böcker W, Denk H, Heitz PU, editors. Pathologie. 3. Auflage ed. München: Elsevier Urban & Fischer; 2004. p. 699-718.

(21) Shen L. Functional morphology of the gastrointestinal tract. Curr Top Microbiol Immunol 2009;337:1-35.

(22) Vereecke L, Beyaert R, van Loo G. Enterocyte death and intestinal barrier maintenance in homeostasis and disease. Trends Mol Med 2011 Oct;17(10):584-593.

(23) Lüllmann-Rauch R. Taschenlehrbuch Histologie. 2. Auflage ed. Stuttgart: Georg Thieme Verlag; 2006.

(24) Marcial MA, Carlson SL, Madara JL. Partitioning of paracellular conductance along the ileal crypt-villus axis: a hypothesis based on structural analysis with detailed consideration of tight junction structure-function relationships. J Membr Biol 1984;80(1):59-70.

(25) Madara JL. Warner-Lambert/Parke-Davis Award lecture. Pathobiology of the intestinal epithelial barrier. Am J Pathol 1990 Dec;137(6):1273-1281.

(26) Cereijido M, Anderson JM. Introduction: Evolution of ideas on the tight junction. In: Cereijido M, Anderson JM, editors. Tight junctions. 2nd ed. Boca Raton: CRC Press LLC; 2001. p. 1-18.

(27) Groschwitz KR, Hogan SP. Intestinal barrier function: molecular regulation and disease pathogenesis. J Allergy Clin Immunol 2009 Jul;124(1):3-20; quiz 21-2.

(28) Anderson JM. Molecular structure of tight junctions and their role in epithelial transport. News Physiol Sci 2001 Jun;16:126-130.

(29) FARQUHAR MG, PALADE GE. Junctional complexes in various epithelia. J Cell Biol 1963 May;17:375-412.

(30) Amasheh S, Fromm M, Gunzel D. Claudins of intestine and nephron - a correlation of molecular tight junction structure and barrier function. Acta Physiol (Oxf) 2011 Jan;201(1):133-140.

(31) Hartsock A, Nelson WJ. Adherens and tight junctions: structure, function and connections to the actin cytoskeleton. Biochim Biophys Acta 2008 Mar;1778(3):660-669.

(32) Franke WW. Discovering the molecular components of intercellular junctions--a historical view. Cold Spring Harb Perspect Biol 2009 Sep;1(3):a003061.

(33) Bjarnason I, MacPherson A, Hollander D. Intestinal permeability: an overview. Gastroenterology 1995 May;108(5):1566-1581.

(34) Anderson JM, Van Itallie CM. Physiology and function of the tight junction. Cold Spring Harb Perspect Biol 2009 Aug;1(2):a002584.

(35) Furuse M. Molecular basis of the core structure of tight junctions. Cold Spring Harb Perspect Biol 2010 Jan;2(1):a002907.

(36) Cunningham KE, Turner JR. Myosin light chain kinase: pulling the strings of epithelial tight junction function. Ann N Y Acad Sci 2012 Jul;1258:34-42.

(37) Bauer HC, Traweger A, Zweimueller-Mayer J, Lehner C, Tempfer H, Krizbai I, et al. New aspects of the molecular constituents of tissue barriers. J Neural Transm 2011 Jan;118(1):7-21.

(38) Harhaj NS, Antonetti DA. Regulation of tight junctions and loss of barrier function in pathophysiology. Int J Biochem Cell Biol 2004 Jul;36(7):1206-1237.

(39) Steed E, Balda MS, Matter K. Dynamics and functions of tight junctions. Trends Cell Biol 2010 Mar;20(3):142-149.

(40) Cummins PM. Occludin: one protein, many forms. Mol Cell Biol 2012 Jan;32(2):242-250.

(41) Feldman GJ, Mullin JM, Ryan MP. Occludin: structure, function and regulation. Adv Drug Deliv Rev 2005 Apr 25;57(6):883-917.

(42) Hartsock A, Nelson WJ. Adherens and tight junctions: structure, function and connections to the actin cytoskeleton. Biochim Biophys Acta 2008 Mar;1778(3):660-669.

(43) Furuse M, Hirase T, Itoh M, Nagafuchi A, Yonemura S, Tsukita S, et al. Occludin: a novel integral membrane protein localizing at tight junctions. J Cell Biol 1993 Dec;123(6 Pt 2):1777-1788.

(44) Saitou M, Fujimoto K, Doi Y, Itoh M, Fujimoto T, Furuse M, et al. Occludin-deficient embryonic stem cells can differentiate into polarized epithelial cells bearing tight junctions. J Cell Biol 1998 Apr 20;141(2):397-408.

(45) Saitou M, Furuse M, Sasaki H, Schulzke JD, Fromm M, Takano H, et al. Complex phenotype of mice lacking occludin, a component of tight junction strands. Mol Biol Cell 2000 Dec;11(12):4131-4142.

(46) Furuse M, Fujita K, Hiiragi T, Fujimoto K, Tsukita S. Claudin-1 and -2: novel integral membrane proteins localizing at tight junctions with no sequence similarity to occludin. J Cell Biol 1998 Jun 29;141(7):1539-1550.

(47) Kubota K, Furuse M, Sasaki H, Sonoda N, Fujita K, Nagafuchi A, et al. Ca(2+)-independent cell-adhesion activity of claudins, a family of integral membrane proteins localized at tight junctions. Curr Biol 1999 Sep 23;9(18):1035-1038.

(48) Will C, Fromm M, Muller D. Claudin tight junction proteins: novel aspects in paracellular transport. Perit Dial Int 2008 Nov-Dec;28(6):577-584.

(49) Furuse M, Sasaki H, Tsukita S. Manner of interaction of heterogeneous claudin species within and between tight junction strands. J Cell Biol 1999 Nov 15;147(4):891-903.

(50) Krause G, Winkler L, Mueller SL, Haseloff RF, Piontek J, Blasig IE. Structure and function of claudins. Biochim Biophys Acta 2008 Mar;1778(3):631-645.

(51) Citi S, Cordenonsi M. Tight junction proteins. Biochim Biophys Acta 1998 Nov 19;1448(1):1-11.

(52) Steinberg MS, Shida H, Giudice GJ, Shida M, Patel NH, Blaschuk OW. On the molecular organization, diversity and functions of desmosomal proteins. Ciba Found Symp 1987;125:3-25.

(53) Shen L, Weber CR, Raleigh DR, Yu D, Turner JR. Tight junction pore and leak pathways: a dynamic duo. Annu Rev Physiol 2011;73:283-309.

(54) Claude P. Morphological factors influencing transepithelial permeability: a model for the resistance of the zonula occludens. J Membr Biol 1978 Mar 10;39(2-3):219-232.

(55) Fihn BM, Sjoqvist A, Jodal M. Permeability of the rat small intestinal epithelium along the villus-crypt axis: effects of glucose transport. Gastroenterology 2000 Oct;119(4):1029-1036.

(56) Turner JR, Rill BK, Carlson SL, Carnes D, Kerner R, Mrsny RJ, et al. Physiological regulation of epithelial tight junctions is associated with myosin light-chain phosphorylation. Am J Physiol 1997 Oct;273(4 Pt 1):C1378-85.

(57) Shen L, Turner JR. Role of epithelial cells in initiation and propagation of intestinal inflammation. Eliminating the static: tight junction dynamics exposed. Am J Physiol Gastrointest Liver Physiol 2006 Apr;290(4):G577-82.

(58) Hollander D. The intestinal permeability barrier. A hypothesis as to its regulation and involvement in Crohn's disease. Scand J Gastroenterol 1992 Sep;27(9):721-726.

(59) Arrieta MC, Bistritz L, Meddings JB. Alterations in intestinal permeability. Gut 2006 Oct;55(10):1512-1520.

(60) Cichoz-Lach H, Celinski K, Slomka M, Kasztelan-Szczerbinska B. Pathophysiology of portal hypertension. J Physiol Pharmacol 2008 Aug;59 Suppl 2:231-238.

(61) Blendis L, Wong F. The hyperdynamic circulation in cirrhosis: an overview. Pharmacol Ther 2001 Mar;89(3):221-231.

(62) Groszmann RJ, Abraldes JG. Pathogenesis of portal hypertension. In: Rodés J, Benhamou J, Blei A, Reichen J, Rizzetto M, editors. Textbook of hepatology: From basic science to clinical practice. 3rd edition ed. Malden, Mass: Blackwell; 2007. p. 630-639.

(63) Hennenberg M, Trebicka J, Sauerbruch T, Heller J. Mechanisms of extrahepatic vasodilation in portal hypertension. Gut 2008 Sep;57(9):1300-1314.

(64) Cubillas R, Rockey DC. Portal hypertensive gastropathy: a review. Liver Int 2010 Sep;30(8):1094-1102.

(65) McCormack TT, Sims J, Eyre-Brook I, Kennedy H, Goepel J, Johnson AG, et al. Gastric lesions in portal hypertension: inflammatory gastritis or congestive gastropathy? Gut 1985 Nov;26(11):1226-1232.

(66) Chapman RW, Angus PW. The effect of liver disease on the gastrointestinal tract. In: Rodés J, Benhamou J, Blei A, Reichen J, Rizzetto M, editors. Textbook of hepatology: From basic science to clinical practice. 3rd edition ed. Malden, Mass: Blackwell; 2007. p. 1798-1803.

(67) Barakat M, Mostafa M, Mahran Z, Soliman AG. Portal hypertensive duodenopathy: clinical, endoscopic, and histopathologic profiles. Am J Gastroenterol 2007 Dec;102(12):2793-2802.

(68) Misra V, Misra SP, Dwivedi M, Gupta SC. Histomorphometric study of portal hypertensive enteropathy. Am J Clin Pathol 1997 Dec;108(6):652-657.

(69) Such J, Guardiola JV, de Juan J, Casellas JA, Pascual S, Aparicio JR, et al. Ultrastructural characteristics of distal duodenum mucosa in patients with cirrhosis. Eur J Gastroenterol Hepatol 2002 Apr;14(4):371-376.

(70) Bhonchal S, Nain CK, Prasad KK, Nada R, Sharma AK, Sinha SK, et al. Functional and morphological alterations in small intestine mucosa of chronic alcoholics. J Gastroenterol Hepatol 2008 Jul;23(7 Pt 2):e43-8.

(71) Shu JC, Li QY, Yang QH, Zhang WR, Li ME, Zhang XY, et al. Ultrastructural changes of duodenal mucosas and their significance in patients with liver cirrhosis. Zhonghua Gan Zang Bing Za Zhi 2007 Apr;15(4):254-257.

(72) Ramachandran A, Balasubramanian KA. Intestinal dysfunction in liver cirrhosis: Its role in spontaneous bacterial peritonitis. J Gastroenterol Hepatol 2001 Jun;16(6):607-612.

(73) Thalheimer U, De Iorio F, Capra F, del Mar Lleo M, Zuliani V, Ghidini V, et al. Altered intestinal function precedes the appearance of bacterial DNA in serum and ascites in patients with cirrhosis: a pilot study. Eur J Gastroenterol Hepatol 2010 Oct;22(10):1228-1234.

(74) Bellot P, Frances R, Such J. Pathological bacterial translocation in cirrhosis: pathophysiology, diagnosis and clinical implications. Liver Int 2012 Oct 11.

(75) Graudal N, Milman N, Kirkegaard E, Korner B, Thomsen AC. Bacteremia in cirrhosis of the liver. Liver 1986 Oct;6(5):297-301.

(76) Arvaniti V, D'Amico G, Fede G, Manousou P, Tsochatzis E, Pleguezuelo M, et al. Infections in patients with cirrhosis increase mortality four-fold and should be used in determining prognosis. Gastroenterology 2010 Oct;139(4):1246-56, 1256.e1-5.

(77) Cirera I, Bauer TM, Navasa M, Vila J, Grande L, Taura P, et al. Bacterial translocation of enteric organisms in patients with cirrhosis. J Hepatol 2001 Jan;34(1):32-37.

(78) Llovet JM, Bartoli R, March F, Planas R, Vinado B, Cabre E, et al. Translocated intestinal bacteria cause spontaneous bacterial peritonitis in cirrhotic rats: molecular epidemiologic evidence. J Hepatol 1998 Feb;28(2):307-313.

(79) Bjarnason I, Peters TJ, Wise RJ. The leaky gut of alcoholism: possible route of entry for toxic compounds. Lancet 1984 Jan 28;1(8370):179-182.

(80) Zuckerman MJ, Menzies IS, Ho H, Gregory GG, Casner NA, Crane RS, et al. Assessment of intestinal permeability and absorption in cirrhotic patients with ascites using combined sugar probes. Dig Dis Sci 2004 Apr;49(4):621-626.

(81) Scarpellini E, Valenza V, Gabrielli M, Lauritano EC, Perotti G, Merra G, et al. Intestinal permeability in cirrhotic patients with and without spontaneous bacterial peritonitis: is the ring closed? Am J Gastroenterol 2010 Feb;105(2):323-327.

(82) Cariello R, Federico A, Sapone A, Tuccillo C, Scialdone VR, Tiso A, et al. Intestinal permeability in patients with chronic liver diseases: Its relationship with the aetiology and the entity of liver damage. Dig Liver Dis 2010 Mar;42(3):200-204.

(83) Hashimoto N, Ohyanagi H. Effect of acute portal hypertension on gut mucosa. Hepatogastroenterology 2002 Nov-Dec;49(48):1567-1570.

(84) Xu WH, Wu XJ, Li JS. Influence of portal pressure change on intestinal permeability in patients with portal hypertension. Hepatobiliary Pancreat Dis Int 2002 Nov;1(4):510-514.

(85) Keshavarzian A, Holmes EW, Patel M, Iber F, Fields JZ, Pethkar S. Leaky gut in alcoholic cirrhosis: a possible mechanism for alcohol-induced liver damage. Am J Gastroenterol 1999 Jan;94(1):200-207.

(86) Wiest R, Groszmann RJ. The paradox of nitric oxide in cirrhosis and portal hypertension: too much, not enough. Hepatology 2002 Feb;35(2):478-491.

(87) Banan A, Fields JZ, Decker H, Zhang Y, Keshavarzian A. Nitric oxide and its metabolites mediate ethanol-induced microtubule disruption and intestinal barrier dysfunction. J Pharmacol Exp Ther 2000 Sep;294(3):997-1008.

(88) Berg RD. Bacterial translocation from the gastrointestinal tract. Trends Microbiol 1995 Apr;3(4):149-154.

(89) Mookerjee RP, Stadlbauer V, Lidder S, Wright GA, Hodges SJ, Davies NA, et al. Neutrophil dysfunction in alcoholic hepatitis superimposed on cirrhosis is reversible and predicts the outcome. Hepatology 2007 Sep;46(3):831-840.

(90) Yang CY, Chang CS, Chen GH. Small-intestinal bacterial overgrowth in patients with liver cirrhosis, diagnosed with glucose H2 or CH4 breath tests. Scand J Gastroenterol 1998 Aug;33(8):867-871.

(91) Pande C, Kumar A, Sarin SK. Small-intestinal bacterial overgrowth in cirrhosis is related to the severity of liver disease. Aliment Pharmacol Ther 2009 Jun 15;29(12):1273-1281.

(92) Guarner C, Soriano G. Bacterial translocation and its consequences in patients with cirrhosis. Eur J Gastroenterol Hepatol 2005 Jan;17(1):27-31.

(93) Perez-Paramo M, Munoz J, Albillos A, Freile I, Portero F, Santos M, et al. Effect of propranolol on the factors promoting bacterial translocation in cirrhotic rats with ascites. Hepatology 2000 Jan;31(1):43-48.

(94) Lumsden AB, Henderson JM, Kutner MH. Endotoxin levels measured by a chromogenic assay in portal, hepatic and peripheral venous blood in patients with cirrhosis. Hepatology 1988 Mar-Apr;8(2):232-236.

(95) Spahr L, Bresson-Hadni S, Amann P, Kern I, Golaz O, Frossard JL, et al. Allopurinol, oxidative stress and intestinal permeability in patients with cirrhosis: an open-label pilot study. Liver Int 2007 Feb;27(1):54-60.

(96) Rasaratnam B, Connelly N, Chin-Dusting J. Nitric oxide and the hyperdynamic circulation in cirrhosis: is there a role for selective intestinal decontamination? Clin Sci (Lond) 2004 Nov;107(5):425-434.

(97) Frances R, Rodriguez E, Munoz C, Zapater P, De la ML, Ndongo M, et al. Intracellular cytokine expression in peritoneal monocyte/macrophages obtained from patients with cirrhosis and presence of bacterial DNA. Eur J Gastroenterol Hepatol 2005 Jan;17(1):45-51.

(98) Salzman AL, Menconi MJ, Unno N, Ezzell RM, Casey DM, Gonzalez PK, et al. Nitric oxide dilates tight junctions and depletes ATP in cultured Caco-2BBe intestinal epithelial monolayers. Am J Physiol 1995 Feb;268(2 Pt 1):G361-73.

(99) Häusinger D, Blei A. Hepatic Encephalopathy. In: Rodés J, Benhamou J, Blei A, Reichen J, Rizzetto M, editors. Textbook of hepatology: From basic science to clinical practice. 3.th ed. Malden, Mass: Blackwell; 2007. p. 728-760.

(100) de Franchis R, Pascal JP, Ancona E, Burroughs AK, Henderson M, Fleig W, et al. Definitions, methodology and therapeutic strategies in portal hypertension. A Consensus Development Workshop, Baveno, Lake Maggiore, Italy, April 5 and 6, 1990. J Hepatol 1992 May;15(1-2):256-261.

(101) Wyatt J, Oberhuber G, Pongratz S, Puspok A, Moser G, Novacek G, et al. Increased gastric and intestinal permeability in patients with Crohn's disease. Am J Gastroenterol 1997 Oct;92(10):1891-1896.

(102) Senzolo M, Fries W, Buda A, Pizzuti D, Nadal E, Sturniolo GC, et al. Oral propranolol decreases intestinal permeability in patients with cirrhosis: another protective mechanism against bleeding? Am J Gastroenterol 2009 Dec;104(12):3115-3116.

(103) Fukuda Y, Bamba H, Okui M, Tamura K, Tanida N, Satomi M, et al. Helicobacter pylori infection increases mucosal permeability of the stomach and intestine. Digestion 2001;63 Suppl 1:93-96.

(104) Assimakopoulos SF, Tsamandas AC, Tsiaoussis GI, Karatza E, Triantos C, Vagianos CE, et al. Altered intestinal tight junctions' expression in patients with liver cirrhosis: a pathogenetic mechanism of intestinal hyperpermeability. Eur J Clin Invest 2012 Apr;42(4):439-446.

(105) Wu LL, Chiu HD, Peng WH, Lin BR, Lu KS, Lu YZ, et al. Epithelial inducible nitric oxide synthase causes bacterial translocation by impairment of enterocytic tight junctions via intracellular signals of Rho-associated kinase and protein kinase C zeta. Crit Care Med 2011 Sep;39(9):2087-2098.

(106) Elmore S. Apoptosis: a review of programmed cell death. Toxicol Pathol 2007 Jun;35(4):495-516.

(107) Tanaka M, Inatsuchi S, Terasaki T, Funaki J, Bandou T, Shimada K, et al. Duodenal mucosal hemodynamics in patients with liver cirrhosis. Acta Med Okayama 1990 Oct;44(5):273-277.

(108) Ikeda H, Suzuki Y, Suzuki M, Koike M, Tamura J, Tong J, et al. Apoptosis is a major mode of cell death caused by ischaemia and ischaemia/reperfusion injury to the rat intestinal epithelium. Gut 1998 Apr;42(4):530-537.

(109) Unno N, Wang H, Menconi MJ, Tytgat SH, Larkin V, Smith M, et al. Inhibition of inducible nitric oxide synthase ameliorates endotoxin-induced gut mucosal barrier dysfunction in rats. Gastroenterology 1997 Oct;113(4):1246-1257.

(110) Ramachandran A, Prabhu R, Thomas S, Reddy JB, Pulimood A, Balasubramanian KA. Intestinal mucosal alterations in experimental cirrhosis in the rat: role of oxygen free radicals. Hepatology 2002 Mar;35(3):622-629.

(111) Zong WX, Thompson CB. Necrotic death as a cell fate. Genes Dev 2006 Jan 1;20(1):1-15.

(112) Kaminski M, Karbowski M, Miyazaki Y, Kedzior J, Spodnik JH, Gil A, et al. Co-existence of apoptotic and necrotic features within one single cell as a result of menadione treatment. Folia Morphol (Warsz) 2002;61(4):217-220.

(113) Köpf-Maier P, Merjer HJ. Atlas der Elektronenmikroskopie: Zellen-Gewebe-Organe. 1st ed. Wien, Berlin: Blackwell Wissenschafts-Verlag; 1989.

(114) Pitelka DR, Taggart BN. Mechanical tension induces lateral movement of intramembrane components of the tight junction: studies on mouse mammary cells in culture. J Cell Biol 1983 Mar;96(3):606-612.

(115) Dickinson E, Tuncer R, Nadler E, Boyle P, Alber S, Watkins S, et al. NOX, a novel nitric oxide scavenger, reduces bacterial translocation in rats after endotoxin challenge. Am J Physiol 1999 Dec;277(6 Pt 1):G1281-7.

(116) Gitter AH, Bendfeldt K, Schulzke JD, Fromm M. Leaks in the epithelial barrier caused by spontaneous and TNF-alpha-induced single-cell apoptosis. FASEB J 2000 Sep;14(12):1749-1753.

(117) Knecht KT, Adachi Y, Bradford BU, Iimuro Y, Kadiiska M, Xuang QH, et al. Free radical adducts in the bile of rats treated chronically with intragastric alcohol: inhibition by destruction of Kupffer cells. Mol Pharmacol 1995 May;47(5):1028-1034.